THEORETICAL STUDIES OF ORGANIC DIRADICALS AND THE THERMAL REARRANGEMENT OF BICYCLOPROPENYLS

Thesis by

James Hubbard Davis

In Partial Fulfillment of the Requirements

for the Degree of

Doctor of Philosophy

California Institute of Technology

Pasadena, California

1977

(Submitted August 6, 1976)

"To me, the tragic alone has that significant beauty which is truth. It is the meaning of life — and the hope. The noblest is eternally the most tragic. The people who succeed and do not push on to a greater failure are the spiritual middle-classers. Their stopping at success is the proof of their compromising insignificance. How petty their dreams must have been!"

Eugene O'Neill

ACKNOWLEDGMENTS

To Bob Bergman and Bill Goddard goes my deepest appreciation for teaching me to think. If I have acquired their insight and their determination in approaching problems, then the last three years will be of immeasurable value. I thank them for their patience in having only part of a graduate student and their understanding for the strange course I am to pursue.

Thanks are also due to all members of the Goddard and Bergman research groups for their stimulating discussions and helpful suggestions.

A special thanks is owed Professor Jerome A. Berson of Yale University who taught me to love and to revere science not as technology but as an art.

I gratefully acknowledge financial support from the California Institute of Technology and from the John and Beverly Stauffer Foundation.

Finally I thank K. C. without whom this thesis would never have been finished on time.

ABSTRACT

Part A. Generalized valence bond calculations on cyclopropene and vinylmethylene lead to the following conclusions: (1) the allyl-type π-system is strongly distorted by the presence of the unpaired sigma electron leading to a methylene-like triplet, $^3A'$, but a 1,3-diradical-like singlet state, $^1A''$; (2) the lowest-lying singlet state of vinylmethylene has the form of a singlet methylene $^1A'$ lying 12 kcal/mole above the triplet ground state, while the diradical singlet state lies at 14 kcal/mole.

Part B. Generalized valence bond calculations on trimethylenemethane indicate that the ground state is the planar triplet with the planar singlet state 26 kcal/mole higher. The rotational barrier for the triplet state is 18 kcal/mole, while one component of the planar singlet prefers the bisected geometry by 7 kcal/mole. Oscillator strengths for vertical transitions and ionization potentials are also reported.

Part C. Generalized valence bond calculations on vinylidene predict that the ground state is a singlet with a methylene-like triplet at 2 eV higher. With extensive CI calculations, we find CC bond energy of $D_0\,(H_2C{=}C) = 150.1$ kcal/mole and a heat of formation of 111.5 kcal/mole at 298°K. The dipole moment for the singlet is calculated to be 2.23D, while the dipole moment for the triplet is 0.55D.

Part D. Generalized valence bond calculations on aminonitrene indicate

that the ground state is a singlet ($^1A_1$) with a low-lying triplet state ($^3A_2$) at 15 kcal/mole. We find the nitrogen-nitrogen bond dissociation energy for the singlet state is 70.4 kcal/mole. The dipole moment is found to be 4.036D for the $^1A_1$ and 2.351D for the $^3A_2$ state of aminonitrene. The ionization potential is calculated to be 9.4 eV.

Part E. The kinetic distribution of isomeric xylenes formed on the thermal aromatization of dl- and meso-1,1'-dimethyl-3,3'-bicyclopropenyl and of 3,3'-dimethyl-3,3'-bicyclopropenyl has been determined by extrapolation of the time-dependent xylene percentages to zero percent conversion. The data is most consistent with a mechanism involving initial cleavage of one of the cyclopropene rings, followed by expansion of the other ring, closure to a Dewar benzene and finally opening of the Dewar benzene to form aromatic products.

PREFACE

Studies on the ring opening of small organic compounds have raised many questions concerning the nature of chemical bonding. The deeper we probe the structure and reactivity of radical centers, the less certain we become of our fundamental concepts. The more we try to distinguish between concerted and diradical pathways, the less certain we become that there is any distinction. Recent work by Berson and Peterson have indicated that very subtle differences in chemical structure can have dramatic effects on the stereochemistry of diradical reactions. This thesis is concerned with probing the effect of structure on diradicals; in particular, we are concerned with the interaction of a radical center with an unsaturated π-system.

In Parts A and B we explore the interaction of a radical center with an allylic π-system. Both of these studies involve intermediates that have received considerable experimental attention: the first concerns the intermediates derived from the ring opening of cyclopropene, while the second concerns the intermediates derived from the ring opening of methylenecyclopropane.

In Parts C and D we study the effect of a π-system on a 1,1'-diradical. The first reactive intermediate is vinylidene, which can be considered to come from cleavage of methylenecyclopropane to give ethylene and vinylidene. The second intermediate studied is the nitrogen analog of vinylidene — aminonitrene.

Neither of these two intermediates have been extensively studied experimentally although work on both is currently underway.

In Part E we present an experimental study on the thermal rearrangement of bicyclopropenyls. Concepts developed in Part A are used to elucidate the mechanism of aromatization.

TABLE OF CONTENTS

PART A: VINYLMETHYLENE AND THE RING OPENING OF CYCLOPROPENE — AB INITIO GENERALIZED VALENCE BOND AND CONFIGURATION INTERACTION STUDIES[1]

I. Introduction

In this paper we examine in some detail the electronic states involved in the ring opening of cyclopropene. Detailed ab initio calculations are performed to determine the electronic nature of these excited states.[2]

Stretching of the C–C bond in cyclopropene (1), without rotation of

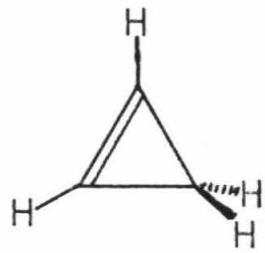

the methylene group, leads to the bisected geometry of the vinylmethylene diradical (2),

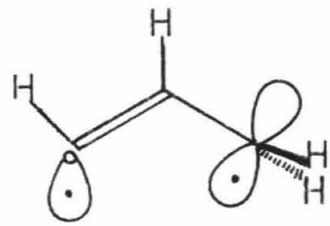

Racemization of 1 can then result from rotation of the methylene group in 2 to give the planar geometry 3 where the circle on the right

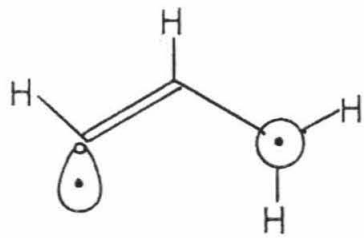

carbon indicates a singly-occupied π-orbital. As suggested by Bergman,[3] this form of the vinylmethylene diradical (3) would be expected to be in resonance with the vinyl carbene (4) so that this planar intermediate

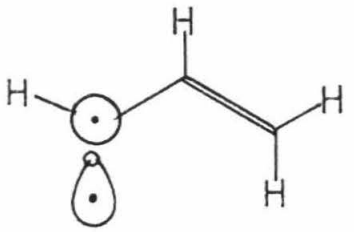

state might be represented as 5,

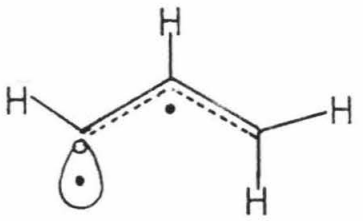

We have carried out ab initio calculations on the states of both the bisected (2) and planar (3, 4, 5) geometries of vinylmethylene and of cyclopropene (1) using Hartree-Fock (HF), generalized valence bond (GVB),[4] and configuration interaction (GVB-CI) wavefunctions. We find that the exchange effects in 3 and 4 are larger than the resonance effects with the result that the triplet state favors 4 while the singlet state favors 3. Thus the form 5 is not an appropriate description of either state.

We have also found a low-lying singlet state of the form 6 which

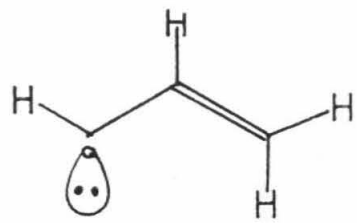

is analogous to singlet carbene and which might play an important role in the racemization of cyclopropene 1. The likely roles of these states in various thermal and photolytic processes is discussed.

In order to provide simple ways of characterizing these states the wavefunctions of 3, 4, and 5 will be referred to as 3π while the wavefunction of 6 is referred to as 2π (indicating in each case the number of electrons in π orbitals). Using standard notation the triplet and singlet states of 3, 4, and 5 are denoted as $^3A''$ and $^1A''$ while the state of 6 is denoted as $^1A'$. Although redundant we will often add a (3π) or (2π) to aid in keeping track of the wavefunctions.

II. Calculational Details

A. Basis Sets and Geometries. Dunning's[5] (4s2p/2s) contraction of Huzinaga's (9s5p/4s) primitive Gaussian basis was used in all calculations. This double zeta basis (DZ) was augmented by a contracted set of polarization d-functions (α = 0.678) on each carbon. This more extensive basis (DZd) had previously been shown to be necessary in calculating the singlet-triplet gap in methylene.[6]

Geometries appropriate for bonding structures 1, 2, 3, 4, 5, and 6 were utilized. The experimental geometry[7] for 1 was used, while for the others, CH bonds were taken as 1.08 Å, CC single bonds as 1.54 Å, CC double bonds as 1.34 Å, and all bond angles, except for the left HCC bond angle, were taken as 120°.

A series of calculations (DZ basis) were carried out for the planar geometry (5) using equal CC bond lengths of 1.38 Å (appropriate for bond order 1.5) and left HCC angles of 120°, 180°, 240°. These calculations showed the triplet 3π state to have the form in 4 and the singlet 3π to have the form in 3. We then repeated the calculations using a DZd basis and geometries appropriate for 3 and for 4 (e.g., in 4, the left HCC angle was taken as 135°).

In the 2π singlet state (6) the left HCC angle was taken as 105° (in analogy with the σ^2 state of methylene). Two different sets of CC bond lengths were considered for 6; initially normal CC single and double bond lengths (1.54 and 1.34 Å) were used. Final calculations on the 2π state used CC bond lengths ($R_{cc-\ell}$ = 1.50 Å and R_{cc-r} = 1.32 Å), values optimized by Salem and Stroher[8] using Hartree-Fock minimum basis set wavefunctions.

B. The GVB calculations. The HF wavefunction for the triplet state of 5 would consist of ten doubly-occupied orbitals and two singly-occupied orbitals:

$$\mathcal{A}[\phi_1^2 \ldots \phi_9^2 \phi_{1\pi}^2 \phi_{2\pi} \phi_\sigma \alpha\beta \ldots \alpha\beta\alpha\beta\alpha\alpha]. \qquad (1)$$

The most serious deficiency in this wavefunction is the lack of correlation between the electrons in the π orbitals, an effect that has been found to be very important in describing unsaturated systems.[9,10] This problem is eliminated by using the GVB(2) wavefunction in which we allow each of the three π-electrons and the one unpaired σ-electron to have their own orbitals. In our calculations we restrict the GVB(2) wavefunction by partitioning the four singly-occupied orbitals into two sets of mutually orthogonal singlet- or triplet-coupled pairs (referred to as the perfect pairing approximation and indicated by the symbol PP). Thus the GVB(2/PP) wavefunction for the triplet state (1) is of the form:

$$\mathcal{A}\{[\phi_1^2 \ldots \phi_9^2 \alpha\beta \ldots \alpha\beta](\phi_{1\pi}\phi_{3\pi} + \phi_{3\pi}\phi_{1\pi})(\alpha\beta)(\phi_{2\pi}\phi_\sigma)(\alpha\alpha)\}. \qquad (2)$$

This wavefunction was then used in all preliminary calculations to obtain the basic qualitative features of bonding.

Since we are concerned with the ordering of states within a few kcal, we also carried out much more extensive calculations in order to include the smaller additional correlation effects that affect excitation energies. For conjugated systems the most important correlation effects ignored in the GVB(2/PP) wavefunction are the interpair correlations involving simultaneous $\sigma \rightarrow \sigma^*$ and $\pi \rightarrow \pi^*$ excitations of the C–C bond pairs.[9,10] In order to include these correlations consistently, we also correlated the CC σ bonds leading to the GVB(4/PP) wavefunction

(this results in localized CC σ bond pairs and provides σ^* orbitals for the interpair terms). These orbitals were then included in a configuration interaction calculation (GVB-CI) to include various residual electron correlation effects.

Finally, we were concerned that the perfect pairing restriction might have prejudiced the localization of the double bond since it allows only one spin coupling. To check for this possibility we relaxed the perfect pairing restriction for the three π-electrons and one σ-electron using the SOGVB program.[11] Thus for example the

$$[\phi_{1\pi}\,\phi_{3\pi} + \phi_{3\pi}\,\varphi_{1\pi})\,\phi_{2\pi}\,\phi_{\sigma}\,\alpha\beta\alpha\alpha]$$

$$= [\phi_{1\pi}\,\phi_{3\pi}\,\phi_{2\pi}\,\phi_{\sigma}\,(\alpha\beta - \beta\alpha)\,\alpha\alpha]$$

part of (2) becomes

$$[\phi_{1\pi}\,\phi_{3\pi}\,\phi_{2\pi}\,\phi_{\sigma}\,\chi]$$

where

$$\chi = C_1\,(\alpha\beta - \beta\alpha)\,\alpha\alpha/\sqrt{2} + C_2\,(\alpha\alpha)(\alpha\beta - \beta\alpha)/\sqrt{2} + C_3[(\alpha\alpha\beta\beta + \beta\beta\alpha\alpha) - \tfrac{1}{2}(\alpha\beta + \beta\alpha)(\alpha\beta + \beta\alpha)]/\sqrt{3}$$

and both the orbitals and spin coupling coefficients (C_1, C_2, C_3) are optimized self-consistently (including self-consistent optimization of the other σ orbitals of GVB(4) wavefunction). Such calculations were carried out for the DZd wavefunction using the appropriate geometry of $\hat{4}$ for the triplet state and of $\hat{3}$ for the singlet state. No change in the extent of delocalization was observed in either case.

Figure 1. Selected GVB orbitals for the $^3A''$, $^1A''$, and $^1A'$ states of planar vinylmethylene based on the GVB(2/PP) wavefunction using the DZ basis set. Long dashes indicate zero amplitude; the spacing between contours is 0.05 a.u. The same conventions are used for all plots.

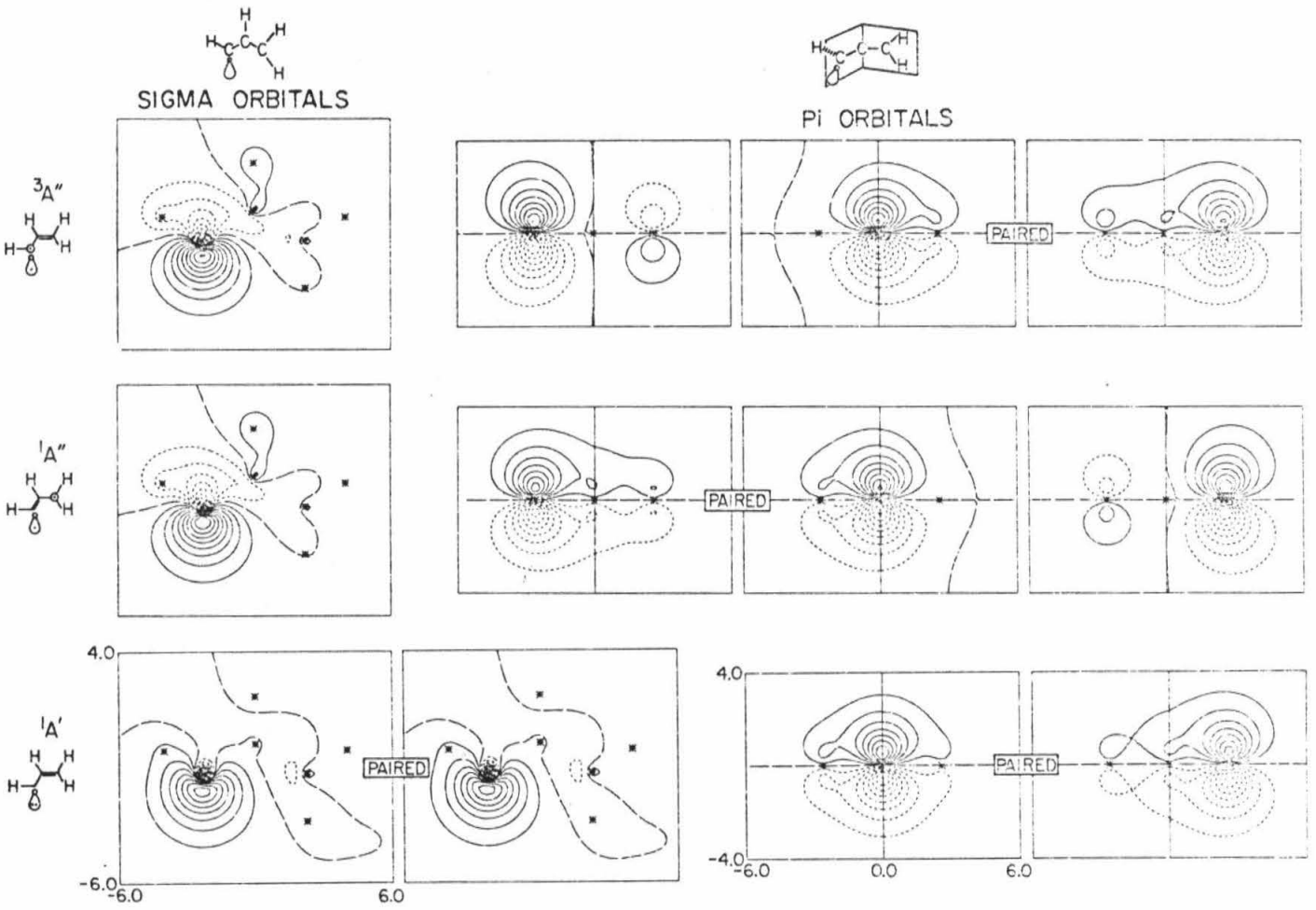
SIGMA ORBITALS
Pi ORBITALS
$^3A''$
$^1A''$
$^1A'$
PAIRED
PAIRED
PAIRED
PAIRED
4.0
-6.0
-6.0
6.0
4.0
-4.0
-6.0
0.0
6.0

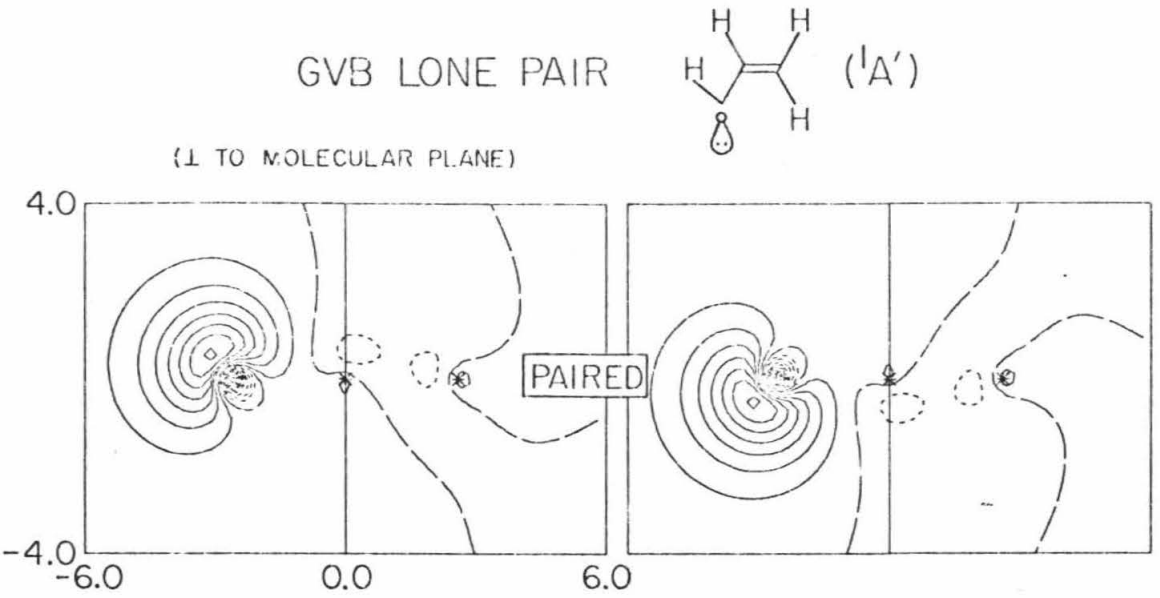
GVB LONE PAIR
H
H
H
H
O
(¹A′)
(⊥ TO MOLECULAR PLANE)
4.0
-4.0
-6.0
0.0
6.0
PAIRED

III. Discussion

A. The GVB Orbitals. The GVB orbitals for the $^3A''$, $^1A'$, and $^1A''$ states are shown in Figure 1. These orbitals come from the calculations [GVB(2/PP)] using the geometry of 5 and a left HCC angle of 120°. By using the equal CC bond lengths of 5, we ensured that our wavefunction would not be biased toward localization. However, as can be seen in Figure 1, the π-system for $^1A''$ and $^3A''$ is well localized.

In the $^3A''$ (3π) state the GVB π-pair is localized on the right CC bond while a singly-occupied π orbital is localized on the left carbon nucleus. Therefore, the $^3A''$ state has the form of a vinylmethylene instead of the allylic form 5. The $^1A''$ (3π) state shows an entirely different type of localized π system in which the π-pair is localized on the left CC bond while the singly-occupied π is on the right nucleus. Thus the $^1A''$ state resembles the 1,3-diradical 3. The $^1A'$ (2π) state resembles the $^3A''$ state in that the π-pair is localized on the right, however the extent of delocalization is somewhat larger for the $^1A'$ state. Some delocalization is expected in $^1A'$ (2π) due to the absence of a π electron on the left carbon; however, such delocalization tends to build up a negative charge on the left center limiting this effect. The $^3A''$ and $^1A'$ states have the form of a vinylmethylene, while the $^1A''$ state resembles a 2,3-diradical.

The two 3π states ($^1A''$ and $^3A''$) had been generally assumed to be a resonance hybrid of 3 and 4, much as in the allyl radical. However, the GVB calculation shows quire conclusively that the presence of the unpaired sigma electron strongly distorts the π-system. The reasons for this are analyzed next. The sigma electron interacts with the

π-system through the exchange terms, resulting in the nondegeneracy of the two resonance contributors (3 and 4). We can represent the energy of each contributor as the sum or difference of a basic energy term, E_0, and an exchange term, $K_{\sigma\pi}$, which describes the interaction between the two unpaired electrons. The triplet state is stabilized by the exchange term as in (3), while the singlet state is destabilized by $K_{\sigma\pi}$ as in (4). The magnitude of the exchange terms

$$E_T = E_0 - K_{\sigma\pi} \tag{3}$$

$$E_S = E_0 - K_{\sigma\pi} \tag{4}$$

$K_{\sigma\pi}$ is related to the proximity of the orbitals. Thus for 4 (where electrons are located on the same carbon), it is large (0.9 eV) but for 3 (where the electrons are well separated) it is small (0.05 eV).[19] Thus eq (1) shows that in the triplet state localized structure 4 will be lower than 3 by 0.05 eV, while from eq (2), in the singlet case state 3 will be lower than 4 by the same amount. The consequences of these exchange terms are the localized orbitals depicted in Figure 1.

B. ResonanceEffects. Since the ideas of resonance provide powerful arguments for qualitative discussions of organic systems we will next analyze our wavefunction semi-quantitatively in terms of the interaction of structures 3 and 4. We can consider the molecular wavefunction for the $^3A''$ state to be composed of two nonequivalent wavefunctions,

$\psi_1 =$  and $\psi_2 =$ 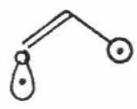 (5)

with energies E_1 and E_2 such that $E_1 < E_2$. Allowing the total wavefunction to have the form

$$\Phi = c_1 \psi_1 + c_2 \psi_2 , \tag{6}$$

we want to determine where the two states of Φ lie in comparison with E_1 and E_2.

The final separation of the resonant and anti-resonant states is calculated from our GVB(2/PP)-CI wavefunctions to be

$$\lambda_2 - \lambda_1 = 3.56 \text{ eV}. \tag{7}$$

In Appendix A we show how to use the excitation energy (7) along with the energy separation

$$E_2 - E_1 = 0.85 \text{ eV} \tag{8}$$

and overlap

$$S = \langle \psi_1 | \psi_2 \rangle = 0.630 \tag{9}$$

of ψ_1 and ψ_2 (from the GVB calculations) to obtain the resonance energy for the wavefunction (6). The result for the triplet state is

$$E^{res} = 6.6 \text{ kcal/mole}$$

which is 60% of the resonance energy, 11.4 kcal/mole, for the allylic system.[12]

The final wavefunction for the resonant state is

$$\phi_1 = 0.728 \psi_1 + 0.366 \psi_2 \tag{10}$$

in terms of nonorthogonal functions. Orthogonalizing (and renormalizing) ψ_2 to ψ_1, wavefunction (10) becomes

$$\phi_1 = 0.959\ \psi_1 + 0.284\ \overline{\psi}_2 \qquad (11)$$

in terms of orthogonal functions. Here we see that the total wavefunction is 92% ψ_1 although the formulation (10) in terms of nonorthogonal orbitals might have suggested greater delocalization.

In order to compare with a case possessing perfect allylic resonance, we set $E_1 = E_2$, obtaining

$$\phi_1 = 0.554\ \psi_1 + 0.554\ \psi_2 \qquad (12)$$

or in terms of orthogonal functions

$$\phi = 0.903\ \psi_1 + 0.430\ \overline{\psi}_2\ . \qquad (13)$$

From (13) we see that the allylic wavefunction is 81% ψ_1 (or ψ_2). Comparing (12) with (10) or (13) with (11), we see that vinylmethylene has about half the resonance or delocalization expected of an allylic pi system.

In the above discussion all numbers were based on the case for equal bond lengths. The optimum geometry for $\hat{4}$ has unequal bond lengths leading to a large increase in E_2-E_1 and as a result will decrease the resonance energy.

C. Inversion Barriers. To study the interconversion of the syn and anti isomers of $\hat{5}$, we carried out calculations at HCC angles of 120° (anti), 180° (linear), and 240° (syn) using the equal bond lengths restrictions of $\hat{5}$. Because of this restriction, the separations between electronic states are not as accurate, but the shapes of the potential surfaces should

be reliable. In the $^3A''$ state the calculations predict relative energies of 0.48, 8.76, and 0.0 kcal for these angles, indicating that the syn and anti forms are nearly degenerate (with syn more stable), but are separated by a relatively large inversion barrier. This barrier compares well with the inversion barrier of triplet methylene (9 kcal/mole)[6] in agreement with our qualitative picture of the $^3A''$ state as a substituted methylene. In the $^1A''$ state the relative energies were 0.0, 1.56, and 0.84 kcal/mole; here there is a small inversion barrier, as one would have expected for a vinyl radical ($\sim$ 2 kcal/mole).[13] Finally, the $^1A'$ state gave energies of 0.0, 18.12, and 1.44 kcal/mole, corresponding to the large barrier observed in the inversion of singlet methylene ($^1A_1$).[6] In all three cases, the inversion barriers compare well with the qualitative picture of a localized π-system.

D. Excitation Energies. The localization of the π-system in the $^3A''$ and $^1A''$ states suggested that the carbon-carbon bond lengths should not be equal as assumed in the previous calculations. Appropriate geometries (see Sec. II. A) were therefore used for the $^3A''$, $^1A''$, and $^1A'$ states. These modified geometries resulted in an energy lowering of 6-8 kcal/mole for each of the three states (see Table I).

In studies on methylene, Hay, Hunt, and Goddard[6] found that the inclusion of 3d polarization functions lowered the $^3B_1$-$^1A_1$ energy separation from 22.4 to 11.0 kcal/mole. In vinyl carbene, inclusion of d-functions lowered the $^3A''$ - $^1A'$ excitation energy by 18 kcal/mole.

The $^3A''$ (3π) - $^1A'(2\pi)$ separation was found to be sensitive not only to inclusion of d-functions but also to inclusion of CC-sigma bond

Figure 2. Electronic states of vinylmethylene (energies in Kcal mole^{-1}) from GVB(4)-CI using DZd basis. CH bonds are omitted in the diagrams. The lowest energy pathway (not shown) involves simultaneous ring opening and methylene rotation.

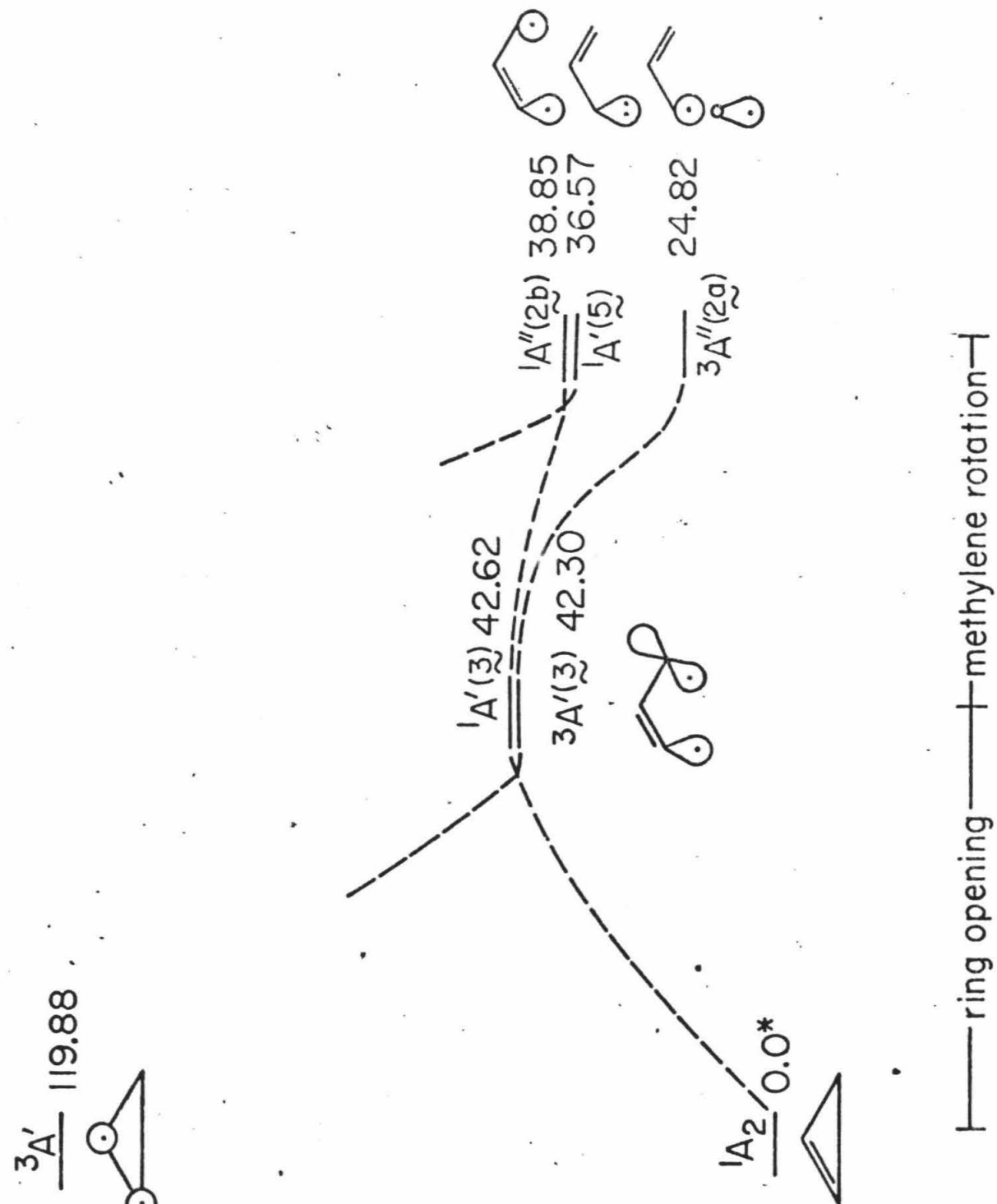
$^3A'$ 119.88
$^1A'(3)$ 42.62
$^3A'(3)$ 42.30
$^1A''(2b)$ 38.85
$^1A'(5)$ 36.57
$^3A''(2a)$ 24.82
$^1A_2$ 0.0*
ring opening
methylene rotation

correlation. Previous calculations[9,10] on systems containing multiple bonds had showed that ($\sigma \rightarrow \sigma^*$, $\pi \rightarrow \pi^*$) excitations are important in obtaining accurate excitation energies. In vinylmethylene these correlations involving CC-σ bonds were included, leading to an increase in the $^3A''$-$^1A'$ excitation energy of 4 kcal/mole.

The excitation energies for the planar states are shown in Figure 2. We predict a $^3A''$ (3π) - $^1A'$ (2π) separation of 11.7 kcal/mole--very close to the separation found for methylene itself (11.0 kcal/mole).[20] The $^1A''$ (3π) state lies only 2.3 kcal/mole above the $^1A'$(2π) state; this $^3A''$ (3π) - $^1A''$ (2π) gap of 14.0 kcal/mole is considerably less than the $^3B_1$ - $^1B_1$ splitting in methylene (44 kcal/mole). Thus, as expected, the vinyl substitution lowers the $^1A''$ (3π) state relative to the $^3A''$ (2π) state by reducing the repulsive exchange interaction through localization of the singly-occupied orbital onto the β-carbon.

Also shown in Figure 2 are the excitation energies for the bisected, twisted geometry $\underset{\sim}{2}$ of vinylmethylene and for cyclopropene. The triplet-singlet splitting for $\underset{\sim}{2}$ is found to be only 0.4 kcal/mole, as expected for a $\sigma\pi$ 1,3-diradical. The triplet-singlet splitting for cyclopropene is found to be 119.9 kcal/mole (compare with 106.1 kcal/mole from similar calculations on ethylene[14]).

E. The Ring Opening of Cyclopropene. As shown in Figure 2, the two states which correlate directly with ground state cyclopropene are the twisted $^1A'$ (2π) state and the planar $^1A''$ (3π) state. The GVB orbitals for cyclopropene and these two states are shown in Figure 3.

Figure 3. GVB orbitals for ring opening of cyclopropene. All valence orbitals are shown for the geometries $\underset{\sim}{1}$, $\underset{\sim}{2}$, and $\underset{\sim}{3}$.

RING OPENING OF CYCLOPROPENE

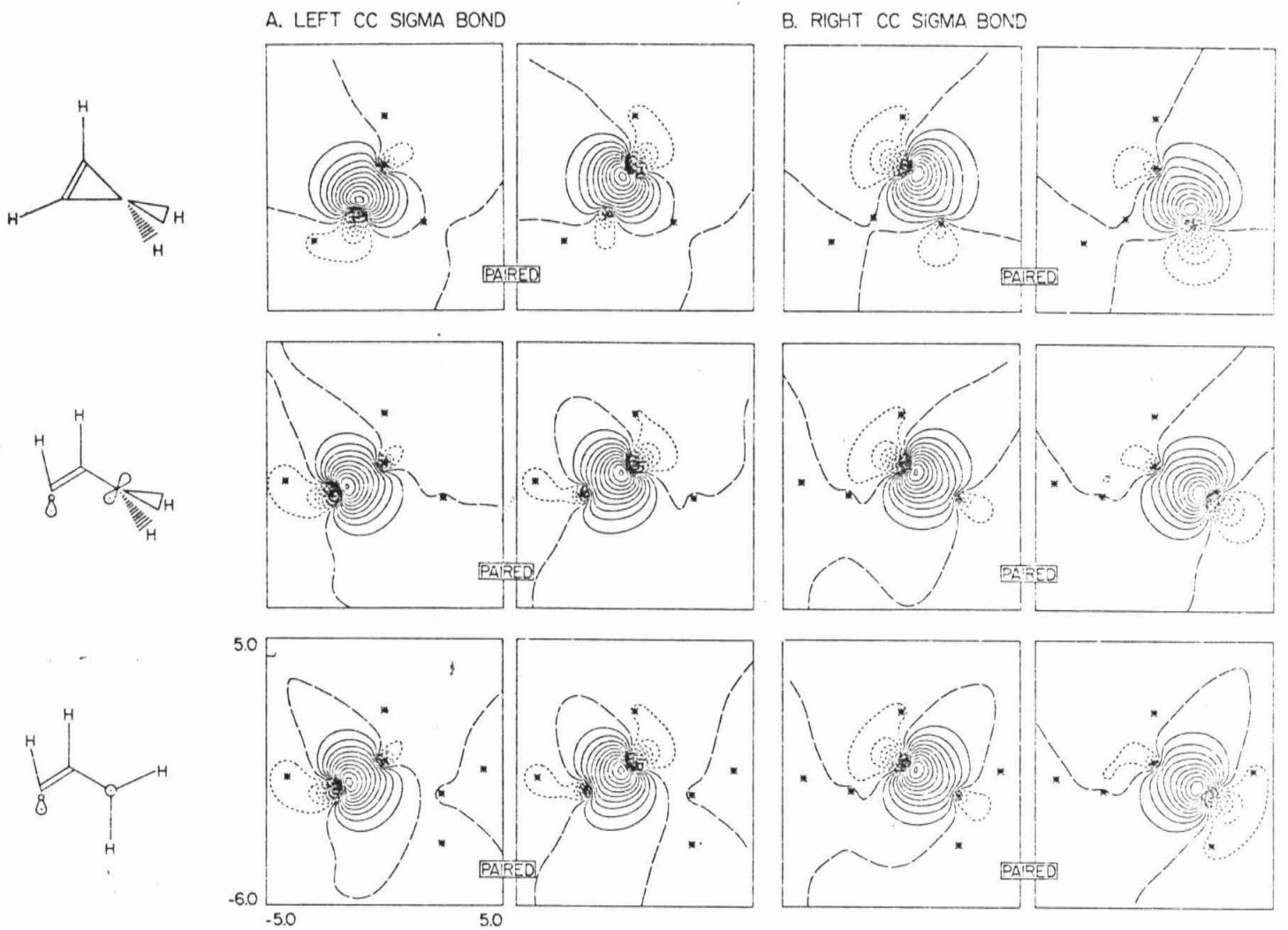

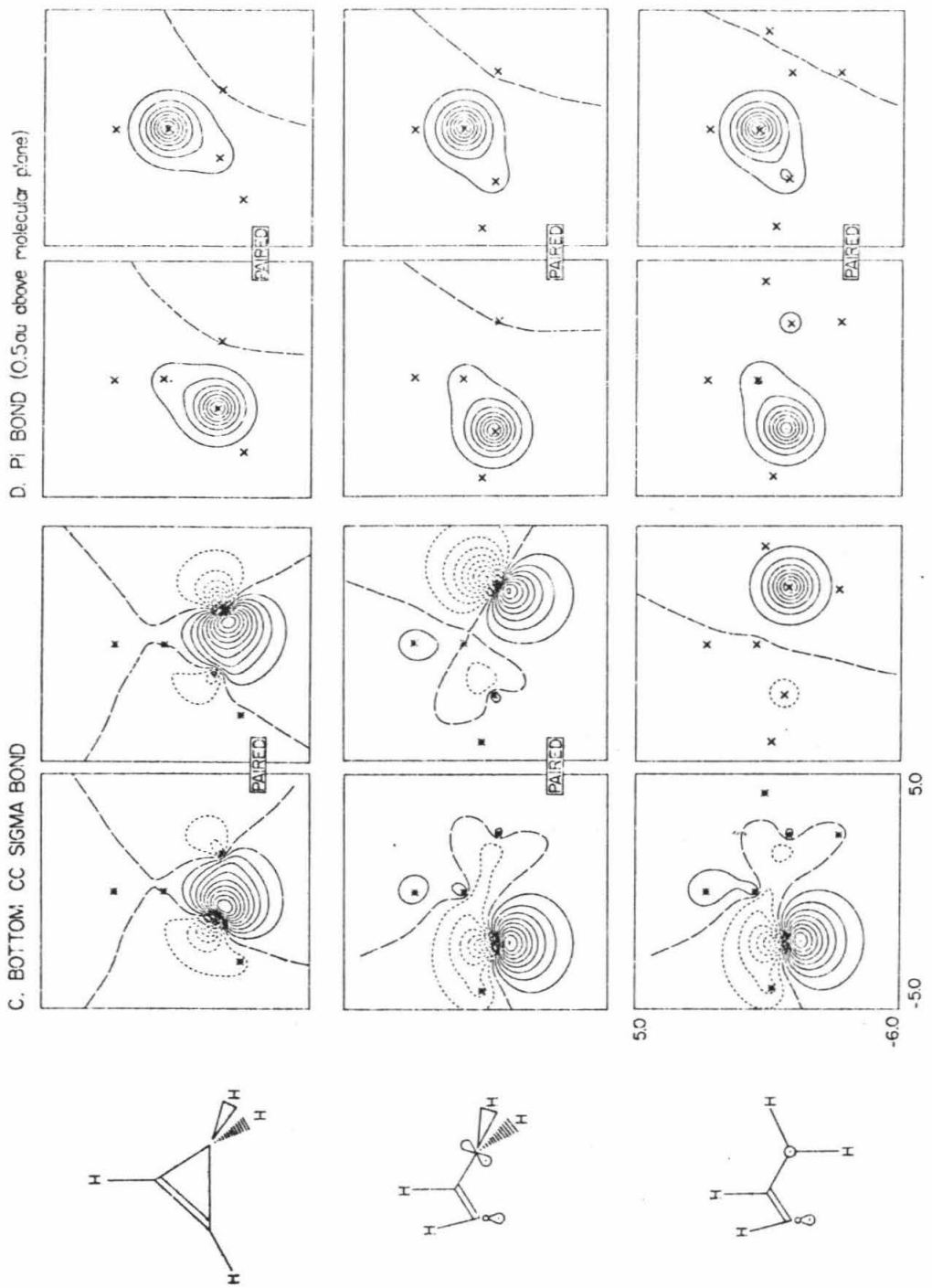
C. BOTTOM: CC SIGMA BOND
D. Pi BOND (0.5au above molecular plane)
PAIRED
PAIRED
PAIRED
PAIRED
PAIRED
PAIRED
5.0
-6.0
5.0
-5.0
H
H
H
H
H
H
H
H
H

In cyclopropene there are two basic types of bonding pairs for the σ-system. The first type of bonding pair is the CC σ bond between centers 1 and 2 and consists of one orbital centered on carbon 1 and hybridized $(sp^{1.6})^{15}$ toward carbon 2 and one orbital on carbon 2 hybridized $(sp^{1.6})$ toward carbon 1. As expected from the symmetry of the molecule, these two orbitals are mirror images of each other. The second type of bonding pair includes the two identical CC bonds between centers 3 and 1 and centers 3 and 2. The orbital in each pair that is centered on carbon 3 is $sp^{3.8}$ hybridized while those on carbons 1 and 2 are $sp^{2.6}$ hybridized. Thus these pairs (sets B and C) consist of orbitals that contain a greater amount of p-character than those of set B; they are less spherical and more directional. Furthermore, each orbital in the pair is not hybridized directly at the opposing carbon but instead is hybridized more toward the outside of the ring. The resulting picture is that of a bowed or strained three-member ring.

Stretching the CC bond of cyclopropene to give the ring opened form--the twisted $^1A'$ state--we can see the effect strain had on the cyclopropene bonds. In sets A and B, the bonding pairs of the two CC σ-bonds now consist of two orbitals pointing directly at the other bonding center. The bowing of the sigma bonds is no longer present. The left CC bond is composed of two orbitals which are $sp^{1.4}$ and $sp^{1.7}$ hybrids on carbons 1 and 2, while the right CC bond is composed of $sp^{2.4}$ and $sp^{2.0}$ hybrids on carbons 3 and 2.

The σ-bond pair corresponding to the broken CC bond (set C) shows extensive rehybridization upon ring opening. The orbital on the left carbon is now an $sp^{5.4}$ hybrid, while the orbital on the right is a pure p-orbital.

As the right methylene group is rotated to give the $^1A''$ state, we see that the two CC sigma bond pairs change very little. In addition, the unpaired sigma orbital on carbon 1 does not change. The only substantial change in the system is that the p-orbital previously in the plane is now perpendicular to the plane. We see further that this singly-occupied π-orbital is largely localized on the right carbon.

The π-bonding pairs for the three states are shown in set D. We see that ring-opening has little effect on the π-system. Rotation of the methylene group leads to only small amounts of delocalization.

In the above discussion we have artifically broken the ring opening of cyclopropene into two modes--bond stretching and methylene rotation. In reality the reaction path near the saddle point no doubt involves simultaneous rotation and bond stretching. Thus the activation energy for ring opening--42.6 kcal/mole--shown in Figure 2 is probably a bit high; we expect the activation energy to lie between 38-42 kcal/mole.

Our calculations show that the 1,3-diradical singlet state ($^1A'$) correlates well with ground state cyclopropene, and therefore suggest that $^1A''$ is the state most important to the isomerization. The "1,3-diradical" state $^1A''$ could possibly decay to the "carbene" states $^1A'$ (2π) and $^3A''$ (3π), leading to products characteristic of singlet and

triplet methylene; however, in this case ring closure must then be preceded by reconversion to $^1A''$.

On the other hand, formation of vinylmethylenes by extrusion of nitrogen from a vinyl diazo-compound should lead directly to $^1A'$, which may react as a carbene, or decay to $^3A''$, which would react as a triplet methylene. We would not expect significant formation of $^1A''$.

F. Comparison with ESR Spectra. Recent ESR experiments by Wasserman[16] and Chapman[17] have reported the observation of two triplet vinylmethylenes having the following zero-field splitting parameters: D = 0.4578 (0.4130), E = 0.0193 (0.0176) and D = 0.4093 (0.4090), E = 0.0224 (0.0233). [Numbers in parentheses refer to Chapman's work.] The two triplets observed were interpreted[16] as the syn and anti $^3A''$ vinylmethylenes.

The low values for the D parameters were interpreted as being indicative of a fully delocalized allyl π-system.

The observation of two triplets in the ESR is in agreement with our calculations, which predict the two isomeric forms of the $^3A''$ to be nearly degenerate (separated by ~ 0.5 kcal) and separated by a substantial barrier (9 kcal/mole). Thus both isomers should be observable in the ESR.

Our calculations, however, do not support the interpretation of a fully delocalized allylic π-system for vinylmethylene. In fact, our calculations suggest a considerable amount of localization. In order to help resolve this apparent discrepancy, we sketch below a simplified calculation of the ESR D value for our wavefunction.

The D value for our total wavefunction Φ [see eq (1)] can be written as

$$D = \langle \Phi | \mathcal{H}_D | \Phi \rangle$$

$$= c_1^2 \langle \psi_1 | \mathcal{H}_D | \psi_1 \rangle + c_2^2 \langle \psi_2 | \mathcal{H}_D | \psi_2 \rangle + 2c_1c_2 \langle \psi_1 | \mathcal{H}_D | \psi_2 \rangle \qquad (14)$$

in terms of our nonorthogonal wavefunctions where $\mathcal{H}_D$ is the spin-spin interaction Hamiltonian. Using the Mullikan approximation

$$\psi_1\psi_2 = \tfrac{1}{2} S(\psi_1\psi_1 + \psi_2\psi_2) \qquad (15)$$

for the cross terms we find

$$D = (c_1^2 + c_1c_2S) \langle \psi_1 | \mathcal{H}_D | \psi_1 \rangle + (c_2^2 + c_1c_2S) \langle \psi_2 | \mathcal{H}_D | \psi_2 \rangle . \qquad (16)$$

The second term of eq (16) represents the spin interaction between an electron in the σ orbital on carbon 1 with an electron in the π orbital on carbon 3. Consequently, the term should be negligible compared with $\langle \psi_1 | \mathcal{H}_D | \psi_1 \rangle$. Thus,

$$D = (c_1^2 + c_1c_2S) \langle \psi_1 | \mathcal{H}_D | \psi_1 \rangle . \qquad (17)$$

Assuming that the one-center integral here is the same (0.627 cm^{-1}) as for methylene[18] (neglecting then possible changes in the "methylene" HCC angles), leads to the following D values:

$$D = 0.627 \text{ cm}^{-1} \text{ for methylene}$$

$$D = 0.438 \text{ cm}^{-1} \text{ for wavefunction (10)}$$

$$D = 0.318 \text{ cm}^{-1} \text{ for wavefunction (12)}$$

where wavefunction (10) is vinylmethylene and wavefunction (12) is vinylmethylene with perfect resonance. Our predicted D of 0.44 is in reasonable agreement with the experimental value of 0.43 (average of syn- and anti-isomers).[16] Thus, because of the cross-term $c_1 c_2 S\langle\psi_1|\mathcal{H}_D|\psi_1\rangle$, even a fairly localized π-system can have substantially smaller zero-field parameters than the perfectly localized system.

IV. Summary

Summarizing, our calculations predict that

1. the allyl-type π-system is strongly distorted by the presence of the unpaired sigma electron leading to a methylene-like triplet, $^3A''$ (4), but a 1,3-diradical-like singlet state, $^1A''$ (3);
2. the lowest-lying singlet state of vinylmethylene has the form of a singlet methylene $^1A'$ (6) lying 12 kcal/mole above the $^3A''$ ground state, while the diradical singlet state $^1A''$ (3) lies at 14 kcal/mole;
3. the $^3A''$ ground state of 4 should exist in two geometrical forms (syn and anti) having nearly the same energy and separated by a large barrier (9 kcal); and
4. the 1,3-diradical singlet state has only a low barrier (2 kcal/mole) between the syn and anti forms while the methylene triplet and singlet states have large barriers.

These results suggest that the ring opening of cyclopropene proceeds directly to a diradical planar intermediate.

Appendix

A. Calculation of Resonance Energy. Since ψ_1 and ψ_2 are non-orthogonal, we will construct a new wavefunction $\bar{\psi}_2$ that is orthogonal to ψ_1. Thus,

$$\bar{\psi}_2 = \frac{\psi_2 - S\psi_1}{\sqrt{1 - S^2}} \tag{1}$$

where

$$S = \langle \psi_1 | \psi_2 \rangle \ . \tag{2}$$

The molecular wavefunction (1) is now rewritten in terms of the orthogonal ψ_1 and $\bar{\psi}_2$ to give

$$\phi = \bar{c}_1 \psi_1 + \bar{c}_2 \bar{\psi}_2 \tag{3}$$

and the solutions are given by

$$\begin{pmatrix} \bar{H}_{11} & \bar{H}_{12} \\ \bar{H}_{21} & \bar{H}_{22} \end{pmatrix} \begin{pmatrix} \bar{c}_1 \\ \bar{c}_2 \end{pmatrix} = \lambda \begin{pmatrix} \bar{c}_1 \\ \bar{c}_2 \end{pmatrix} \tag{4}$$

where

$$\bar{H}_{11} = \langle \psi_1 | \mathcal{H} | \psi_1 \rangle = E_1$$

$$\bar{H}_{12} = \langle \psi_1 | \mathcal{H} | \bar{\psi}_2 \rangle = (H_{12} - SE_1)/\sqrt{1 - S^2}$$

$$\bar{H}_{22} = \langle \bar{\psi}_2 | \mathcal{H} | \bar{\psi}_2 \rangle = (E_2 - 2SH_{12} + S^2E_1)/(1 - S^2)$$

$$= E_2 + [S(E_1 + E_2) - 2H_{12}]\, S/(1 - S^2) \ .$$

Taking E_1 as our energy zero leads to the following expressions,

$$\bar{H}_{11} = 0$$

$$\bar{H}_{12} = H_{12}/\sqrt{1 - S^2}$$

$$\bar{H}_{22} = E_2 + [S(E_2) - 2H_{12}]\, S/(1 - S^2)$$

Figure 4. Resonance effects in vinylmethylene. Numbers based on the $^3A''$ (3π) state using equal bond lengths.

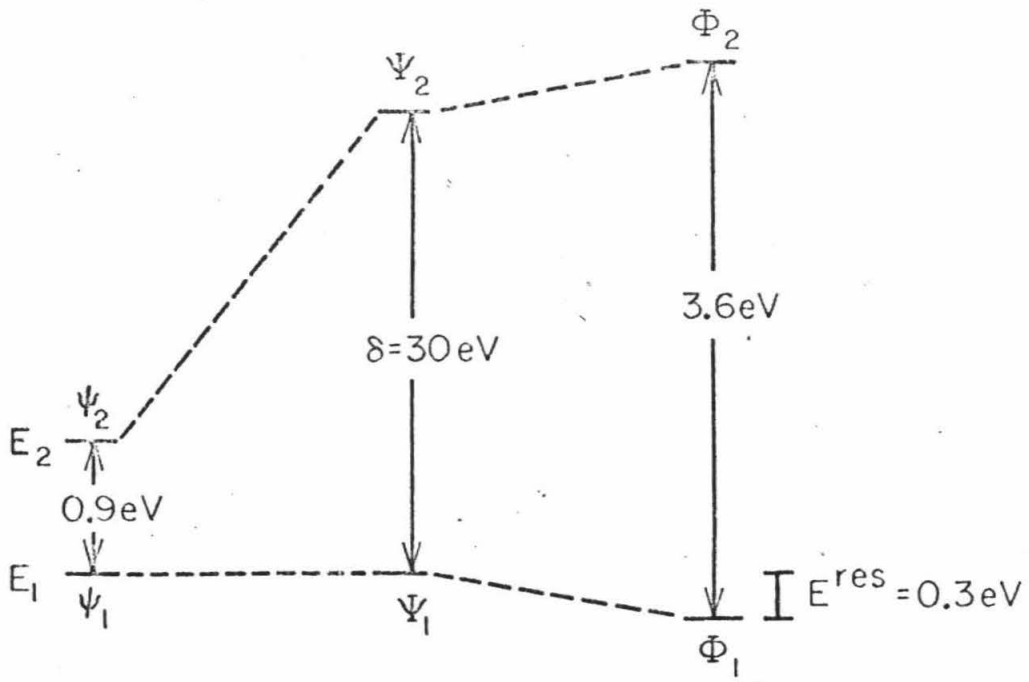
Φ_2
Ψ_2
3.6eV
δ=30eV
Ψ_2
E_2
0.9eV
E_1
Ψ_1
Ψ_1
E^{res}=0.3eV
Φ_1
Non-orthogonal Wavefunctions
Orthogonal Wavefunctions
Final Resonating Wavefunctions

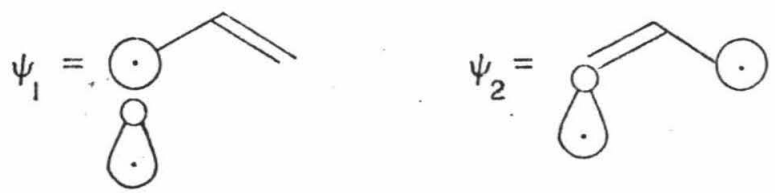
Ψ_1 =
Ψ_2 =

$$= E_2 + d$$

$$= \delta$$

where

$$d = [S(E_2) - 2H_{12}]\, S/(1 - S^2).$$

The energy E_2 now represents the difference in energy between ψ_1 and ψ_2 before orthogonalization, while the energy δ is the difference in energy between ψ_1 and $\overline{\psi}_2$ (i.e., after orthogonalization). The solutions of (4) have energies

$$\lambda = E_1 + \tfrac{1}{2}\delta \pm \sqrt{\tfrac{1}{4}\delta^2 + H_{12}^2/(1 - S^2)}\,. \qquad (5)$$

The lower energy solution uses the minus sign in (5), leading to an energy we can represent as

$$\lambda_1 = E_1 - E^{res}$$

where

$$E^{res} = -RH_{12}/(1 + S)$$

$$R = \left\{ \sqrt{\left(S + \frac{E_2}{2H_{12}}\right)^2 + (1 - S^2)} \; - \; \left(S + \frac{E_2}{H_{12}}\right) \right\} /(1 - S).$$

The quantity E^{res} is the stabilization or <u>resonance energy</u> of the state ψ_1 due to mixing in of state $\overline{\psi}_2$; R = 1 for $E_1 = E_2$ and decreases toward zero as $E_2 - E_1$ increases. The full resonance, R = 1 is obtained when $E_1 = E_2$ as for example in allyl radical.

The upper state of $\underset{\frown}{5}$ has energy

$$\lambda_2 = E_1 + \delta + E^{res}.$$

Thus in terms of the non-orthogonal functions the anti-resonance energy is

$$E^{res} + \delta - (E_2 - E_1) .$$

B. Calculation of Zero-Field Parameter D. Expanding the molecular wavefunction Φ in terms of ψ_1 and ψ_2 leads to

$$D = \langle \Phi | \mathcal{H}_D | \Phi \rangle = \langle c_1\psi_1 + c_2\psi_2 | \mathcal{H}_D | c_1\psi_1 + c_2\psi_2 \rangle$$
$$= c_1^2 \langle \psi_1 | \mathcal{H}_D | \psi_1 \rangle + c_2 \langle \psi_2 | \mathcal{H}_D | \psi_2 \rangle + 2c_1c_2 \langle \psi_1 | \mathcal{H}_D | \psi_2 \rangle .$$

Using the Mullikan approximation that

$$\langle \psi_1 | \hat{p} | \psi_2 \rangle = \tfrac{1}{2} \langle \psi_1 | \psi_2 \rangle [\langle \psi_1 | \hat{p} | \psi_1 \rangle + \langle \psi_2 | \hat{p} | \psi_2 \rangle] ,$$

for a one-electron operator $\hat{p}$,

$$D = (c_1^2 + c_1c_2S) \langle \psi_1 | \mathcal{H}_D | \psi_1 \rangle + (c_2^2 + c_1c_2S) \langle \psi_2 | \mathcal{H}_D | \psi_2 \rangle$$

where

$$S = \langle \psi_1 | \psi_2 \rangle .$$

For a totally localized wavefunction $c_1 = 1$ and $c_2 = 0$, and hence

$$D = \langle \psi_1 | \mathcal{H}_D | \psi_1 \rangle .$$

The ψ_1 and ψ_2 in the above represent the many-electron wavefunction which we found to be $S = 0.630$ for the triplet state of vinylmethylene (DZ basis, equal bond lengths). Since the overlap of the singly-occupied π orbital of ψ_1 with the singly-occupied π orbital of ψ_2 is 0.631, we can consider ψ_1 as the product of $\sigma\pi_\ell$ and ψ_2 as $\sigma\pi_r$, and hence the use of the Mullikan approximation seems justified.

Table I. Total Energies for Vinylmethylene for Various Wavefunctions. Energies in atomic units, 1 h = 27.2116 eV.

Wave-function	Basis	States					
		Geometries			Energies		
		$^3A''$	$^1A''$	$^1A'$	$^3A''$	$^1A''$	$^1A'$
HF	DZ	5	5	5	-115.77162	-115.74380	-115.73399
GVB(2)	DZ	5	5	5	-115.78984	-115.76500	-115.76939
GVB(2) - CI	DZ	5	5	5	-115.81669	-115.77557	-115.77317
GVB(2)	DZ	-	3	6	--	-115.78055	-115.77826
GVB(2) - CI	DZ	-	3	6	--	-115.78780	-115.78228
HF	DZD	4	3	6	-115.81458	-115.79666	-115.78991
GVB(2)	DZD	4	3	6	-115.83625	-115.81935	-115.83144
GVB(2) - CI	DZD	4	3	6	-115.85135	-115.82981	-115.83804
GVB(4)	DZD	4	3	6	-115.85975	-115.84327	-115.85538
SOGVB(4)	DZD	4	3	-	-115.86579	-115.84332	--
GVB(4) - CI	DZD	4	3	6	-115.90144	-115.87908	-115.88271

References

(1) This work was supported by a John and Beverly Stauffer Foundation Fellowship, 1975-1976.

(2) See J. H. Davis, W. A. Goddard III, and R. G. Bergman, J. Am. Chem. Soc., 98, 4015 (1976) for preliminary communication.

(3) E. J. York, W. Dittmar, J. R. Stevenson, and R. G. Bergman, J. Am. Chem. Soc., 94, 2882 (1972); 95, 5681 (1973).

(4) W. A. Goddard III, T. H. Dunning, Jr., W. J. Hunt and P. J. Hay, Accts. Chem. Res., 6, 368 (1973).

(5) T. H. Dunning, Jr., J. Chem. Phys., 53, 2823 (1970).

(6) P. J. Hay, W. J. Hunt, and W. A. Goddard III, Chem. Phys. Lett., 13, 30 (1972).

(7) P. H. Kasai, R. J. Meyers, D. F. Eggers, and K. B. Wiberg, J. Chem. Phys., 30, 512 (1959).

(8) L. Salem and W. Stroher (private communication) optimized the geometry for the $^1A'$ state using the Hartree-Fock wavefunction and an STO-36 basis set.

(9) L. B. Harding and W. A. Goddard III, J. Am. Chem. Soc., 97, 6293 (1975); 97, 6300 (1975).

(10) L. B. Harding and W. A. Goddard III, J. Am. Chem. Soc., (in press).

(11) F. W. Bobrowicz, Ph. D. Thesis, California Institute of Technology, 1974.

(12) G. Levin and W. A. Goddard III, J. Am. Chem. Soc., 97, 1649 (1975).

(13) R. W. Fessendon and R. H. Schuler, J. Chem. Phys., 39, 2147 (1963).

(14) L. B. Harding and W. A. Goddard III, unpublished results.

(15) Hybridization was calculated using Mullikan population analysis of GVB orbitals.

(16) R. S. Hutton, M. L. Manion, H. D. Roth, and E. Wasserman, J. Am. Chem. Soc., 96, 4680 (1974).

(17) a) O. L. Chapman, Pure Appl. Chem., 511 (1975);
b) O. L. Chapman, M. Chedekel, N. Rosenquist, R. S. Sheridan, J. Pocansky, and R. Roth, private communication.

(18) a) E. Wasserman, V. J. Kuck, R. S. Hutton, and W. A. Yager, J. Am. Chem. Soc., 92, 7491 (1970);
b) J. F. Harrison, Accts. Chem. Res., 7, 378 (1974).

(19) These energies were evaluated by using the $^3A''$ (3π) orbitals in the singlet wavefunction leading to an energy increase of 0.9 eV which we identify as $K_{\sigma\pi}$ for 4 and by using the $^1A''$ (3π) orbitals in the triplet wavefunction leading to an energy decrease of 0.05 eV which we identify as $K_{\sigma\pi}$ for 3.

(20) Inclusion of p basis functions on the hydrogen and much more extensive correlation effects lead to an increase in the triplet-singlet separation in CH_2 to 16 Kcal. Recent experimental results[21] lead to 19 Kcal. For vinylmethylene, these effects should be smaller, and we expect that the $^3A''$ (3π) - $^1A''$ (3π) separation will be unchanged, while the $^3A''$ (3π) - $^1A'$ (2π)

separation may increase by 3 Kcal.

(21) P. F. Zittel, G. B. Ellison, S. V. ONeil, E. Herbst, W. C. Lineberger, and W. P. Reinhardt, J. Am. Chem. Soc., 98, 3731 (1976).

PART B: ELECTRONIC STATES OF TRIMETHYLENEMETHANE[1]

I. Introduction

Trimethylenemethane 1 has been a subject of much theoretical discussion since the work of Moffitt.[2] Only recently, however, has the molecule become a subject of serious experimental and theoretical work. In 1966, Dowd[3] reported the first preparation of 1 from the pyrolysis of the pyrazoline system 2:

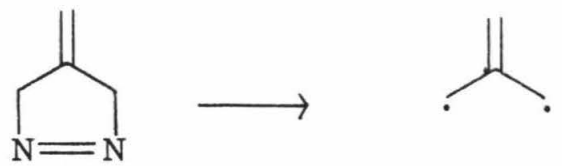

1 2

The early work of Dowd has been summarized in a review article[4] and will not be discussed. In 1971, Berson[5] prepared the trimethylenemethane diyl analog 3 from the diazo compound 4, and extensive research has been conducted since then. Early esr experiments showed 3 to have a triplet ground state, and CIDNP studies showed the dimerization of 3 had to include at least one triplet reactive species.

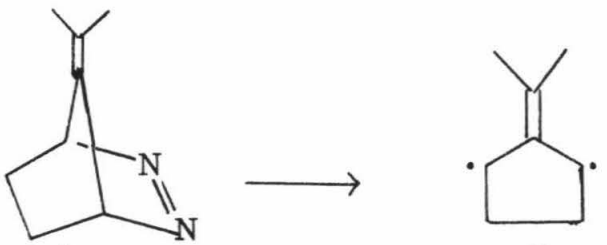

4 3

Additional studies[6-9] have shown that at least two distinct electronic states are involved in the pyrolysis of the diazo precursor 4. Berson has postulated that the two reactive species are a bisected singlet 5

and a planar triplet 6.

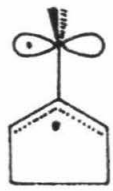

5

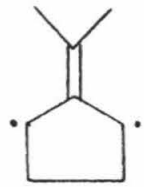

6

Previous theoretical studies on trimethylenemethane diradical 1 have led to contradictory results. Most workers agree that for the planar geometry the lowest state is a triplet state; however, calculations of the lowest planar singlet state lead to energies of 21,[10] 68,[10] and 70[11] kcal/mole from ab initio Hartree-Fock (HF) wavefunctions and 35 and 57 kcal/mole[12] from semi-empirical Hartree-Fock wavefunctions. Part of the problem here is a special difficulty with spatial symmetry for the Hartree-Fock wavefunction of the lowest singlet state.[13]

We report here the results of ab initio configuration interaction (CI) calculations based on generalized valence bond[14] (GVB) wavefunctions of both the planar (1) and the bisected (7) geometries of

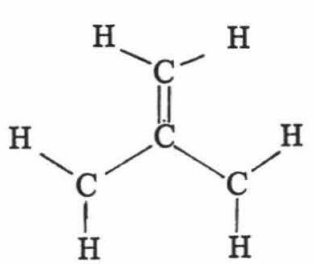

1

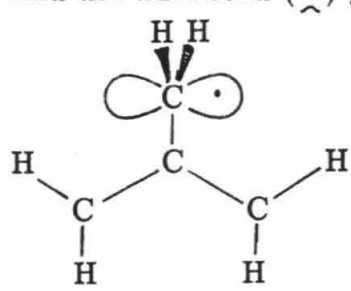

7

trimethylenemethane which eliminate the above difficulties and provide a description of the other excited states, including the transition

oscillator strengths. A summary of these results was communicated earlier.[15]

II. Calculational Details

For all calculations, a contracted Gaussian basis set equivalent to a double-zeta (DZ) basis was used. For carbon, Dunning's contraction[16] (3s,2p) of Huzinaga's (9s,5p) basis set was utilized, while for hydrogen a comparable (4s/2s) contraction was used with each Gaussian exponent multiplied by a scale factor of 1.44 corresponding to a Slater exponent of $\zeta = 1.2$.

Our objective in these studies was to establish the overall character of the states of planar and bisected trimethylenemethane. Hence we have used a geometry of each form roughly appropriate for the ground state: C–C bond lengths of 1.40 Å, CH bond lengths of 1.086 Å and bond angles of 120°. Since these geometries are roughly appropriate for the ground state, we obtain vertical excitation energies and ionization potentials. Geometry optimization would be particularly important for the rotation barriers.

In the GVB calculations the π bond pair of the triplet state was correlated with all orbitals described as symmetry functions (for the appropriate symmetry group). For the planar configuration this led to four occupied π orbitals. In the configuration interaction (CI) calculations for the planar case,a full CI was carried out over these four orbitals plus the four remaining (virtual) π orbitals for the DZ basis. Thus the ground state sigma orbitals were used for all excited

and ion states. This is adequate for the valence excited states and reasonably adequate for the lower ion states.

For the bisected configuration this GVB calculation leads to four non-closed shell orbitals, three π and one σ. For the CI this was supplemented with three additional π and one additional σ (virtual) functions obtained by starting with the most diffuse π function on each of the three unrotated carbons plus the corresponding σ-like orbital in the rotated carbon and orthogonalizing to all original orbitals. In additional CI calculations including single excitations from the combination of CH orbitals on the rotated carbon, we concluded that such excitations are unimportant.

All HF and GVB calculations were carried out with Bobrowicz-Wadt-Goddard program[17] using the fully self-consistent techniques of Hunt, Hay and Goddard.[18] The CI calculations were carried out with the Caltech CI porgram (Bobrowicz, Winter, Ladner, Moss, Harding, Walch, and Goddard).[19]

III. Results

The ground state energies for the planar and bisected geometries of trimethylenemethane were calculated using HF, GVB, and GVB-CI wavefunctions. These results are shown in Table I.

The results of CI calculations on the excited states are presented in Tables II and III where we have also listed the dominant configurations for each state. Because of the use of the GVB orbitals there are few dominant configurations.

Table I. Total Energies for the Ground State of Trimethylenemethane (Hartrees)

State	HF	GVB	GVB-CI
$^3A_2$ (planar)	-154.82362	-154.83639	-154.87378
$^3B_1$ (bisected)	-154.79619	-154.81169	-154.84478

Table II. Excitation Energies and Dominant Configurations for Planar Trimethylenemethane [GVB-CI]. All configurations contributing more than 0.010 hartree = 6.275 kcal/mole are included.

State Symmetry		Excitation Energy	Configuration[a]								Energy Lowering[b]
D_{3h}	C_{2v}	(kcal/mole)	$\pi_1(a_2'')$	$\pi_2(e_y'')$	$\pi_3(e_x'')$	$\pi_4(e_y'')$	$\pi_5^*(a_2'')$	$\pi_6^*(a_2'')$	$\pi_7^*(e_x'')$	$\pi_8^*(e_y'')$	(hartree)
$^1A_2'$	$^1B_2$	0.0	2	0	1	1	0	0	0	0	--
			1	1	1	1	0	0	0	0	0.036
			0	2	1	1	0	0	0	0	0.013
$^1E'$	$^1B_2$	26.4	2	0	1	1	0	0	0	0	--
			1	0	2	1	0	0	0	0	0.060
			2	1	0	1	0	0	0	0	0.043
	$^1A_1$	26.4	2	0	2	0	0	0	0	0	--
			2	0	0	2	0	0	0	0	--
			1	0	1	2	0	0	0	0	0.061
			2	1	1	0	0	0	0	0	0.043
$^3E'$	$^3B_2$	107.6	1	0	2	0	0	0	0	0	--
			2	1	0	1	0	0	0	0	0.089
			1	1	1	1	0	0	0	0	0.049
			2	0	0	1	1	0	0	0	0.021
			0	1	2	1	0	0	0	0	0.015
			1	2	0	1	0	0	0	0	0.015
	$^3A_1$	107.6	1	0	1	2	0	0	0	0	--
			2	1	1	0	0	0	0	0	0.089
			1	1	0	2	0	0	0	0	0.029
			1	1	2	0	0	0	0	0	0.029
			2	0	1	0	1	0	0	0	0.021
			0	1	1	2	0	0	0	0	0.015
			1	2	1	0	0	0	0	0	0.015
$^1A_1'$	$^1A_1$	125.4	0	0	2	2	0	0	0	0	--
			2	0	0	2	0	0	0	0	0.015
			2	0	2	0	0	0	0	0	0.015
$^3A_1'$	$^3A_1$	195.9	2	1	1	0	0	0	0	0	--
			2	0	1	0	1	0	0	0	0.036
			1	0	1	2	0	0	0	0	0.013

[a] The first four orbitals are the GVB orbitals while the last four are the remaining (virtual) pi orbitals for the DZ basis.

[b] The energy increase upon deleting this configuration from the wavefunction.

Table III. Excitation Energies and Dominant Configurations for Bisected Trimethylenemethane [GVB-CI]. All configurations contributing more than 0.010 hartree = 6.275 kcal/mole are included.

State Symmetry C_{2v}	Excitation Energy (kcal/mole)	Configuration $o(b_2)$	$\pi_1(b_1)$	$\pi_2(b_1)$	$\pi_3(a_2)$	$\sigma_2^*(b_2)$	$\pi_4(b_1)$	$\pi_5(b_1)$	$\pi_6(a_2)$	Energy Lowering
$^3B_1$	18.2	1	2	0	1	0	0	0	0	--
		1	1	1	1	0	0	0	0	0.023
		1	0	2	1	0	0	0	0	0.017
$^1A_1$	139.0	2	2	0	0	0	0	0	0	--
		1	2	0	0	1	0	0	0	0 043
		2	0	0	2	0	0	0	0	0.026
		2	1	1	0	0	0	0	0	0.011
$^3B_1$	155.6	1	1	1	1	0	0	0	0	--
		1	1	0	1	0	0	0	0	0.025
$^1A_1$	160.1	0	2	0	2	0	0	0	0	--
		0	2	2	0	0	0	0	0	0.016
		0	1	1	2	0	0	0	0	0.011
$^1B_1$	20.2	1	2	0	1	0	0	0	0	--
		1	1	1	1	0	0	0	0	0.025
		1	0	2	1	0	0	0	0	0.017
$^3A_2$	98.7	1	1	0	2	0	0	0	0	--
		1	2	1	0	0	0	0	0	0.11
		1	1	2	0	0	0	0	0	0.026
		1	0	1	2	0	0	0	0	0.024
$^1A_2$	99.9	1	1	0	2	0	0	0	0	--
		1	2	1	0	0	0	0	0	0.11
		1	1	2	0	0	0	0	0	0.026
		1	0	1	2	0	0	0	0	0.025
		1	2	0	0	0	0	1	0	0.011

The CI results for the lower ion states of planar and bisected trimethylenemethane are shown in Tables IV and V.

In Table VI we compare our results to those of previous workers. Our numbers are in good agreement with the HF calculations of Yakony and Schaefer[10]. (We avoided the ambiguity in the energy of the $^1E'$ state by carrying out CI.) The early HF calculations by Hehre et al.[11] and Mindo calculations by Dewar[12] led to excitation energies high by a factor of two.

IV. Qualitative Description

First we will consider the excited states of the planar geometry. Given four orbitals each with one electron, we can form six states (referred to as covalent or valence states): two singlets, three triplets, one quintet. The quintet state is expected to be of high energy and was not calculated.

The ground state triplet, $^3A_2'$ can best be described with the three outer orbitals high-spin coupled ($S = \frac{3}{2}$) and the central carbon orbital low-spin coupled to all three (leading to $S = 1$):

$^3A_2'$ = 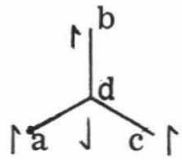 = 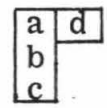 (1)

(See Appendix for the precise expansion of the wavefunction).[20] Rotating, say, the upper CH_2 group to the bisected form leads to a loss of bonding between centers b and d and hence to a higher energy (by

Table IV: Ionization Potentials and Dominant Configurations for Planar Tetrethylenemethane [CVTE-CI]. All configurations contributing more than 0.010 hartree (~6.275 kcal/mole) are included.

State Symmetry		Excitation Energy	Configuration								Energy Lowering
D_{3h}	C_{2v}	(eV)	$\pi_1(a_2'')$	$\pi_2(a_2'')$	$\pi_3(e_x'')$	$\pi_4(e_y'')$	$\pi_5^*(a_2'')$	$\pi_6^*(a_2'')$	$\pi_7^*(e_x'')$	$\pi_8^*(e_y'')$	(hartree)
$^2E''$	$^2B_1$	8.30	2	0	0	1	0	0	0	0	--
			1	0	1	1	0	0	0	0	0.028
			0	0	2	1	0	0	0	0	
$^2E''$	$^2A_2$	8.30	2	0	1	0	0	0	0	0	--
			1	0	2	0	0	0	0	0	0.016
			1	0	0	2	0	0	0	0	0.016
			0	0	1	2	0	0	0	0	0.013
$^4A_1''$	$^4B_1$	11.30	1	0	1	1	0	0	0	0	--
			0	0	1	1	0	0	0	1	0.006
$^2A_1''$	$^2A_2$	12.41	2	1	0	0	0	0	0	0	--
			2	0	0	0	1	0	0	0	0.033
			1	0	0	2	0	0	0	0	0.018
			1	0	2	0	0	0	0	0	0.018
			1	2	0	0	0	0	0	0	0.012
			0	1	0	2	0	0	0	0	0.012
			0	1	2	0	0	0	0	0	0.012
$^2E''$	$^2B_1$	14.12	1	0	1	1	0	0	0	0	--
			1	1	0	1	0	0	0	0	0.060
			0	0	2	1	0	0	0	0	0.013
			2	0	0	1	0	0	0	0	0.012
			0	1	1	1	0	0	0	0	0.011
$^2E''$	$^2A_2$	14.12	1	0	2	0	0	0	0	0	--
			1	0	0	2	0	0	0	0	0.070
			1	1	1	0	0	0	0	0	0.060
			0	0	1	2	0	0	0	0	0.013
			2	0	1	0	0	0	0	0	0.012
$^2A_2''$	$^2B_1$	14.45	1	0	1	1	0	0	0	0	--
			0	1	1	1	0	0	0	0	

Table V. Ionization Potentials and Dominant Configurations for Bi-ected Trimethylenemethane [GVB-CI]. All configurations contributing more than 0.010 hartree = 6.275 kcal/mole are included.

State Symmetry C_{2v}	Excitation Energy	Configurations								Energy Lowering (hartree)
		$\sigma(b_2)$	$\pi_1(b_2)$	$\pi_2(b_1)$	$\pi_3(a_2)$	$\sigma_2^*(b_2)$	$\pi_4(a_1)$	$\pi_5(b_1)$	$\sigma(a_2)$	
$^2B_2$	8.89	1	2	0	0	0	0	0	0	--
		1	0	0	2	0	0	0	0	0.019
$^2A_2$	10.55	0	2	0	1	0	0	0	0	--
		0	1	1	1	0	0	0	0	0.035
		0	0	2	1	0	0	0	0	0.016
$^4A_1$	11.65	1	1	0	1	0	0	0	0	--
		1	1	0	0	0	0	0	1	0.006
$^2B_1$	14.03	0	2	1	0	0	0	0	0	--
		0	1	0	2	0	0	0	0	0.094
		0	0	1	2	0	0	0	0	0.040
		0	1	2	0	0	0	0	0	0.013
		0	2	0	0	0	0	1	0	0.013
$^2B_2$	16.90	1	1	1	0	0	0	0	0	--
		1	1	0	0	0	0	1	0	0.013

Table VI. Excitation Energy for Various Calculations

			Dewar and Wasson[a] (MINDO/2)	Hehre, Salem and Willcott[b] (HF-CI)	Yarkony and Schaefer[c] (HF)	Davidson and Borden[d] (HF)	This Work (GVB-CI)
Planar	$^3A_2'$		0.0	0.0	0.0 (-154.8252h)	0.0 (-152.9654h)	0.0 (-154.87378h)
	$^1E'$	D_{3h}	-	70.4	68.6		-
		C_{2v}[e]	36, 57	-, -	212, -	26.2, 116.3	26.4, 26.4
	$^1A_1$		-		128.8	123.5	125.4
Bisected	$^3B_1$		9	-	16.9	-	18.2
	$^1B_1$		12	18.3	18.5	-	20.2

[a]Ref. 12.

[b]Ref. 11, total energy not reported.

[c]Ref. 10

[d]Ref. 13. Note this work also reported the results of full π-CI on the $^1E'$ state resulting in a degenerate state.

[e]The two values correspond to the $^1B_2$ and $^1A_1$ components in sequence.

Figure 1. Electronic states of trimethylenemethane (energies in kcal mole^{-1}).

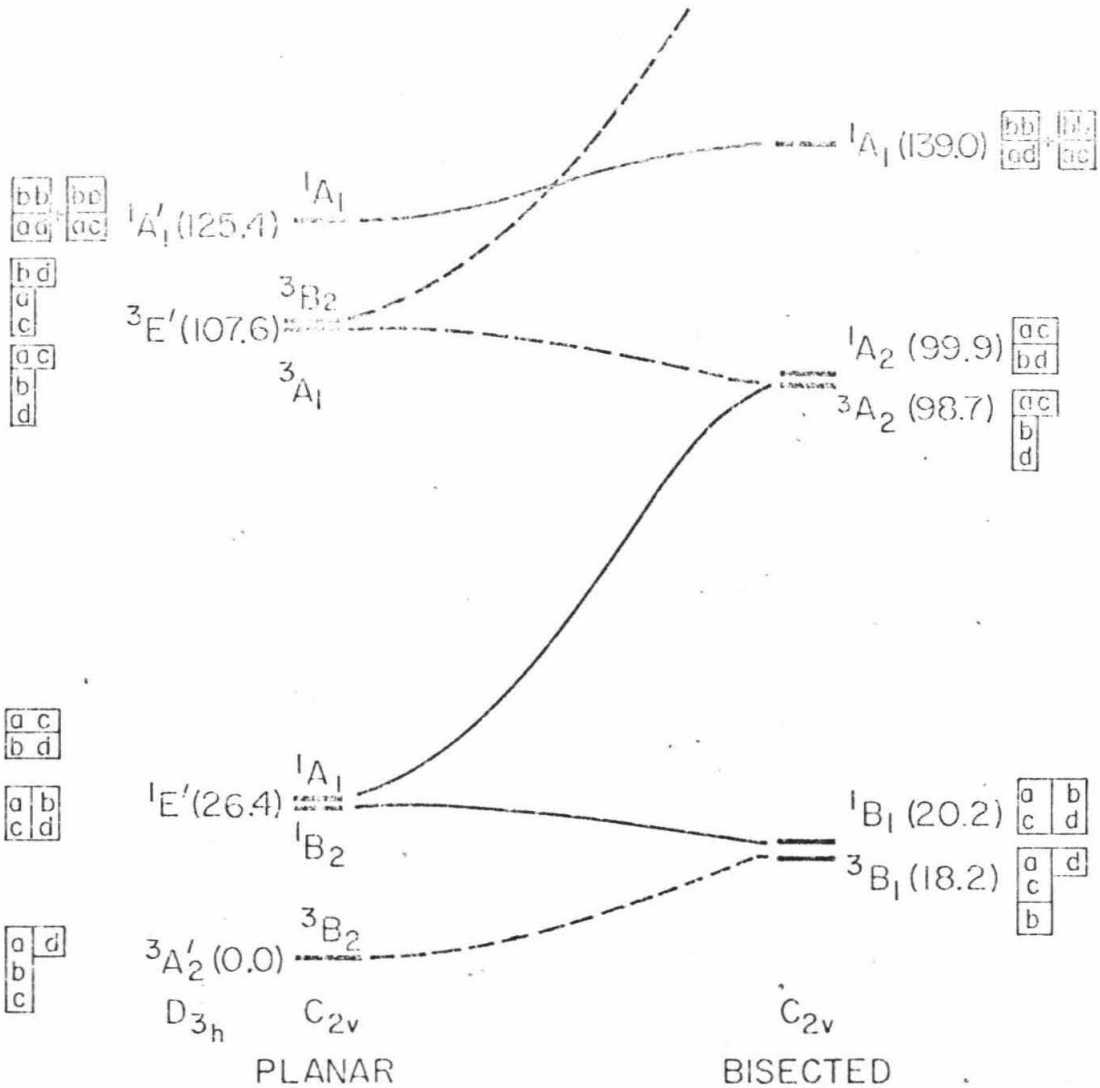

GEOMETRY

TRIMETHYLENEMETHANE

18.2 kcal mole^{-1}) as indicated in Figure 1.

The other two valence triplet states are degenerate, $^3E'$, lying 107.6 kcal mole^{-1} above the ground state. These states can each be represented as the singlet coupling of two orbitals and triplet pairing of the other two:

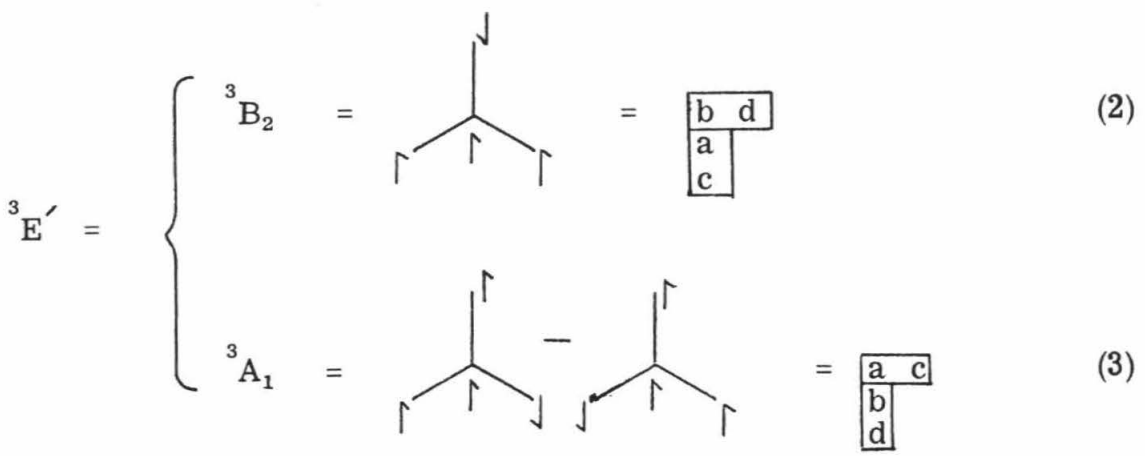

Notice that the $^3B_2$ state (2) has a bonding interaction between centers b and d, while the $^3A_1$ state (3) has an antibonding interaction between these centers. As a consequence,rotation of the upper methylene group leads to a lowering of energy for the $^3A_1$ state (by 8.9 kcal) and a raising of energy for the $^3B_2$ state (by 48.0 kcal).

Turning to the planar singlet states, we find two degenerate states 26.4 kcal/mole about the triplet ground state. These can be represented, respectively, as either the coupling of b and d into a triplet, the coupling of a and c into a triplet and then the coupling of these two pairs into an overall singlet state

$^1B_2$ = 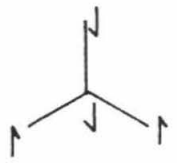 =  (4)

or as the coupling of b and d into a singlet, the coupling of a and c into a singlet and then the coupling of these two pairs into an overall singlet state.

$^1A_1$ = 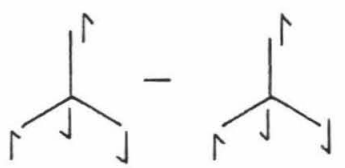 =  (5)

Examining the net bonding-antibonding interactions, we see that both states have two bonding and one antibonding interactions and hence should be degenerate. Rotating the upper methylene group to the bisected form removes a repulsive triplet pairing for $^1B_2$ (4), stabilizing this state by 6.2 kcal, but removes an attractive singlet pairing for $^1A_1$ (5), destabilizing this state by 73.3 kcal. These changes parallel the changes in the triplet case.

Thus the overall picture for the five valence states for planar trimethylenemethane is summarized in Figure 1.

Now we will examine the excited states of the bisected trimethylenemethane. Considering the bisected trimethylenemethane to be the union of the pi system of allyl radical with the sigma radical orbital of methyl radical

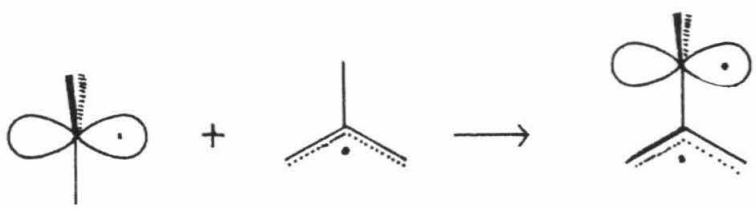

allows us to build up the excited states as follows.

The ground state of allyl has the form (6)

$^3A_2$ = 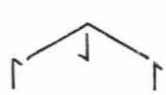 =  (6)

(corresponding to the resonance form ), leading to $^2A_2$ (π^3) symmetry. Combining this with the in-plane sigma p-orbital [$^2B_2$ (σ) symmetry] leads to $^3B_2$ ($\sigma\pi^3$) (7) and $^1B_1$ ($\sigma\pi^3$) (8) states

$^3B_1$ = 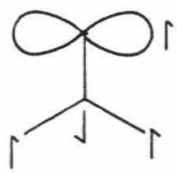 = 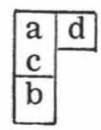 (7)

$^1B_1$ = 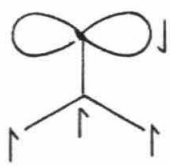 = 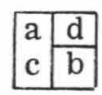 (8)

that should be nearly degenerate (separated by a two-center $\sigma\pi$ exchange integral). As expected, we find a $^3B_1$ ground state for the bisected geometry with the $^1B_1$ excited state lying 1.8 kcal/mole^{-1} higher in energy. Rotating the upper methylene group to the planar form leads to a bonding interaction for $^3B_1$, stabilizing the state, and leads to an anti-bonding interaction for $^1B_1$, destabilizing this state.

The first excited state of allyl is the antiresonant state

(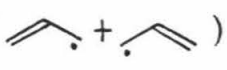)

$^2B_1$ = 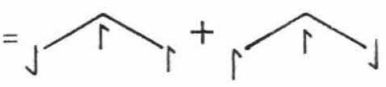 =  (9)

which is $^2B_1$ symmetry and lies 3.2 eV[21] above the resonant state (6). Combining this anti-resonant form of allyl with the sigma p-orbital ($^2B_2$) leads to the $^3A_2$ (10) and $^1A_2$ (11) states

$^3A_2$ = 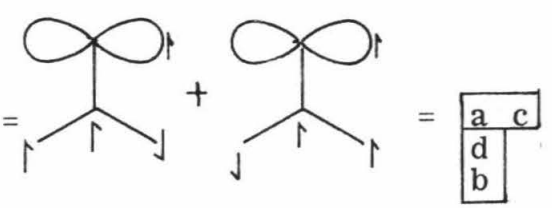 = (10)

$^1A_2$ = 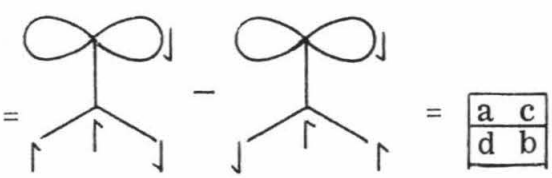 = (11)

which should be ~3.2 eV above the $^{3,1}B_1$ states and nearly degenerate (separated by a two center $\sigma-\pi$ exchange integral). In fact we find the $^3A_2$ and $^1A_2$ states at 3.3 eV above the $^3B_1$ ground state with a triplet-singlet splitting of only 1.2 kcal/mole^{-1}. Rotating the upper methylene group to the planar geometry destabilizes the $^3A_2$ while stabilizing the $^1A_2$ state. These results are shown in Figure 1 .

Summarizing the above discussion, we find that the states correlate as shown in Figure 1.

Additional excited states are also given in Tables II and III . Since our basis does not contain diffuse basis functions, these states must be of ionic (zwitterionic) character. For such states one would expect significant changes in the sigma orbitals and hence our energies should be significantly too high.

The cation states can be easily understood in terms of the above description. Ionization of one of the unpaired π-electrons in the planar $^3A_2'$ ground state results in a degenerate pair of doublet states ($^2E''$) lying at 8.3 eV. Rotation of a methylene group splits the degeneracy of the states leading to a $^2B_2$ ion at 8.9 eV and a $^2A_2$ ion at 10.6. The $^2B_2$ state has a $\sigma\pi^2$ configuration in which the π-system is an allylic cation; the higher energy $^2A_2$ ion has the charge localized on the rotated methylene. Ionization of a bonding π-electron leads to three different planar states: a $^4A_2''$ at 11.3 eV, and two doublets, $^2E''$ and $^2B_1$, at 14.1 and 14.5 eV, respectively. Once again rotating the methylene group to the bisected form raises the energy, since we decrease the delocalization. Other ion states involving simultaneous ionization and excitation are listed in Tables IV and V.

V. Comparison to Experiment

A. Spectroscopic Data. Thus far little spectroscopic data have yet been reported (Berson and Platz[22] are attempting to observe these transitions in the low-temperature ultraviolet spectrum). For comparison with future experimental results we have calculated the intensities of the various transitions as shown in Table VII.

For the planar geometry we calculated that the vertical transition energy from ground state $^3A_2'$ to $^3E'$ ($^3B_2$ and $^3A_1$) corresponds to λ_{max} = 266 nm with an oscillator strength of $f = 1.7 \times 10^{-3}$. For the bisected geometry we find that the first vertical transition energy from the lowest singlet state ($^1A_2 \leftarrow {}^1B_1$) corresponds to λ_{max} = 359 nm with $f = 7.9 \times 10^{-4}$. For the planar geometry the first absorption of the singlet state is calculated as λ_{max} = 289 nm with f = 0.10 This planar singlet state, however, may be too short-lived for sufficient population to observe the transition in absorption experiments.

On the basis of the ionization potentials Rydberg transitions are expected at ~4.6 to 4.9 eV (270 to 250 nm) [$^3A_2' \rightarrow {}^3E''$ (3s)] and ~5.6 to 6.7 eV (220 to 200 nm) [$^3A_2' \rightarrow {}^3E'$ (3p)]. Since we did not include diffuse basis functions, we have not calculated these states directly.

B. Pyrolysis. The pyrolysis date of Berson[5-8] corresponds qualitatively to the energy surface as we have calculated. We expect that the pyrolysis of the diazo compound 4 gives planar excited singlet ($^1E_1$); the $^1B_2$ component quickly undergoes methylene rotation to give the bisected $^1B_1$. This singlet then intersystem crosses to give the $^3B_1$ state which quickly rotates to the $^3A_2'$ ground state. Thus, since

Table VII. Transition Strengths

Geometry	Transition	Transition Energy (nm)	Dipole Matrix Element (a.u.)	f
Planar	$1\,^3A_2' \rightarrow 2\,^3E$	266	0.08638	1.7×10^{-3}
	$1\,^3A_2' \rightarrow 2\,^3A_2'$	146	-1.54566	5.0×10^{-1}
	$1\,^1E' \rightarrow 1\,^1A_2$	289	1.40141	1.0×10^{-1}
Bisected	$1\,^1B_1 \rightarrow {}^1A_2$	359	0.09641	7.9×10^{-4}

intersystem crossing might be slow compared to trapping of the diradical, we believe that the reactive species observed by Berson are the planar $^3A_2'$ and the bisected $^1B_1$.

A possibly significant difference between $\underset{\frown}{1}$ and $\underset{\frown}{3}$ is that the lowest ^1E state of $\underset{\frown}{1}$ splits into two nondegenerate states ($^1A_1$ and $^1B_2$) of $\underset{\frown}{4}$. Of these, the $^1A_1$ state seems more likely formed. If $^1A_1$ is lower than $^1B_2$ for the planar geometry (only the $^1B_2$ states prefers twisting to the bisected form), the $^1A_1$ state may live long enough to do some chemistry or to convert (intersystem cross) directly to the lower triplet state. In this circumstance there could be three reactive forms of trimethylenemethane (planar $^3B_2$ and $^1A_1$ and bisected $^1B_2$). With proper substituents on $\underset{\frown}{3}$ it may be possible to stabilize planar $^1A_1$ lower than bisected $^1B_2$ so that all the chemistry would involve the two planar states. Such possibilities could be probed by observing the absorptions at 266 nm (planar $^3B_2$), 359 nm (bisected $^1B_1$), and 289 nm (planar $^1A_1$) as a function of reaction conditions and time for various substituents.

C. Photoionization. Thus far photoionization experiments have not been reported. Starting with the planar triplet state the prominent vertical photoionization potentials are calculated to be 8.3 eV to $^2E''$, 14.1 eV to $^2E''$ and 14.5 eV to $^2A_2''$. Other cation states involve excitation simultaneous with ionization.

Starting with the bisected singlet state $^2B_1$, the prominent IP's are 10.6 eV for ionizing the σ orbital and 10.6 and 17.0 eV for ionizing a π orbital.

Starting with the component of planar ^1E that could be stable for planar geometries the IP's are 8.3 and 14.12 eV.

VI. Summary

Our calculations predict that the ground state of trimethylenemethane is the planar triplet with the planar singlet state 26 Kcal/mole higher. The rotational barrier for the triplet state is 18 Kcal/mole, while one component of the planar singlet prefers the bisected geometry by 7 Kcal/mole. We predict the transitions for the chemically interesting states as follows: planar triplet: λ_{max} = 266 nm with f = 0.002; bisected singlet: λ_{max} = 359 nm with f = 0.0008; and planar singlet: λ_{max} = 289 nm with f = 0.10. The vertical ionization potential is calculated at 8.3 eV.

Appendix

The tableaux representation used in Section IV describes the precise coupling of orbitals and spins for each wavefunction. Two orbitals in a horizontal box indicate that the orbitals are singlet coupled

$$\boxed{a\ b} \equiv \mathcal{A}[\phi_a \phi_b (\alpha\beta - \beta\alpha)]$$

while two orbitals in vertical boxed indicate that the orbitals are high-spin or triplet coupled.

$$\begin{array}{|c|}\hline a \\ \hline b \\ \hline \end{array} \equiv \mathcal{A}[\phi_a \phi_b (\alpha\beta + \beta\alpha)]$$

The cases used in this paper are:

$$\begin{array}{|c|c|}\hline a & c \\ \hline b \\ \cline{1-1} \end{array} \equiv \mathcal{A}\{\phi_a \phi_b \phi_c [\alpha\alpha\beta - \tfrac{1}{2}(\alpha\beta + \beta\alpha)\alpha]\}$$

$$\begin{array}{|c|c|}\hline a & c \\ \hline b \\ \cline{1-1} \end{array} \equiv \mathcal{A}\{\phi_a \phi_c \phi_b (\alpha\beta - \beta\alpha)\alpha\}$$

$$\begin{array}{|c|c|}\hline a & c \\ \hline b & d \\ \hline \end{array} \equiv \mathcal{A}\{\phi_a \phi_b \phi_c \phi_d [\alpha\alpha\beta\beta + \beta\beta\alpha\alpha - \tfrac{1}{2}(\alpha\beta + \beta\alpha)(\alpha\beta + \beta\alpha)]\}$$

$$\begin{array}{|c|c|}\hline a & c \\ \hline b & d \\ \hline \end{array} \equiv \mathcal{A}\{\phi_a \phi_c \phi_b \phi_d (\alpha\beta - \beta\alpha)(\alpha\beta - \beta\alpha)\}$$

$$\begin{array}{|c|c|}\hline a & d \\ \hline b \\ \cline{1-1} c \\ \cline{1-1} \end{array} \equiv \mathcal{A}\{\phi_a \phi_d \phi_b \phi_c (\alpha\beta - \beta\alpha)(\alpha\beta + \beta\alpha)\}$$

$$\begin{array}{|c|c|}\hline a & d \\ \hline b \\ \cline{1-1} c \\ \cline{1-1}\end{array} \equiv \mathcal{A}\{\phi_a \phi_b \phi_c \phi_d [\alpha\alpha\alpha\beta - \tfrac{1}{3}(\alpha\alpha\beta + \alpha\beta\alpha + \beta\alpha\alpha)\alpha]\}$$

$$\begin{array}{|c|c|}\hline a & c \\ \hline b \\ \cline{1-1} d \\ \cline{1-1}\end{array} \equiv \mathcal{A}\{\phi_a \phi_b \phi_c \phi_d [\alpha\alpha\beta\alpha - \tfrac{1}{2}(\alpha\beta + \beta\alpha)\alpha\alpha]\}$$

References

(1) This work was supported by a John and Beverly Stauffer Foundation Fellowship, 1975-1976.

(2) C. A. Coulson, J. Chim. Phys. Physicochim. Biol., 45, 243 (1948).

(3) P. Dowd, J. Am. Chem. Soc., 88, 2587 (1966).

(4) P. Dowd, Accts. Chem. Res., 5, 242 (1972).

(5) J. A. Berson, R. J. Bushby, J. M. McBride, and M. Tremelling, J. Am. Chem. Soc., 93, 1545 (1971).

(6) J. A. Berson, L. R. Corwin, and J. H. Davis, J. Am. Chem. Soc., 96, 6177 (1974).

(7) J. A. Berson, D. M. McDaniel, L. R. Corwin, and J. H. Davis, J. Am. Chem. Soc., 94, 5508 (1972).

(8) J. A. Berson, L. R. Corwin, and C. D. Duncan, J. Am. Chem. Soc., 96, 6175 (1974).

(9) J. A. Berson, D. M. McDaniel, and L. R. Corwin, J. Am. Chem. Soc., 94, 5509 (1972).

(10) D. R. Yarkony and H. F. Schaefer III, J. Am. Chem. Soc., 96, 3754 (1974).

(11) W. J. Hehre, L. Salem, and M. R. Wilcott, J. Am. Chem. Soc., 96, 4328 (1974).

(12) M. J. S. Dewar and J. S. Wasson, J. Am. Chem. Soc., 93, 3081 (1971).

(13) W. T. Borden, J. Am. Chem. Soc., 97, 2906 (1975).

(14) W. A. Goddard III, T. H. Dunning, Jr., W. J. Hunt, and P. J. Hay, Accts. Chem. Res., 6, 368 (1973).

(15) J. H. Davis and W. A. Goddard III, J. Am. Chem. Soc., 98, 303 (1976).

(16) T. H. Dunning, Jr., private communication.

(17) F. W. Bobrowicz, Ph.D. Thesis, California Institute of Technology, 1974.

(18) W. J. Hunt, P. J. Hay, and W. A. Goddard III, J. Chem. Phys., 57, 738 (1972).

(19) R. C. Ladner, Ph.D. Thesis, California Institute of Technology, 1971; see also ref. 17.

(20) The spin coupling represented by the arrows in Eq. (1) indicates the coupling qualitatively. The precise coupling is indicated by the tableaux representation. (See ref. 14.)

(21) G. Levin and W. A. Goddard III, J. Am. Chem. Soc., 97, 1649 (1975).

(22) J. A. Berson, private communication.

(23) The conversion between energy units is 1 hartree = 27.2116 eV = 627.5096 Kcal $mole^{-1}$ = 149.9784 KJ $mole^{-1}$ = 455.6334 nm; taken from E. R. Cohen and B. N. Taylor, J. Phys. Chem. Ref. Data, 2, 717 (1973).

PART C: THEORETICAL STUDIES OF THE LOW-LYING STATES OF VINYLIDENE [1]

I. Introduction

Recent experimental results of Stang and co-workers[2] have suggested that the ground state of vinylidene 1 is a closed-shell singlet state. The difficulty in generating unsaturated carbenes has precluded

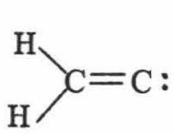

1

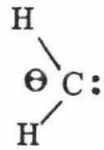

2

any direct measurement of the singlet-triplet energy difference. By considering the effect of the HCH bond angle, θ, on the singlet-triplet gap of methylene 2, Hoffmann and Gleiter[3] had predicted that vinylidene might have a singlet ground state. Numerous theoretical calculations on methylene[4] have shown that as θ is decreased below 135°, the energy of the $^3B_2$ state

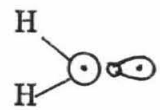

(1)

rises and the energy of the $^1A_1$ state

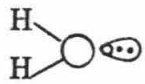

(2)

drops. At θ = 105°, the singlet also begins to rise. At angles less than 98°, the $^1A_1$ state is actually lower than the $^3B_1$. In analogy vinylidene represents the case where θ = 0 (or considering a double-bond as two bent "banana-bonds", θ = 30 to 60°), and thus on the basis of

Figure 1. The energies of the electronic states of methylene as a function of bond angle. Data from reference 4.

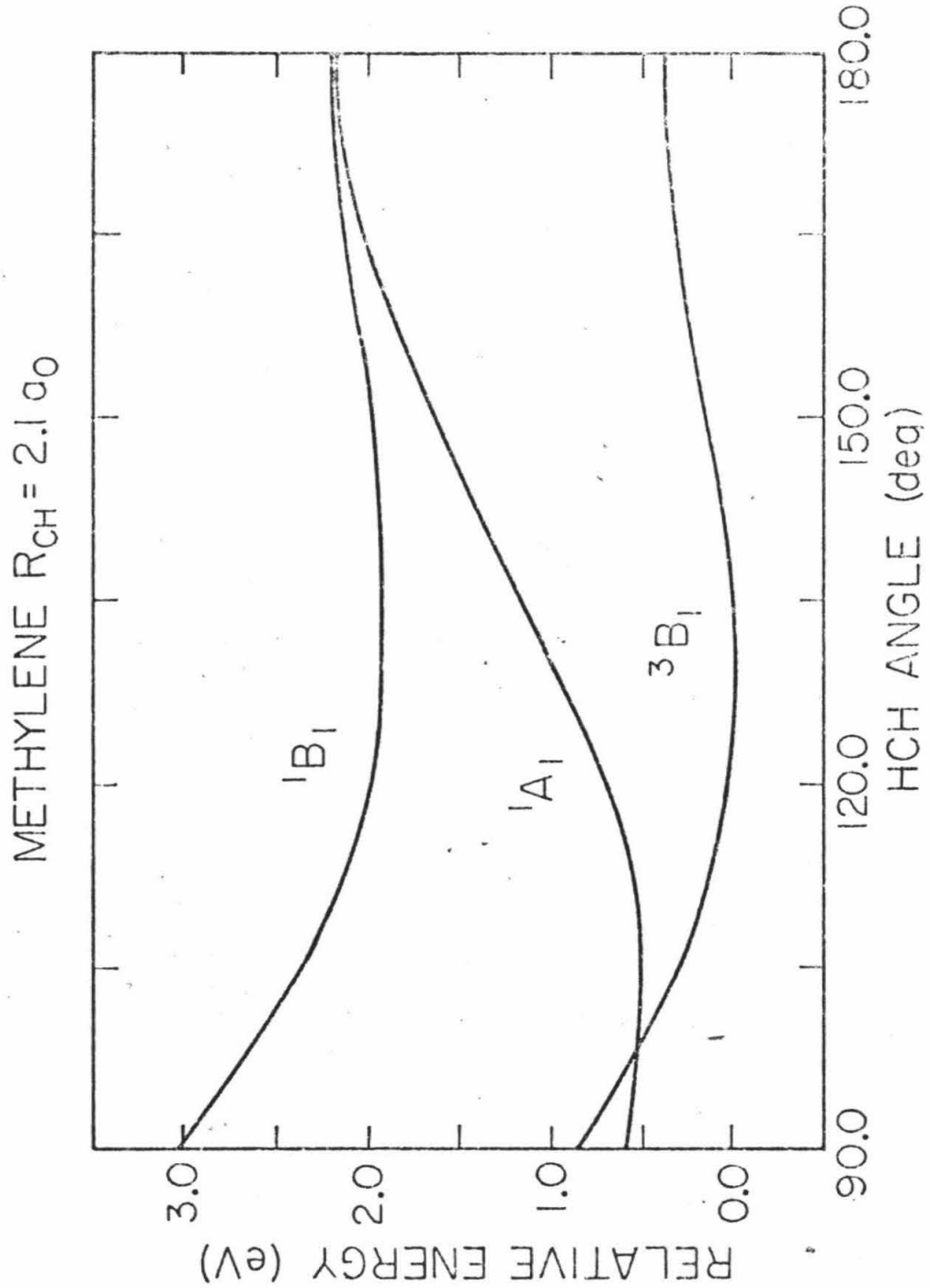
METHYLENE R_{CH} = 2.1 a_0
$^1B_1$
$^1A_1$
$^3B_1$
3.0
2.0
1.0
0.0
RELATIVE ENERGY (eV)
90.0
120.0
150.0
180.0
HCH ANGLE (deg)

these arguments we would expect $\underset{\wedge}{1}$ to be a singlet ground state.

Despite the experimental interest in unsaturated carbenes, no extensive theoretical treatment of vinylidene has been published. We can consider vinylidene to be composed of methylene and a carbon atom. Joining ground state methylene ($^3B_1$) and ground state carbon atom (^3P) gives $^1A_1$ vinylidene (denoted σ^2)

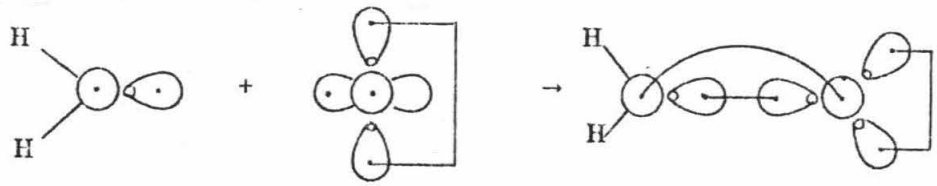

(3)

and $^3B_2$ vinylidene (denoted $\sigma\bar{\pi}$)[5]

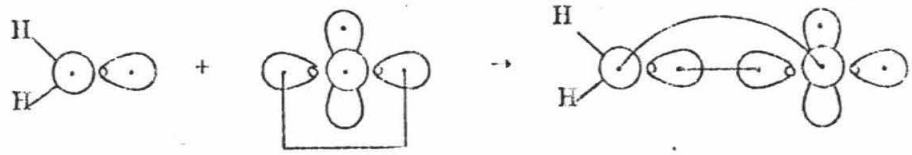

(4)

The second configuration ($\sigma\bar{\pi}$) also gives rise to a singlet state, $^1B_2$. It is these three states which are considered below.

II. Calculations Details

A. Basis Set and Geometries. Dunning's[6] (4s,2p/2s) contraction of Huzinaga's[7] (9s5p/4s) primitive Gaussian basis was used in all calculations. Since polarization functions are known to be important in the singlet-triplet energy difference for methylene, we included one set of d-polarization functions (α = 0.6769) on each carbon.[8]

The geometry used maintained C_{2v} symmetry and used the following parameters: R_{C-H} = 1.076; $\angle$HCH = 116.6°. Since the most likely difference in geometry between the σ^2 and $\sigma\bar{\pi}$ states was expected

to be in the carbon-carbon bond length, this parameter was optimized using a parabolic fit to three points: R_{C-C} = 1.25, 1.33 and 1.41 Å. The $^1A_1$ state was found to have an optimum bond length of 1.35 Å, while the $^3B_2$ state had a bond length of 1.36 Å. These optimum values were used in all subsequent calculations.

B. The GVB Calculations. To accurately describe the variation of the energy with bond length, we must consider those bonds which are directly affected by modifying the geometry. The Hartree-Fock (HF) wavefunction for the $^1A_1$ state of vinylidene would have seven doubly occupied orbitals. Breaking the carbon-carbon bond to give $^3B_1$ methylene and ^3P carbon atom requires HF wavefunctions consisting of five doubly occupied and four singly occupied orbitals. Thus the HF wavefunction for vinylidene cannot properly describe the dissociation of the CC bond.

The GVB wavefunction allows every electron to have its own orbital. However, to properly describe the dissociation of the CC bond, it is sufficient that only three HF pairs be correlated or split into pairs of nonorthogonal singly occupied orbitals. The first two pairs correspond to the CC sigma and pi bonding pairs. These are the pairs directly involved in breaking the CC bond. We also correlated the doubly-occupied "carbon" orbital; this orbital was split to make it consistent with our treatment of the $^3B_2$ state, in which the "carbene" carbon has two singly occupied orbitals. This GVB wavefunction which has three pairs of singly occupied orbitals is denoted as GVB(3).[9] It is the GVB(3) wavefunction which was used in the geometry optimization.

Although the GVB(3) wavefunction is adequate for describing the excitation energies of vinylidene, accurate bond strengths generally require close attention to small correlation effects not included in this wavefunction. In order to include all possible correlations that might affect the CC bond energy, we increased the complexity of our GVB(3) wavefunction by also correlating the two pairs of orbitals corresponding to the CH bonding pairs. This GVB(5) [or GVB(5/10) where the 10 refers to the total number of GVB orbitals] wavefunction allows us to account for any differential correlation in the CH pairs between vinylidene and methylene. From previous studies on ethylene[10] it was found that accurate CC bond strengths required the inclusion of two additional correlating orbitals for each of the CC bond pairs. Thus our GVB(5/10) wavefunction becomes a GVB(5/14) wavefunction which was used for the $^3B_2$ state. For the $^1A_1$ state we also included an additional correlating orbital for the lone pair leading to a GVB(5/15) wavefunction.

C. CI Calculations. Three different levels of CI wavefunctions were used. In the bond length determinations a full GVB(3)-CI was carried out. This utilized all configurations with six or more distributed among the six GVB orbitals ($CC\sigma\sigma^*$, $CC\pi\pi^*$, $LP\sigma\sigma^*$). This resulted in 50 spatial configurations (104 determinants) for $^1A_1$ and 27 spatial configurations (65 determinants) for $^3B_2$.

In determining the CC bond energy we carried out considerably more extensive CI calculations [referred to as GVB(5/15)-CI(1)]. The reason is that it was necessary to include a consistent level of

correlation effects for both vinylidene and the separated molecule (i.e., $:CH_2$ and $\cdot\dot{C}:$). To account for all correlation effects about the CC sigma and pi bond, we allowed up to quadruple excitations within the set of eight orbitals $(\sigma\sigma_1^*\sigma_2^*\sigma_3^*\pi\pi_1^*\pi_2^*\pi_3^*)$ describing the four electrons of the CC bond, with the restriction that there be no excitations between the σ and π sets. To this set of configurations we added another set to account for correlation effects available to separated molecules but not normally utilized in vinylidene. This set involved all five pairs of GVB orbitals: A = CC $(\sigma\sigma^*)$; B = CC $(\pi\pi^*)$; C = CH $(\sigma\sigma^*)$ + CH_2 $(\sigma\sigma^*)$; D = LP $(\sigma\sigma^*)$. Double excitations in set A and in set B and single excitations within set C and within set D were allowed (with the restriction that no quintruple of higher excitations be included); no excitations between sets were allowed. In addition all single excitations from the dominant configurations[11] were included and finally we allowed all excitations from the doubly occupied CC σ into the three π virtuals This CI led to 166 spatial configurations (296 spin eigenfunctions) for the $^1A_1$ state.

The final CI calculations [referred to as GVB(5/15)-CI(2)] was identical to the one just discussed except that double excitations within set D were allowed. This led to 166 spatial configurations (296 spin eigenfunctions) for the $^1A_1$ state and 136 spatial configurations (542 spin eigenfunctions) for the $^3B_2$ state. This CI was used to establish the most accurate estimate of the singlet-triplet energy gap.

The CI calculations for the IP's were carried out as follows. For the σ^2 state $^2B_1$ we used the GVB orbitals of the $^1A_1(\sigma^2)$ state, for

all other states we used the GVB orbitals of the $^3B_2(\sigma\bar{\pi})$ state. The CI calculations were then carried out as for the ground state except that CI excitations were based on the dominant configurations[11] of the various ion states.

III. The GVB Orbitals

A. The $^1A_1$ State. The ground state GVB(5) orbitals are shown in Figures 2 and 3. We find that the orbitals localize in different regions and have the basic character of valence bond wavefunctions.

In the σ-system there are three different bonding pairs. The first pair corresponds to the CC sigma bond; one orbital centered on the central carbon is hybridized $(sp^{1.59})^{12}$ toward the terminal carbon while the other orbital centered on the terminal carbon is hybridized $(sp^{1.78})$ toward the central carbon. The other two pairs correspond to CH σ bonds--one centered on the upper hydrogen and the other on the lower hydrogen. The two pairs are identical and consist of two orbitals: one centered on the hydrogen is essentially spherical with some delocalization toward the central carbon, while the other is an sp^2-type orbital (actually $sp^{1.88}$) centered on the central carbon and hybridized toward the hydrogen.

The other pair of orbitals in the sigma system corresponds to the doubly occupied lone-pair orbital on the terminal carbon. The orbitals of this pair have the hybridization $sp^{0.63}$. Thus they are mainly s-like with high overlap as appropriate for singlet paired orbitals.

The π system consists of two p-orbitals centered on each carbon

Figure 2. GVB orbitals for the $^1A_1$ state of vinylidene based on the GVB(5/15) wavefunction. Long dashes indicate zero amplitude; the spacing between contours is 0.05 a.u. The same conventions are used for all plots.

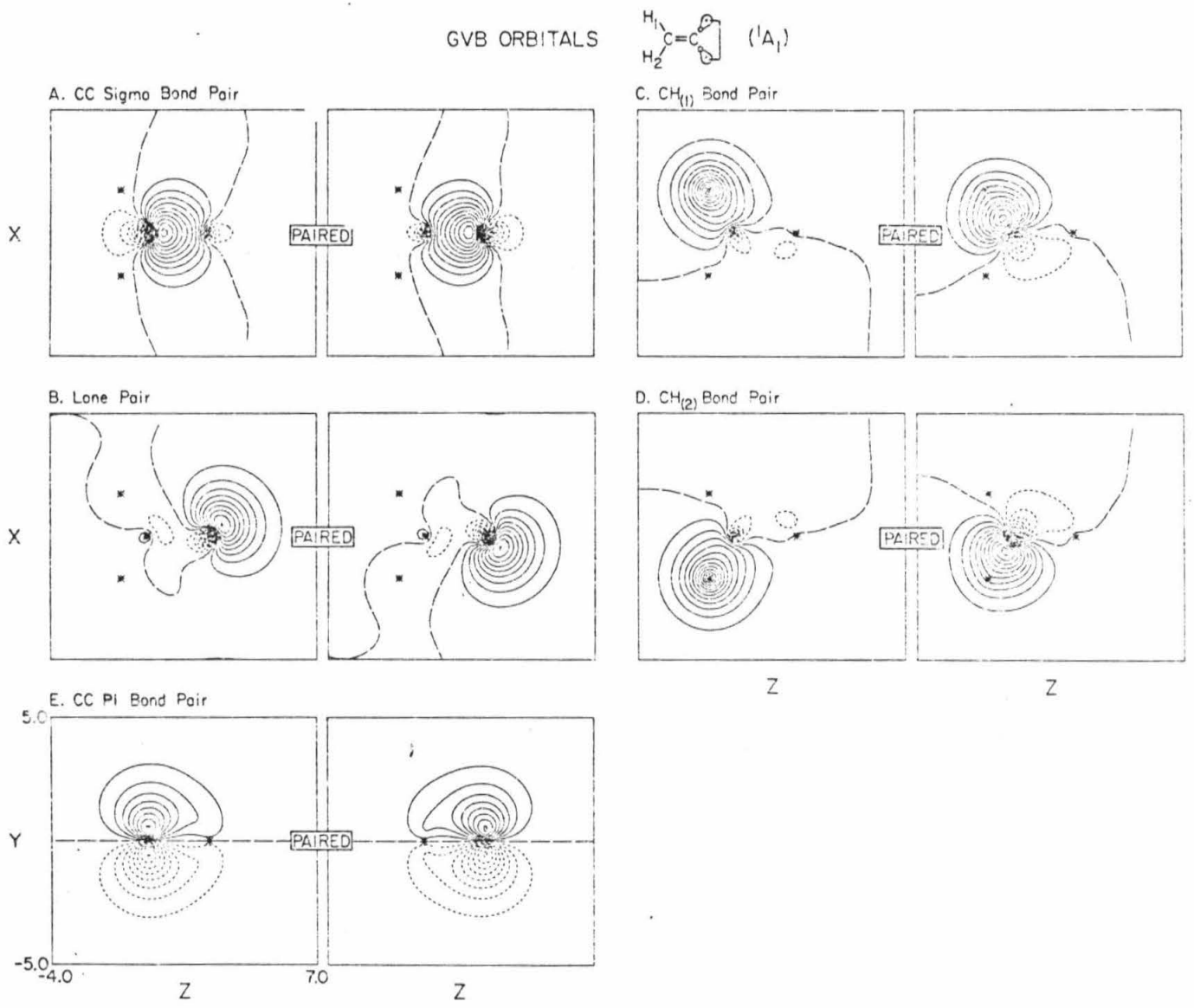
GVB ORBITALS
$^1A_1$
A. CC Sigma Bond Pair
C. $CH_{(1)}$ Bond Pair
B. Lone Pair
D. $CH_{(2)}$ Bond Pair
E. CC Pi Bond Pair
PAIRED
X
Y
Z
5.0
-5.0
-4.0
7.0

Figure 3. GVB orbitals for the $^3B_2$ state of vinylidene based on the GVB(5/14) wavefunction.

GVB ORBITALS 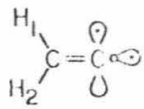 ($^3B_2$)

A. CC Sigma Bond

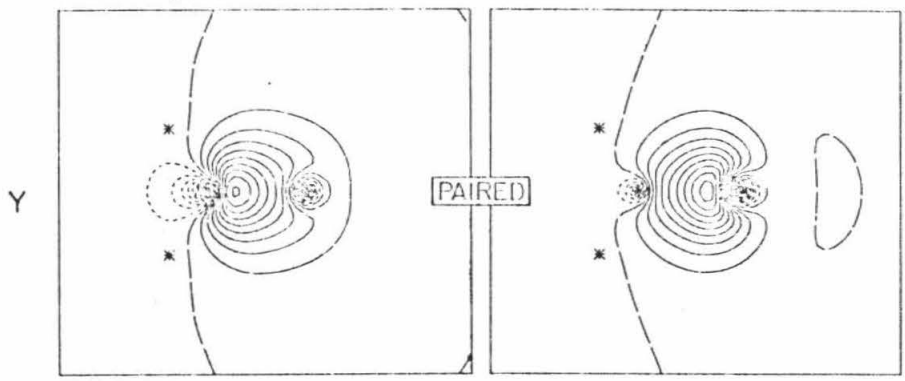

B. a_1 Orbital

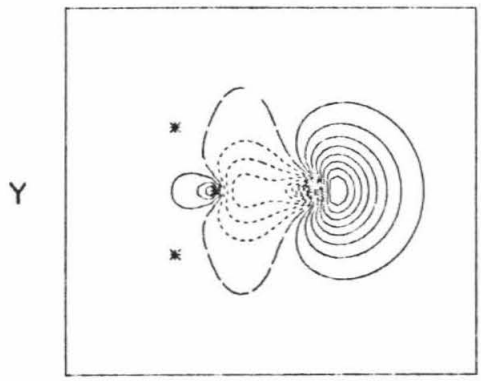

C. b_2 Orbital

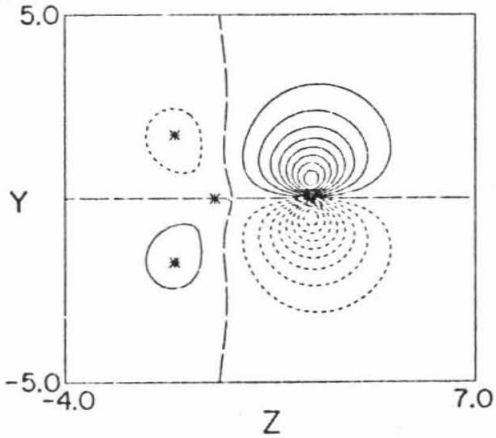

Table I. GVB Pair Information

State	Energy (h)	Pair	Overlap	Energy Lowering (h)
$^1A_1$	-76.88407	CC - Pair	0.6593	0.0323
		CC - Sigma	0.8889	0.0148
		CH - Left	0.8450	0.0142
		CH - Right	0.8450	0.0142
		Lone Pair	0.7170	0.0272
$^3B_1$	-76.81089	CC - Pi	0.6445	0.0333
		CC - Sigma	0.9043	0.0106
		CH - Left	0.8460	0.0106
		CH - Right	0.8460	0.0141

and hybridized toward the other carbon.

The overlaps and energy lowering for these pairs are summarized in Table I.

B. The $^3B_2$ State. The bonding pairs corresponding to the CH bonds and the CC π-bond are not shown, since they are essentially identical with the corresponding $^1A_1$ orbitals.

The CC σ-bond, however, shows greater delocalization toward the terminal carbon than was present in the $^1A_1$ case. The orbital on the terminal carbon is $sp^{0.45}$ hybridized, while the orbital on the central carbon is $sp^{1.66}$. This is due to the change in the lone pair from a singlet coupled pair to triplet coupled orbitals. As can be seen, the triplet pair of orbitals (the "methylene" orbitals) now have the character of a singly occupied p_x orbital and a singly occupied $sp_z^{1.8}$ orbital.

IV. Discussion

A. Heat of Formation. Since our GVB(5/15)-CI wavefunction for vinylidene is sufficiently correlated to describe accurately the breaking of the carbon-carbon bond to give $^3B_1$ methylene and ^3P carbon atom, we can calculate the carbon-carbon bond strength, $D(H_2C{=}C{:})$. The energies of $H_2C{=}C{:}$, $H_2C{:}$, and C are shown in Table II and lead to an energy difference of $D_e(H_2C{=}C{:}) = 155.7$ Kcal mole^{-1}. The inappropriateness of the HF wavefunction for bond-breaking processes is illustrated by the low bond energy calculated using this wavefunction. In addition Table II shows that even second-order correlation

Table II. Comparison of Calculated Bond Energies from Various Wavefunctions

	HF	GVB(3)	GVB(5/10)	GVB(5/15)	CI(1)	
$H_2CC\,(^1A_1)$:	-76.77066	-76.82951	-76.85744	-76.87130	-76.85908	-76.88407
$H_2C\,(^3B_1)$:	-38.9202[a]	-38.9202[a]	-38.9483[b]	-38.9483[b]	-38.92647[d]	--
$C\,(^3P)$:	-37.6845[a]	-37.7033[b]	-37.7033[b]	-37.7033[b]	-37.6845[a]	-37.7033[b]
$D_e\,(H_2C{=}C)$ (Kcal mole^{-1})	104.1	129.3	129.2	137.9	155.7	--

[a] HF

[b] GVB(1)

[c] GVB(2)

[d] GVB(2)-CI

effects can lead to a bond energy as much as 18 Kcal $mole^{-1}$ too weak.

Since an experimental determination of this bond energy would include the difference in zero point energies of the molecule and fragments, it is necessary to apply a zero-point vibrational energy correction to D_e. Estimating the vibrational frequencies for vinylidene based on the average frequencies of ethylene[13] as shown in Table III and using the experimental values for methylene,[13] we calculate a zero-point correction of 5.6 Kcal $mole^{-1}$. Thus we predict the bond dissociation energy for vinylidene to be $D_0(H_2C{=}C{:}) = 150.1$ Kcal $mole^{-1}$. For comparison similar calculations on ethylene by Harding and Goddard lead to $D_0(H_2C{=}CH_2) = 167$ Kcal $mole^{-1}$ as compared to the experimental value of 170 Kcal $mole^{-1}$.

Using the experimental values for the heat of formation of methylene ($^3B_1$) and carbon atom (^3P) and the theoretical D_0, we calculate the heat of formation for vinylidene as

$$\Delta H^\circ_{f_{0\,^\circ K}}(H_2C{=}C{:}) = 92.2 + 169.6 - 150.1 = 111.7 \text{ Kcal mole}^{-1}$$

Correcting[13] to 298°K leads to $\Delta H^\circ_{f_{298}}(H_2C{=}C{:}) = 111.5$ Kcal $mole^{-1}$.

There is currently considerable uncertainty in the heat of formation of vinyl radical,

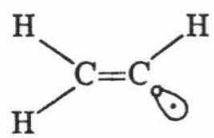

estimates ranging[14] from $\Delta H_f = 62$ to 71 Kcal $mole^{-1}$. Using our

Table III. Vibrational Frequencies Used in Zero-Point Energy Calculation

Vibration		H_2CC (estimated cm^{-1})	H_2C (experimental cm^{-1})
CH	a_1	3062	2960
	b_2	3131	3200
CH_2	a_1	1393	1114
	b_2	1023	-
	b_1	946	-
CC	a_1	1623	-
Total zero-point energy (kcal $mole^{-1}$)		31.96	20.80

calculated ΔH_f° for H_2CC we find that the bond energy $D_0(H_2CC\text{-}H)$ of vinyl is 101 to 92 Kcal $mole^{-1}$, respectively, while the CH bond of ethylene[15] is 101 to 110 Kcal $mole^{-1}$. These results would seem most reasonable for ΔH_f (H_2CCH) $\approx$ 70 Kcal $mole^{-1}$.

B. The Singlet-Triplet Splitting. As expected, we find that the singlet state has a considerably lower energy, 45.9 Kcal $mole^{-1}$, than the triplet state (see Table IV)[16]. The large $^3B_2$-$^1A_1$ splitting is consistent with experimental observations[2] that the only reactive species is a singlet state.

In methylene the triplet state is 41.5 Kcal $mole^{-1}$ below the singlet state for a HCH bond angle of 180°, 20.8 Kcal mole below for an angle of 135°, and nearly degenerate for ~100°. That is, two electrons in the nonbonding a_1 orbital are favored for small bond angles; hence for bond angles less than 90° the singlet state is below the triplet. In vinylidene the carbon is double bonded to another carbon; this double bond is equivalent to reducing the bond angle to an angle much less than 90° and hence leads to a singlet ground state.

The $^1B_2$ state is calculated to be at 116.5 Kcal $mole^{-1}$ relative to ground state. The resulting $^3B_2$-$^1B_2$ difference (2.9 eV) is considerably larger than that found in methylene (1.9 eV at $\angle$HCH = 135°). This might seem strange since in the simplest description this energy difference is just twice the exchange integral between the open shell orbitals (denoted as σ and $\bar{\pi}$),

$$E(^1B_2) - E(^3B_2) = 2K_{\sigma\bar{\pi}} \ .$$

Table IV. Excitation Energies and Dominant Configurations [GVB(5/15)-CI(2)] for Vinylidene.

State	Excitation Energy	Dominant Configurations																		Energy Lowering
		CH Bonds				CC Bonds										Lone Pair				
						sigma				pi										
		a_1	a_1^*	b_2	b_2^*	σ	σ^*	σ^*	$\bar{\pi}$	π	π^*	π^*	π^*	a_1	b_2	a_1				
$^1A_1$	0.0	2	0	2	0	2	0	0	0	2	0	0	0	2	0	0				-
		2	0	2	0	2	0	0	0	0	2	0	0	2	0	0				0.0202
		2	0	2	0	2	0	0	0	2	0	0	0	0	2	0				0.0190
		2	0	2	0	1	1	0	0	1	1	0	0	2	0	0				0.0101
$^3B_2$	1.99	2	0	2	0	2	0	0	0	2	0	0	0	1	1	-				-
		2	0	2	0	2	0	0	0	0	2	0	0	1	1	-				0.0239
		2	0	2	0	2	0	0	0	1	1	0	0	1	1	-				0.0051
		2	0	2	0	1	1	0	0	1	1	0	0	1	1	-				0.0051
$^1B_2$	4.88	2	0	2	0	2	0	0	0	2	0	0	0	1	1	-				-
		2	0	2	0	1	0	0	0	2	0	0	0	2	1	-				0.0185
		2	0	2	0	2	0	0	0	0	2	0	0	1	1	-				0.0197
		1	0	2	0	2	0	0	0	2	0	0	0	2	1	-				0.0011
$^3A_1$	5.49	2	0	2	0	2	0	0	0	1	1	0	0	2	0	0				-
($\pi-\pi^*$)		2	0	2	0	2	0	0	0	1	1	0	0	0	2	0				0.019
		2	0	2	0	2	0	0	0	1	1	0	0	0	0	2				0.0064
		2	0	2	0	0	2	0	0	1	1	0	0	2	0	0				0.0085
$^3B_2$	8.85	2	0	2	0	2	0	0	0	1	1	0	0	1	1	-				-
($\pi-\pi^*$)		2	0	2	0	2	0	0	0	2	0	0	0	1	1	-				-0.0048
		2	0	2	0	1	0	0	0	2	0	0	0	1	2	-				0.0074
		1	0	2	0	2	0	0	0	2	0	0	0	2	1	-				0.0024
$^1A_1$	10.49	2	0	2	0	2	0	0	0	1	1	0	0	2	0	0				-
($\pi-\pi^*$)		2	0	1	0	2	0	0	0	2	0	0	0	2	1	0				0.0874
		2	0	1	0	2	0	0	0	1	1	0	0	2	1	0				0.0273
		2	0	1	0	2	0	0	1	2	0	0	0	2	0	0				0.0271

Table V. Contributions to the Dipole Moment of Vinylidene. Based on the GVB(5/15) Wavefunction.

[All quantities in atomic units unless states otherwise; 1 a.u. = 2.541765 D.

State	Core (1s)		CH Bonds				CC-Bond				Lone Pair				Total		
			left		right		sigma		pi		a_1		b_2				
	x	z	x	z	x	z	x	z	x	z	x	z	x	z	x	z	z (D)
$^3B_2$	0.0	0.0	0.587	0.284	-0.587	0.284	0.0	-0.353	0.0	0.116	0.0	-0.640	0.0	0.091	0.0	-0.218	-0.554
$^1A_1$	0.0	0.0001	0.592	0.261	-0.592	0.261	0.0	0.036	0.0	0.189	0.0	-1.626	—	—	0.0	-0.878	-2.233

However, this exchange integral is a function of the hybridization of the σ orbital and for CH_2 increases from 2K = 1.8 eV at 180° to 1.9 at 135° to 2.2 at 90°. Thus a value of 2K = 3.0 eV for vinylidene is consistent with a very small effective bond angle (see Figure 1).

C. Dipole Moments. In GVB wavefunctions, the orbitals are unique and have clear valence bond characteristics which make it useful to analyze properties such as dipole moments in terms of orbital contributions. In order for the dipole moment to be independent of origin we associate with the electron of each orbital a unit nuclear charge centered at the nucleus on which the orbital is centered (in the VB model). This leads to the results shown in Table V.

In the $^1A_1$ case we see that the largest contribution comes from the lone pair on the terminal carbon which is strongly polarized away from the carbon. (The CH pairs are also polarized away from the central carbon.) This polarization is partially compensated by the π system which is polarized toward the central carbon. Hence the total dipole moment for the $^1A_1$ state is 2.232 D pointing toward the "carbene" carbon.

In the $^3B_2$ state, unlike the $^1A_1$, the CC sigma bond is strongly polarized toward the terminal carbon. All other orbital contributions are approximately the same except for the diminished polarization of the now singly occupied a_1 orbital. Thus the overall dipole moment is 0.554 D, only one quarter of the moment of the $^1A_1$ state.

Figure 4. Electronic states of vinylidene and vinylidene cation. Energies in electron volts. (1hartree = 27.2116 eV = 627.5096 kcal $mole^{-1}$)

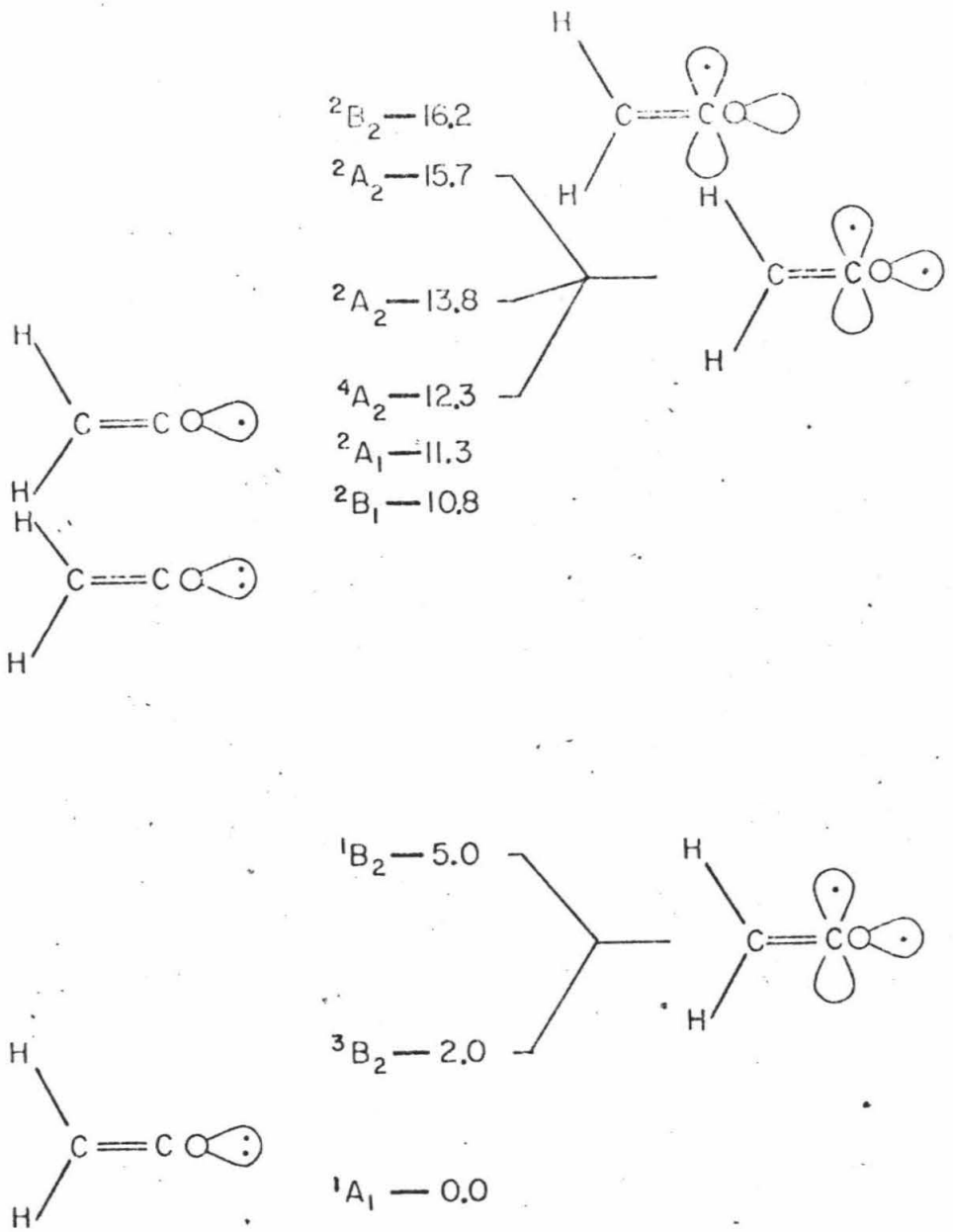
$^2B_2$ — 16.2
$^2A_2$ — 15.7
$^2A_2$ — 13.8
$^4A_2$ — 12.3
$^2A_1$ — 11.3
$^2B_1$ — 10.8
$^1B_2$ — 5.0
$^3B_2$ — 2.0
$^1A_1$ — 0.0

D. Ionization Potentials and Higher Excited States. Since the methylene and ethylene ionization potentials are comparable, we can expect several lower positive ion states for vinylidene. We carried out CI calculations (vide supra) for these states leading to the results in Figure 4 (all vertical ionizations). The first ionization is out of the π-system leading to $^2B_1$ at 10.8 eV, just 0.3 eV above the corresponding IP of ethylene.[17] The second ionization potential (the $^2A_1$) is at 11.3 eV, and results from ionization of the $\bar{\pi}$-electron of the $^3B_2$ state. The analogous ionization in methylene is at 11.4 eV.[17] Ionization of an electron in the π-system of the $^3B_2$ state leads to a $^4A_2$ ion at 12.3 eV and two $^2A_2$ ions at 13.8 and 15.7 eV. Finally, ionization of the σ-electron of the $^3B_2$ state yields a $^2B_2$ ion at 16.2 eV.

On the basis of the IP and in analogy with ethylene, we expect the first Rydberg transition to be at 7.4 eV (compared to 7.1 eV for ethylene).

We have also carried out CI calculations (vide supra) for the $\pi \rightarrow \pi^*$ transitions. The $\pi \rightarrow \pi^*$ triplet state ($^3A_1$) was found at 5.5 eV, which is about 1 eV higher than the corresponding state of ethylene. (This calculated energy may be high by ~ 0.5 eV since the orbitals were not solved for self-consistently.) The $\pi \rightarrow \pi^*$ singlet state ($^1A_1$) state was found at 10.5 eV. It is well known that a $\pi \rightarrow \pi^*$ singlet state such as for vinylidene requires diffuse basis functions. Since we did not include diffuse functions and since we did not even solve self-consistently for this state, we expect to calculate an energy considerably too high.

Table V. Ionization Potentials and Dominant Configurations [GVB(5-15)-CI(2)] for Vinylidene.

State	Ionization Potential	Dominant Configurations																Energy Lowering
		CH Bonds				CC Bonds								Lone Pair				
						sigma				pi								
		a_1	a_1^*	b_2	b_2^*	σ	σ^*	σ'	$\overline{\pi}$	π	π^*	$\overline{\pi}^*$	π^*	a_1	b_2	a_1		
$^2B_1$	10.82	2	0	2	0	2	0	0	0	1	0	0	0	2	0	0		-
		2	0	2	0	2	0	0	0	1	0	0	0	0	2	0		0.0212
		2	0	1	1	2	0	0	0	1	0	0	0	2	0	0		0.0106
		2	0	2	0	2	0	0	0	2	0	0	0	0	1	0		0.0065
$^2A_1$	11.28	2	0	2	0	2	0	0	0	2	0	0	0	1	0	-		-
		2	0	1	0	2	0	0	0	2	0	0	0	1	1	-		0.0229
		2	0	2	0	2	0	0	0	1	1	0	0	1	0	-		0.0133
		2	0	1	0	2	0	0	0	1	0	1	0	1	0	-		0.0065
$^4A_2$	12.26	2	0	2	0	2	0	0	0	1	0	0	0	1	1	-		-
		2	0	2	0	2	0	0	0	0	1	0	0	1	1	-		0.0031
		2	0	2	0	2	0	0	0	0	0	1	0	1	1	-		0.0070
		2	0	1	1	2	0	0	0	1	0	0	0	1	1	-		0.0097
$^2A_2$	13.76	2	0	2	0	2	0	0	0	1	0	0	0	1	1	-		-
		2	0	1	1	2	0	0	0	1	0	0	0	1	1	-		0.0084
		2	0	2	0	1	1	0	0	0	1	0	0	1	1	-		0.0080
		2	0	2	0	2	0	0	0	0	0	1	0	1	1	-		0.0070
$^2A_2$	15.72	2	0	2	0	2	0	0	0	1	0	0	0	1	1	-		-
		2	0	2	0	2	0	0	1	1	0	0	0	1	0	-		0.0128
		2	0	1	1	2	0	0	0	1	0	0	0	1	1	-		0.0089
		2	0	2	0	1	0	0	0	1	0	0	0	2	1	-		0.0073
$^2B_2$	16.24	2	0	2	0	2	0	0	0	2	0	0	0	0	1	-		-
		2	0	2	0	1	0	0	0	2	0	0	0	1	1	-		0.0349
		1	0	2	0	2	0	0	0	2	0	0	0	1	1	-		0.0233
		2	0	2	0	2	0	0	0	0	2	0	0	0	1	-		0.0161

V. Summary

We find the ground state of vinylidene is the singlet state ($^1A_1$) with the methylene-like triplet at 2.0 eV. The lower ionization potentials are close to the values expected from the corresponding ionizations of ethylene or methylene.

We find the carbon-carbon bond dissociation energy for vinylidene to be 150.1 Kcal $mole^{-1}$ as compared to a dissociation energy of 169.9 Kcal $mole^{-1}$ for ethylene.

The dipole moment is found to be 0.554 D for the $^3B_2$ and 2.232 for the $^1A_1$ state of vinylidene.

References

(1) This work was supported by a John and Beverly Stauffer Foundation Fellowship, 1975-1976.

(2) P. J. Stang and M. G. Mangum, J. Am. Chem. Soc., 97, 1459 (1975), 97, 6478 (1975), 97, 3854 (1975).

(3) R. Gleiter and R. Hoffmann, J. Am. Chem. Soc., 94, 9095 (1972).

(4) W. Wadt and W. A. Goddard III, J. Am. Chem. Soc., 96, 5996 (1974).

(5) An orbital which is symmetric with respect to the molecular plane but antisymmetric with respect to the perpendicular plane passing through the CC axis is denoted by $\bar{\pi}$.

(6) T. H. Dunning, Jr., J. Chem. Phys., 53, 2823 (1970).

(7) S. Huzinaga, J. Chem. Phys., 42, 1293 (1965).

(8) P. J. Hay, W. J. Hunt, and W. A. Goddard III, Chem. Phys. Lett., 13, 30 (1972).

(9) Our calculations also restrict the GVB(3) wavefunction by partitioning the singly occupied orbitals into mutually orthogonal singlet- or triplet-coupled pairs; this perfect pairing approximation is generally indicated by the notation GVB(3/PP). In this paper we will use the simpler notation GVB(3) in place of the notation GVB(3/PP). The effects of such restrictions are relaxed by the CI and in vinylidene are of minor importance.

(10) L. B. Harding and W. A. Goddard III, unpublished results.

(11) Single excitations were performed from the dominant configuration of each state. In addition it was found that inclusion of all single

excitations from the three configurations involving single excitations within the GVB pairs (sets A, B, and D) led to an energy lowering of 6 Kcal $mole^{-1}$.

(12) Hybridization was determined by Mullikan Population Analysis of the GVB orbitals.

(13) JANAF Thermochemical Tables, NSRDS-NBS 37, U.S. Government Printing Office, 1970.

(14) a) F. P. Lossing, Can. J. Chem., 49, 357 (1971);
b) S. W. Benson, 'Thermochemical Kinetics", John Wiley & Sons, New York (1968).

(15) Calculated using $\Delta H_{f_{298}^{\circ}}(H_2C{=}CH_2)$ = 12.5 Kcal $mole^{-1}$, see ref. 13.

(16) Inclusion of p basis functions on the hydrogens and extensive correlation lead to an increase in the triplet-singlet separation of methylene from 11 to 16 Kcal $mole^{-1}$ (L. B. Harding and W. A. Goddard III, unpublished results). Recent experimental results[18] lead to 19 Kcal $mole^{-1}$. For vinylidene these effects are expected to be small (< 1 Kcal).

(17) G. Herzberg, "Molecular Spectra and Molecular Structures", Vol. III, D. Van Nostrand Co., Inc., Princeton (1966).

(18) P. F. Zittel, G. B. Ellison, S. V. ONeil, E. Herbst, W. C. Lineberger, and W. P. Reinhardt, J. Am. Chem. Soc., 98, 3731 (1976).

PART D: THEORETICAL STUDIES OF THE LOW-LYING STATES OF AMINONITRENE [1]

I. Introduction

A number of chemically interesting systems incorporating molecular dinitrogen bonded to an organic or inorganic framework are currently under extensive investigation by various groups.

Using transition metals it has been possible to bond N_2 to a single metal complex[2]

M–N–N

and to incorporate N_2 bridging two metal complexes[3]

M–N–N–M .

From such complexes it has been possible to reduce the N_2 to hydrazine (N_2H_4) or ammonia (NH_3) by reaction with hydrogen.

An exciting area of organic dinitrogen systems has been with ring systems such as

1

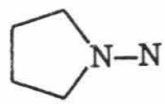

2

where the extrusion of nitrogen may lead either to formation of biradical intermediates or to concerted eliminations.[4] An unusual application of such systems has recently been advanced by Dervan[5] who has suggested that decomposition of systems such as 1 or 2 may lead to vibrationally excited N_2 and that such a system could be the basis of a chemical laser.

Of particular theoretical interest is the electronic structure and

bond energies of aminonitrenes

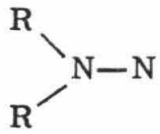

3

such as in 2 since these systems seem to be poorly understood. It is generally presumed[6] that the ground state of 3 is a singlet state as would be expected from the valence bond diagram

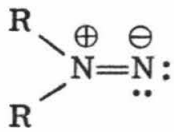

(1)

However, nitrenes

generally have a triplet ground state, with the first singlet state much higher (44 Kcal mole^{-1} for NH). The only reported theoretical ab initio studies of aminonitrene

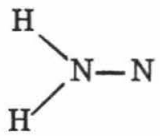

4

resulted in a triplet ground state with the singlet state 26.3 Kcal mole^{-1} higher.[7]

In this paper we will concentrate on aminonitrene, 4. We carried out Hartree Fock (HF), generalized valence bond[8] (GVB), and configuration interaction (GVB-CI) calculations on both the singlet and triplet states with geometry optimization. From these studies we conclude that the ground state is the singlet state with the triplet 15 Kcal $mole^{-1}$ higher.

In addition we obtained bond energies and dipole moments of these states and examined several other excited states and cation states for the optimum ground state geometry.

First (section II) we will summarize the quantitative results while presenting a qualitative description of the states of 4. This is followed by section III presenting the details of the calculations, and section IV discussing the more theoretical aspects of the results.

II. Qualitative Description and Summary of Results

The ground state of N is ^4S and has the configuration $(1s)^2(2s)^2(2p)^3$. Ignoring the 1s and 2s pairs we can represent this wavefunction as

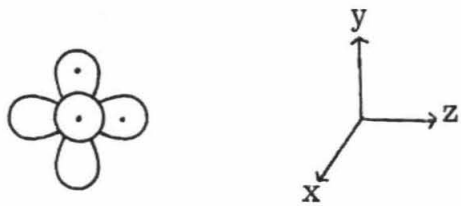

(2)

where ∞ , ∞ , and $\bigcirc$ represent p_z, p_y, and p_x orbitals and each dot indicates one electron in the orbital. With three electrons in the p orbitals we can also construct the ^2D and ^2S states lying at 2.4 eV and 3.6 eV above the ^4S state.[9] Configurations such as

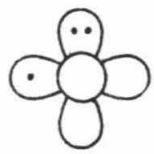

(3)

must lead to a doublet state; the single configuration (3) is half ^2D and half ^2P.

Bonding an H to (2) leads to

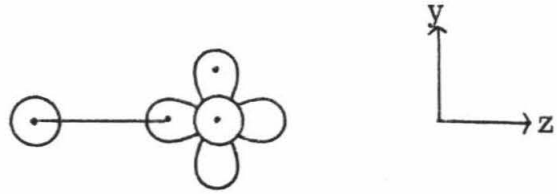

(4)

where the line indicates a singlet bonding pair. Triplet pairing of the p_x and p_y orbitals of (4), as in (2), leads to the $^3\Sigma^-$ ground state of NH. Other couplings and occupations of the p_x and p_y orbitals lead to the $^1\Delta$ and $^1\Sigma^+$ states of NH lying[10] at 1.6 eV and 2.7 eV above $^3\Sigma^-$. The wavefunctions for these states have the form

$$^3\Sigma^- : \quad (p_x p_y - p_y p_x)\ (\alpha\beta + \beta\alpha) \tag{5a}$$

$$^1\Delta^- : \quad (p_x p_y + p_y p_x)\ (\alpha\beta - \beta\alpha) \tag{5b}$$

$$^1\Delta^+ : \quad (p_x p_x - p_y p_y)\ (\alpha\beta - \beta\alpha) \tag{5c}$$

$$^1\Sigma^+ : \quad (p_x p_x + p_y p_y)\ (\alpha\beta - \beta\alpha) \tag{5d}$$

where we have ignored the bond pairs and closed shell orbitals which should be similar for the various states. In this description

$$E(^1\Delta) = E(^3\Sigma^-) + 2K_{xy} \tag{6a}$$

$$E(^1\Sigma^+) = E(^3\Sigma^-) + 4K_{xy} \tag{6b}$$

and hence since K_{xy} is necessarily positive the states are ordered $^3\Sigma^-$, $^1\Delta_1$ and $^1\Sigma^+$ with $^3\Sigma^-$ lowest. The $^3\Sigma^- - {}^1\Delta$ and $^1\Delta - {}^1\Sigma^+$ separations are nearly equal, 1.6 eV and 1.1 eV, respectively, indicating the validity of this simple description. Simple alkyl nitrenes, RN, such as

$$CH_3—N$$

$$\underset{\sim}{5}$$

should lead to a very similar bonding description.

We can now consider the effect of replacing the H- group of nitrene with an amino group to give aminonitrene $\underset{\sim}{4}$. Joining an amino radical ($^2A_1$) with (2), to form a planar molecule $\underset{\sim}{4}$ leads to

$\pi\bar{\pi}$:

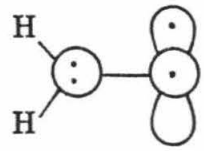

(7)

where the sigma bond is represented as a line and only the three non-bonded orbitals are indicated explicitly. This configuration (7) is referred to as $\pi\bar{\pi}$, indicating that there is one electron in the π- orbital and one electron in the $\bar{\pi}$ orbital.[11] Triplet and singlet pairing of the singly occupied orbitals of (7) leads to the $^3A_2(\pi\bar{\pi})$, $^1A_2(\pi\bar{\pi})$ states of $\underset{\sim}{4}$ analogous to the $^3\Sigma^-$ and $^1\Delta^-$ states of NH, (5a) and (5b) respectively. The main difference between the $\pi\bar{\pi}$ states in aminonitrene and in nitrene is the presence of the π-lone pair on the amino nitrogen; however the interaction of this pair with the nitrene π-electron should be equivalent in both the $^1A_2(\pi\bar{\pi})$ and $^3A_2(\pi\bar{\pi})$ states. Therefore we

Figure 1. Energies of the valence states of nitrene (HN) and aminonitrene (H_2NN).

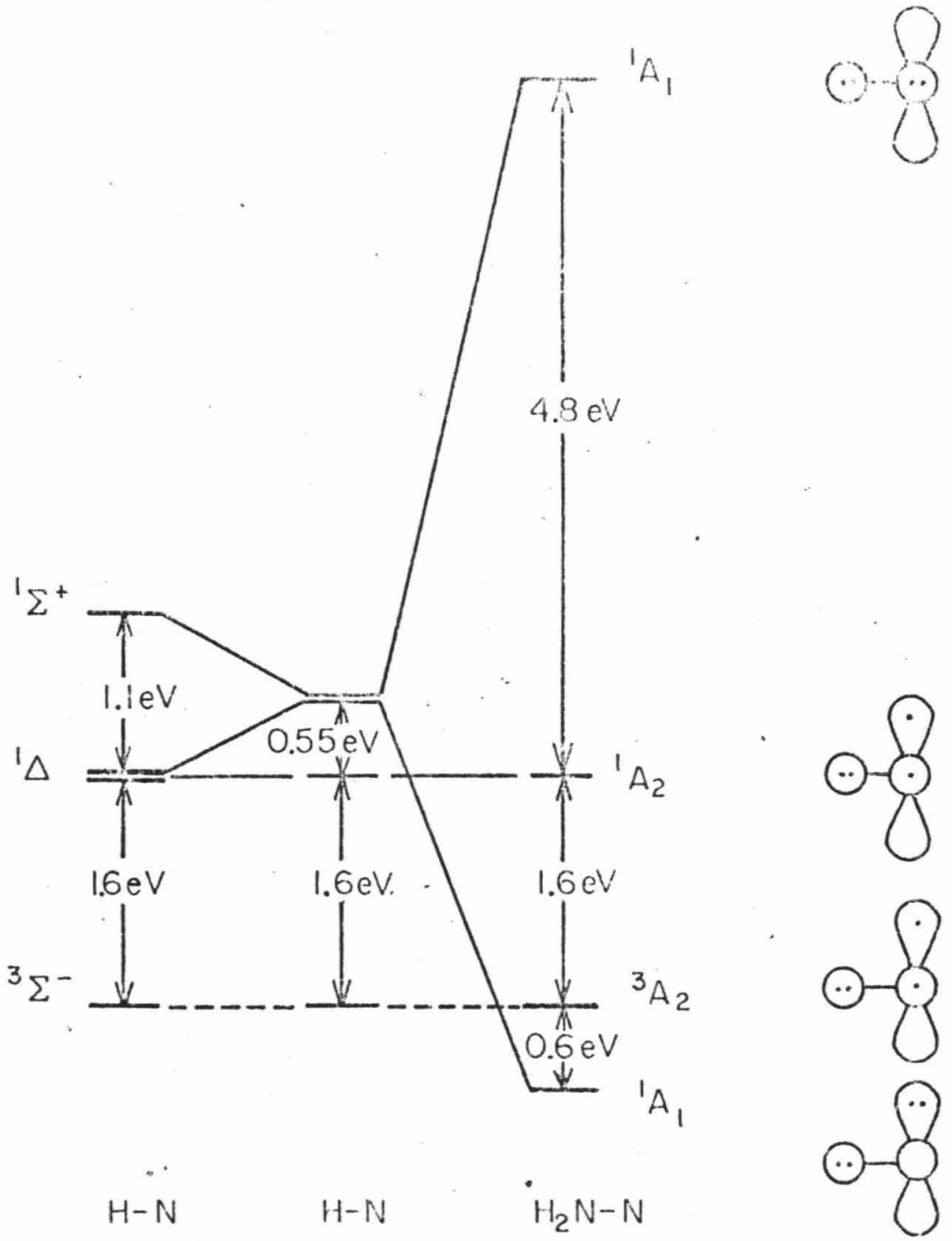

NITRENE VALENCE STATES

would expect the $^1A_2$-$^3A_2$ separation in aminonitrene to be ~ 1.6 eV just as in NH.

The results of our calculations are illustrated in Figure 1. As can be seen the $^1A_2$-$^3A_2$ separation is in fact 1.6 eV in complete agreement with our predictions.

We now want to determine the effect of the amino lone pair on the $^1\Delta^+$ and $^1\Sigma^+$ states of nitrene. Each of these states is combination of two configurations (8) and (9)

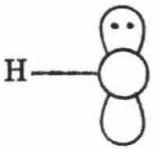

(8)

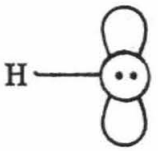

(9)

In nitrene the two configurations are equivalent and can mix leading to a resonant combination ($^1\Delta^+$)

(10)

and to an anti-resonance combination ($^1\Sigma^+$)

(11)

In aminonitrene configurations (8) and (9) become

$\bar{\pi}^2$:

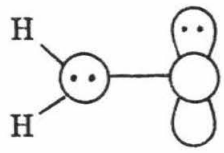

(12)

and

π^2 :

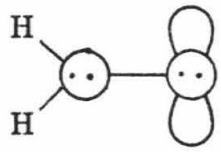

(13)

Now we find great differences due to the effect of the π-pair of the NH_2 group. In (12) this pair can delocalize into the empty π orbital of the terminal N whereas in (13) there are two doubly occupied π orbitals and hence very repulsive interactions (arising from the Pauli principle). These interactions with the NH_2 group split the states (12) and (13) by ~ 7 eV. Since this is far greater than the favorable interaction due to the resonance interaction observed in (10) and (11) for NH, we expect no significant interaction between (12) and (13).

Ignoring the interaction with the NH_2 group the configurations (12) and (13) would be expected to lie about 2.2 eV above the $^3A_2$ $(\pi\bar{\pi})$ state in analogy to NH, see Figure 1. In fact we find that $^1A_1$ $(\bar{\pi}^2)$ is

0.6 eV <u>below</u> $^3A_2$ ($\pi\bar{\pi}$) indicating about 2.8 eV of bonding in the π orbitals of (12). Indeed the pi system of $^1A_1$ ($\bar{\pi}^2$) is quite delocalized, strongly resembling the pi orbitals of a normal π bond, as shown in Fig. 2. Similarly, the calculated NH bond length of $^1A_1$ ($\bar{\pi}^2$) is 1.24 Å, quite close to the value[12] of 1.23 Å for dimide 6.

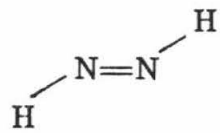

6

This indicates that the bond order for $^1A_1$ aminonitrene is very close to 2. In addition the dipole moment for the $^1A_1$ state is 4.0 Debye (negative end on nitrene) indicating that dipolar species such as (1) contribute heavily.

The calculated location of $^1A_1$ (π^2) indicates about 4.2 eV of repulsive interaction due to the two pi pairs.

So far we have considered the states of aminonitrene assuming a planar geometry. The π^2 configuration (13) is expected to adopt a pyrimidal geometry, to reduce the overlap (and thus the repulsion) of the two doubly-occupied orbitals. Similarly, configuration (12) would undoubtedly prefer a planar configuration to maximize the pi bonding.

On the other hand, the optimum geometry for configuration (7) is not so obvious from such qualitative considerations. Here there are two opposing forces: 1) a pyramidal geometry would reduce the anti-bonding interaction of the singly occupied π orbital with the doubly occupied amino π group (Pauli principle); 2) a planar geometry could

allow delocalization of the amino π-pair onto the nitrene nitrogen, leading to a 3-electron, 2-center bond. Our calculations indicate that the delocalization effects are slightly more important than the repulsion effects leading to an optimum planar geometry. This delocalization is clear in the shape of the π orbitals, Fig. 3, and is reflected in the optimum bond length (R_{NN} = 1.37 Å) for the $^3A_2$ state. While this bond is longer than the 1.24 Å of the $^1A_1(\pi)$ state, it is considerably shorter than the typical single NN bond length (e.g., 1.45 Å in hydrazine[12]). This delocalization is also reflected in the dipole moment, which is calculated to be 2.4 Debye.

Normally a doubly occupied amino π pair prefers a pyramidal geometry, thus the inversion barrier of NH_3 is 6 Kcal. However, for the $^3A_2(\pi\bar{\pi})$ state we find a very flat potential surface (planar favored by 0.1 Kcal over the pyramidal). This indicates ~6 Kcal of bonding due to the 3-electron pi bond of the planar configuration.

III. Calculational Details

A. Basis Set and Geometries. Dunning's (3s2p/2s) contraction of Huzinaga's (9s5p/4s) primitive Gaussian basis was used in all calculations. We also included one set of d-polarization functions (α = 0.8000) for each nitrogen. Such functions are important in calculating the singlet-triplet energy difference for methylene and, thus, should also be important in the analogous nitrene.

In the planar states, we considered only geometries with C_{2v} symmetry and used the following parameters: R_{N-H} = 1.016 Å; ∠ HNH = 115.4°. Since the most likely difference in geometry between

the $\pi\bar{\pi}$ and $\bar{\pi}^2$ states was expected to be in the nitrogen-nitrogen bond length, this parameter was optimized (a cubic spline fit to four points: R_{N-H} = 1.23, 1.33, 1.43, and 1.53 Å). The $^1A_1$ state was found to have an optimum bond length of 1.246 Å, while the $^3A_2$ state has a bond length of 1.374 Å. These optimum values were used in all subsequent calculations.

To determine the optimum pyramidal geometry for the lowest triplet state, the N–N and N—H bond lengths were fixed at 1.016 Å and 1.374 Å, while the HNH and NNH bond angles were varied linearly.

We compared the geometries from Hartree-Fock minimal basis set calculations on N_2H_4, H_2N_2, and NH_3 by Pople and coworkers with experimental values of N_2H_4 and NH_3 and estimated that pyramidal H_2N_2 would have $\measuredangle$ HNH = 107.0° and $\measuredangle$ NNH = 119.0°, while planar H_2N_2 $^3A_2$ ($\pi\bar{\pi}^2$) would have $\measuredangle$ HNH = 115.4° and $\measuredangle$ NNH = 122.3°. Extrapolating linearly we included a third point $\measuredangle$ HNH = 102.1° and $\measuredangle$ NHH = 117.1°. Converting to an inversion coordinate θ, where the planar corresponds to $\theta = 0$, and requiring that $\frac{dE}{d\theta} = 0$ at $\theta = 0$, the above three calculations correspond to five points. We fitted them to a cubic spline fit to obtain the optimum geometry.

B. The GVB Calculations. To describe accurately the variation of energy with bond length, we must consider those bonds which are directly involved in stretching. The Hartree-Fock (HF) wavefunction for the $^1A_1$ state of aminonitrene has eight doubly occupied orbitals. Breaking the nitrogen-nitrogen bond, retaining the planar geometry, yields the $^2A_1$ amino radical and ^2P nitrogen atom and hence requires HF wavefunctions consisting of seven doubly occupied orbitals and two

singly occupied orbitals. Thus a HF wavefunction does not properly describe the dissociation of the NN bond. Indeed as discussed in section I, the HF wavefunction leads to the wrong ground state, putting $^3A_2\,(\pi\bar{\pi})$ below $^1A_1\,(\bar{\pi}^2)$.

The GVB wavefunction allows every electron to have its own orbital. However, to describe properly the dissociation of the NN bond of the $^1A_1\,(\bar{\pi}^2)$ state, it is sufficient that only two HF pairs be correlated or split into pairs of non-orthogonal singly-occupied orbitals. The first pair corresponds to the NN sigma bond, which is directly involved in bond breaking. The second pair is the doubly-occupied π orbital on the central nitrogen.

Near R_e we expected and found that the amino lone pair exhibits delocalization characteristic of a pi bond pair and, hence, we need also to correlate this pair. For large R the most important correlation for the amino lone pair will be in-out correlation in which one electron occupies a more contracted orbital while the other occupies a more diffuse orbital. Near R_e the most important correlation is left-right (between the two nitrogens). A consistent description should allow both correlations, requiring three natural orbital for this π pair. Since the NH σ bond pair is described by two natural orbitals, the resulting wavefunction has two electron pairs that are not closed-shell (doubly occupied) and these two pairs are described with a total of five natural orbitals; thus this wavefunction is denoted GVB(2/5).

For the $^3A_2\,(\pi\bar{\pi})$ state the wavefunction in which the σ bond is correlated is denoted as GVB(2) [or GVB(2/4)] since there are two pairs of electrons that are not closed-shell. To be consistent with our

description of the $^1A_1$ ($\bar{\pi}^2$) state we also correlated the amino π pair using three natural orbitals, leading hence to a GVB(3/7) wavefunction for $^3A_2$ ($\pi\bar{\pi}$).

Although the above wavefunctions are expected to be adequate for geometry optimization, accurate excitation energies and bond strengths require close attention to small correlation effects not included in these wavefunctions.

To obtain reliable excitation energies requires correlation of the $\bar{\pi}$ pairs of the $^1A_1$ state (the $^3A_2$ state with only one electron in π and $\bar{\pi}$ leads to little correlation error), leading to a GVB(3/7) wavefunction for both $^1A_1$ and $^3A_2$.

To obtain an accurate NN bond energy requires correlation of other pairs localized near the NN bond since there will be interpair correlation effects important near R_e. Thus we increased the complexity of our GVB wavefunction by also correlating the orbitals corresponding to the two CH bonding pairs and the 2s non-bonding pair on the terminal nitrogen. This lead to GVB(6/13) wavefunctions for the $^3A_2$ and $^1A_1$ states. The GVB(6/13) wavefunction allows us to account for any differential correlation in the NH bond pairs between aminonitrene and amidogen. From previous studies on ethylene, it was found that accurate bond strenghts required the inclusion of two additional natural orbitals for the correlated CC sigma bond. In analogy we have included this correlation in our NN bond leading to a GVB(6/15) wavefunction.

C. CI Calculations. Two different levels of CI wavefunctions were used. In determining the NN bond length we carried out a full CI over the active orbitals of the GVB(2/5) wavefunction for $^1A_1$ and the GVB(3/7) wavefunction for $^3A_2$. For the singlet this utilized all configurations of the GVB pairs and the nitrene lone pair ($NN\sigma\sigma^*$, $LP_1\pi\pi_1^*\pi_2^*$, $LP_2\bar{\pi}^2$) leading to 50 spatial configurations (104 determinants) of the proper spin and spatial symmetry. The analogous CI was performed for the triplet, resulting in 27 spatial configurations (65 determinants). Note here that by optimizing the orbitals of the GVB wavefunction we allow high orders of correlation in just a few configurations.

In determining the NN bond energy we carried out considerably more complicated CI calculations. The reason is that it was necessary to include a consistent level of correlation effects for both N-aminonitrene and the separated molecules (i.e., NH_2 and N). a.) To account for all correlation effects about the NN sigma bond and π-orbitals, we allowed up to quadruple excitations within the set of seven GVB orbitals ($\sigma\sigma_1^*\sigma_2^*\sigma_3^*\pi\pi_1^*\pi_2^*$) describing the four electrons of the NN bond and π-lone pair, with the restriction that there be no excitations between the σ and π sets. [In the $^3A_2$ case we also included in this CI the singly-occupied π orbital on the terminal nitrogen.] b.) In the $^1A_1$ case, to allow for correlation of the $\bar{\pi}$ lone pair by the π-orbitals, we added to this set another set involving quadruple excitation within the space ($\sigma\sigma_1^*\sigma_2^*\sigma_3^*\bar{\pi}\pi_1^*\pi_2^*$). At large R such excitations are required to describe the ^2D and ^2P states of N atoms. c.) In order to account for correlation effects available to the separated molecules but not normally utilized

in aminonitrene, and to include interpair correlation effects important in the molecule we added another set of configurations involving all six pairs of GVB orbitals: A = NN ($\sigma\sigma^*$); B = LP_1 ($\pi\pi^*$); C = NH_1 ($\sigma\sigma^*$) + NH_2 ($\sigma\sigma^*$); D = 2s ($\sigma\sigma^*$); E = LP_2 ($\overline{\pi},\overline{\pi}^*$) for $^1A_1$ or E = LP_2 ($\pi,\overline{\pi}$) for $^3A_2$. Here we allowed all double excitations in set A, in set B and in set C simultaneous with all single excitations within set D and within set E but with the restrictions that (i) no excitations higher than quadruple be included and (ii) no excitations between sets be allowed. d.) In addition to the above, all single excitations from the dominant configurations were included. The results of a, b, c, and d are 139 spatial configurations (256 spin eigenfunctions) of the proper symmetry for the $^1A_1$ case and 181 spatial configurations (687 spin eigenfunctions) of the proper symmetry for the $^3A_2$ case.

We should emphasize here that despite only a moderate number of configurations this wavefunction contains a very intensive level of correlation effects including a vast number of triple and quadruple excitations. This is possible since we have self-consistently determined the optimum correlating orbitals by carrying out the GVB calculations. This does two things for us. First it reduces the number of orbitals that need be considered in the CI, greatly reducing the number of configurations resulting from a given level of CI. Secondly since the GVB orbitals are localized with chemically identifiable character, we can develop conceptual schemes identifying which higher order correlations are essential. This serves the purpose of keeping down the total number of excitations (while including all important effects) but just as important, the conceptual scheme resulting from the GVB wavefunction

allows us to compare wavefunctions of different states and geometries and thereby to establish (before calculations) consistent levels of correlation sufficient to trust excitation energies, bond energies, etc. Thus we have benefitted here from studies on ethylene and methylene which established guidelines on consistent levels of correlation that apply also to the states of aminonitrene.

IV. The GVB Orbitals

A. The $^1A_1$ State. The GVB(6) orbitals of the $^1A_1$ ($\bar{\pi}$) ground state are shown in Fig. 2. We find that the orbitals localize in different regions and have the basic character of valence bond wavefunctions.

In the σ-system there are five different bonding pairs. The first pair (A) corresponds to the NN sigma bond; one orbital centered on the central nitrogen is hybridized[13] ($sp^{2.8}$) toward the terminal nitrogen, while the other orbital centered on the terminal nitrogen is hybridized ($sp^{3.3}$) toward the central nitrogen. The next two pairs (C,D) correspond to the NH σ bonds--one pair for each bond. The two pairs are identical and consist of two orbitals: one centered on the hydrogen is essentially spherical with some delocalization toward the central nitrogen, while the other is an sp^2-type orbital (actually $sp^{1.7}$) centered on the central nitrogen and hybridized toward the hydrogen.

In section II the description of the $^1A_1$ ($\bar{\pi}^2$) state involved a $\bar{\pi}$ lone pair

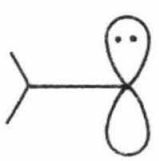

(14)

and a N 2s pair

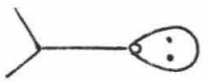

(15)

However, with the GVB(6) wavefunction we find the orbitals (E, F) of Fig. 2 can be represented as

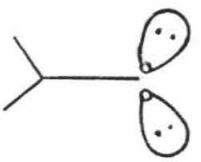

(16)

[ignoring in (16) the correlation within each lone pair] where each lone pair has hybridization of $sp^{1.4}$. For a (closed shell) HF wavefunction the energy of (16) and

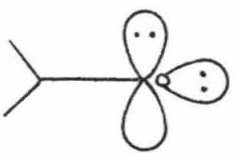

(17)

would be identical (corresponding to combining columns of the determinant wavefunction). However, for the GVB wavefunction, (16) and (17) lead to different energies with (16) being favored. On the other hand, the energy of the GVB(6) wavefunction of form (17) [contracted from the orbitals of the GVB(6) wavefunction for (16)] is only 6.0 kcal higher than those of (16) so that the distortion between (16) and (17) is energetically of only little importance. Exciting or ionizing one electron out of one of the lone pair orbitals leads to

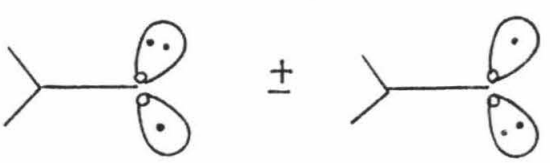

(18)

based on (16) and

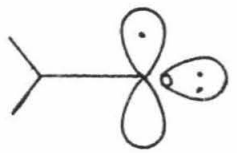

(19a)

or

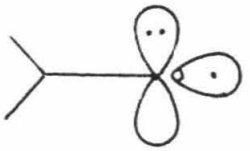

(19b)

based on (17). Again these descriptions are nearly equivalent; however (19) is simpler to represent and hence is preferred for discussing excited and cation states. Thus we continue to use (17) in describing $^1A_1$ ($\overline{\pi}^2$) although the orbitals can best be described as (16).
It is interesting to note that the two lone pairs and the NN σ bond are essentially trigonal about the terminal nitrogen, having hybridization of $sp^{1.7}$, $sp^{1.4}$, and $sp^{1.4}$.

From Figure 2, we can see that the π system consisting of a doubly occupied lone pair orbital (B) on the central nitrogen is considerably delocalized onto the terminal nitrogen as expected from our earlier discussion (see section II).

Energy lowerings and overlaps for these GVB orbitals are listed in Table I.

B. The $^3A_2$ State. The bonding pairs corresponding to the NH bonds (not shown) and NN σ-bond are essentially identical with the corresponding $^1A_1$ orbitals (see Fig. 3).

The two triplet coupled orbitals (π and $\overline{\pi}$) are essentially pure p_x and p_y orbitals centered on the terminal nitrogen. The π lone pair on the central nitrogen is delocalized somewhat onto the terminal

nitrogen, with a corresponding amount of antibonding character in the singly occupied π orbital.

The remaining orbital on the nitrene N corresponds to a doubly occupied, N 2s-like orbital [hybridized (sp^2) along the z-axis].

Thus the triplet state can best be represented:

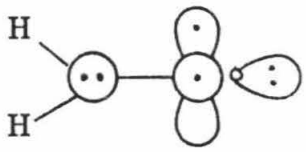

In Fig. 4 we show the orbitals for the $^3A''$ state which corresponds to bending the hydrogens of the $^3A_2$ state out of the plane. The major change is that the delocalization of the π-lone pair is reduced.

V. Additional Quantitative Results

A. Inversion Barrier. As in NH_3 the H configuration about an amino N is generally nonplanar and hence for the $^3A_2$ ($\pi\overline{\pi}$) state we carried out calculations to determine the geometry and energy barrier. With the GVB(3/7) wavefunction we found a pyramidal geometry (the angle between the H_2N plane and the NN axis being 43.7°) with an inversion barrier of 1.7 kcal mole^{-1}. For comparison NH_3 has an angle[12] of 61.3° and a barrier[14] of 5.8 kcal mole^{-1}, while H_2N-NH_2 has pyramidal angles[12] of 49.6° and a barrier[12] of 2.8 kcal mole^{-1}. With minimum basis HF, Pople et al.[15] found a pyramidal geometry for H_2NN of 36.6°. However, including all the correlation effects for the GVB(6/13)-CI at the planar and optimum pyramidal geometries led to the planar geometry being favored by 0.1 Kcal mole^{-1}.

Figure 2. GVB orbitals of the $^1A_1$ state of aminonitrene based on the GVB(6/13) wavefunction. Long dashes indicate zero amplitude; the spacing between contours is 0.05 a.u. The same conventions are used for all plots.

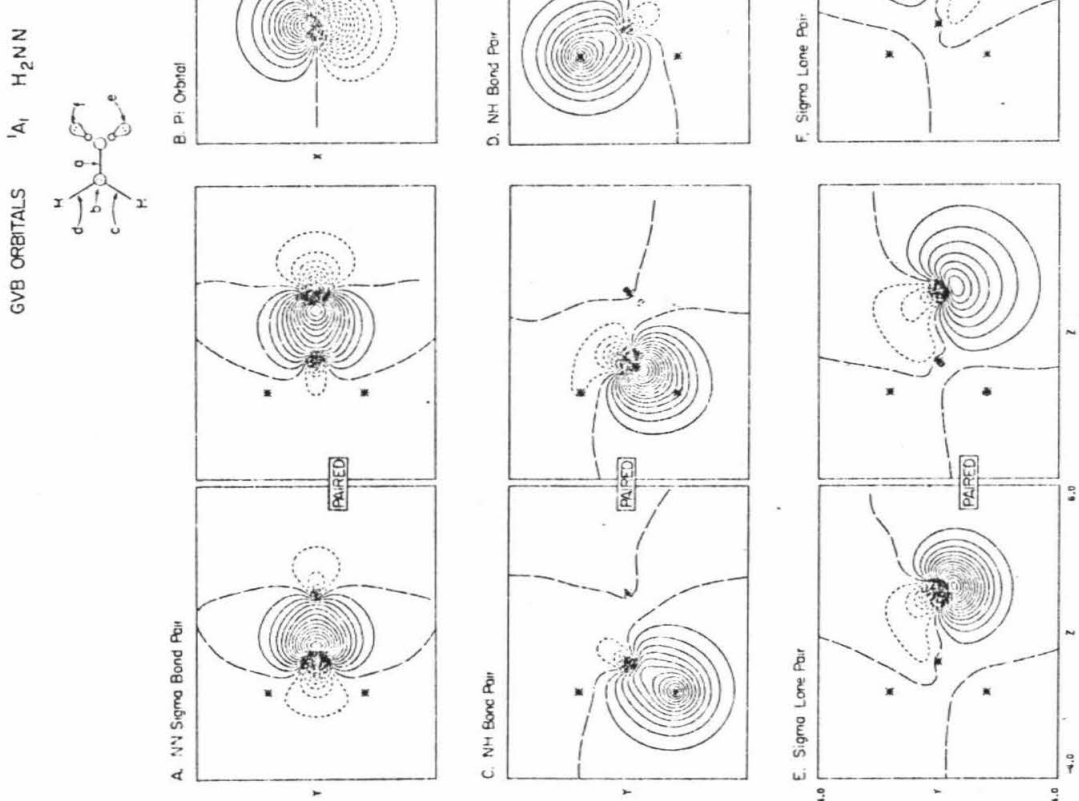
GVB ORBITALS $^1A_1$ H_2NN
A. NN Sigma Bond Pair
B. Pi Orbital
C. NH Bond Pair
D. NH Bond Pair
E. Sigma Lone Pair
F. Sigma Lone Pair
PAIRED
PAIRED
PAIRED
PAIRED
PAIRED
PAIRED
X
Y
Z
Z
Z
Z
6.0
-4.0
6.0
-4.0

Figure 3. Selected GVB orbitals of the $^3A_2$ state of aminonitrene based on the GVB(6/13) wavefunction.

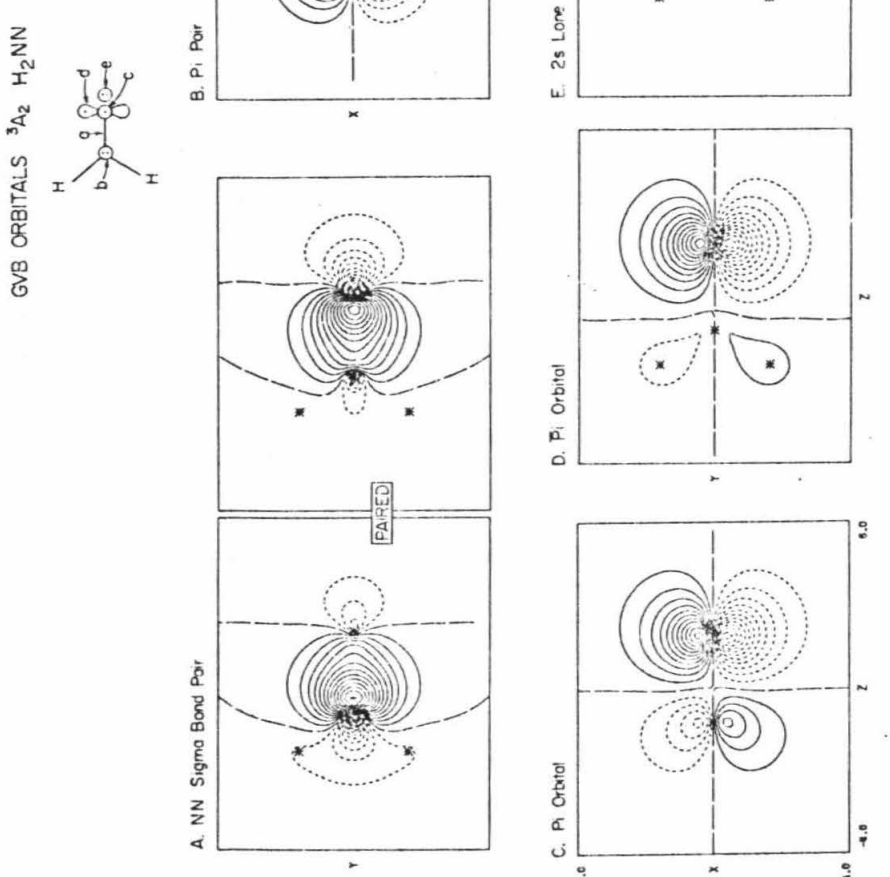
GVB ORBITALS $^3A_2$ H_2NN
A. NN Sigma Bond Pair
PAIRED
B. Pi Pair
PAIRED
C. Pi Orbital
D. Pi Orbital
E. 2s Lone Pair
PAIRED
H
H
a
b
c
d
e
g
f
X
Y
Z
6.0
-6.0

Table I. Pair Quantities for the GVB(6/15) Calculations

State	Energy	Pair	Overlap	Energy lowering (a.u.)
$^1A_1$	-110.10915	NH-sigma	0.872	0.0181
		NH-left	0.840	0.0172
		NH-right	0.840	0.0172
		π-lone pair/bond	0.712	0.0293
		$\bar{\pi}$-lone pair	0.876	0.0095
		2s-lone pair	0.876	0.0095
$^3A_2$	-110.08525	NN-sigma	0.831	0.0233
		NH-left	0.844	0.0162
		NH-right	0.844	0.0162
		π-lone pair	0.882	0.0083
		2s-lone pair	0.919	0.0048
$^3A''$ (pyramidal)	-110.08513	NN-sigma	0.827	0.0237
		NH-left	0.840	0.0167
		NH-right	0.840	0.0167
		π-lone pair	0.881	0.0106
		2s-lone pair	0.919	0.0048

Table II. Excitation Energies and Dominant Configurations for Aminonitrene [GVB(6/15)-CI

State	Excitation Energy[a] (eV)	Configuration																Energy Lowering (hartrees)
		NH Bonds				NN-sigma bond				pi lone pair				lone pair		2s lone pair		
		a_1	a_1^*	b_2	b_2^*	σ	σ^*	σ^*	$\bar{\pi}$	π	π^*	π^*		π	$\bar{\pi}$	σ	σ^*	
$^1A_1$	0.00[b]	2	0	2	0	2	0	0	0	2	0	0		0	2	2	0	--
		2	0	2	0	2	0	0	0	0	2	0		0	2	2	0	0.0167
		2	0	2	0	1	1	0	0	1	1	0		0	2	2	0	0.0142
		2	0	2	0	0	2	0	0	2	0	0		0	2	2	0	0.0103
$^3A_2$	0.65	2	0	2	0	2	0	0	0	2	0	0		1	1	2	0	--
		2	0	2	0	0	2	0	0	2	0	0		1	1	2	0	0.0155
		2	0	1	1	2	0	0	0	1	1	0		1	1	2	0	0.0078
		2	0	2	0	1	1	0	0	1	0	0		1	1	2	0	0.0074
$^1A_2$	2.22	2	0	2	0	2	0	0	0	2	0	0		1	1	2	0	--
		2	0	2	0	2	0	0	0	1	0	0		2	1	2	0	0.0149
		2	0	2	0	0	2	0	0	2	0	0		1	1	2	0	0.0143
		2	0	2	0	1	1	0	0	1	0	0		2	1	2	0	0.0127
$^1A'$	7.06[c]	2	0	2	0	2	0	0	0	2	0	0		2	0	2	0	--
		2	0	2	0	2	0	0	0	1	0	0		1	2	2	0	0.0071
		2	0	2	0	1	1	0	0	1	0	0		1	2	2	0	0.0019
		2	0	2	0	2	0	0	0	0	0	0		2	2	2	0	0.0013
$^3A_2$	8.84	2	0	2	0	2	0	0	0	1	0	0		2	1	2	0	--
		2	0	2	0	1	1	0	0	1	0	0		2	1	2	0	0.0341
		2	0	2	0	1	1	0	0	2	0	0		1	1	2	0	0.0095
		2	0	2	0	0	1	0	0	1	0	0		2	1	2	0	0.0075
$^1A_2$	9.26	2	0	2	0	2	0	0	0	1	0	0		2	1	2	0	--
		2	0	2	0	1	1	0	0	1	0	0		2	1	2	0	0.0355
		2	0	2	0	1	1	0	0	2	0	0		1	1	2	0	0.0096
		2	0	2	0	0	2	0	0	1	0	0		2	1	2	0	0.0080
$^1A_1$	13.29[b]	2	0	2	0	2	0	0	0	1	1	0		0	2	2	0	--
		2	0	2	0	2	0	0	0	0	2	0		0	2	2	0	0.0234
		2	0	2	0	1	1	0	0	2	0	0		0	2	2	0	0.0200
		2	0	2	0	2	0	0	0	2	0	0		1	1	2	0	0.0139

[a] Planar triplet geometry unless specified.

[b] Planar singlet geometry.

[c] Pyramidal triplet geometry.

Figure 4. Selected GVB orbitals of the pyramidal $^3A''$ state of aminonitrene based on the GVB(6/13) wavefunction.

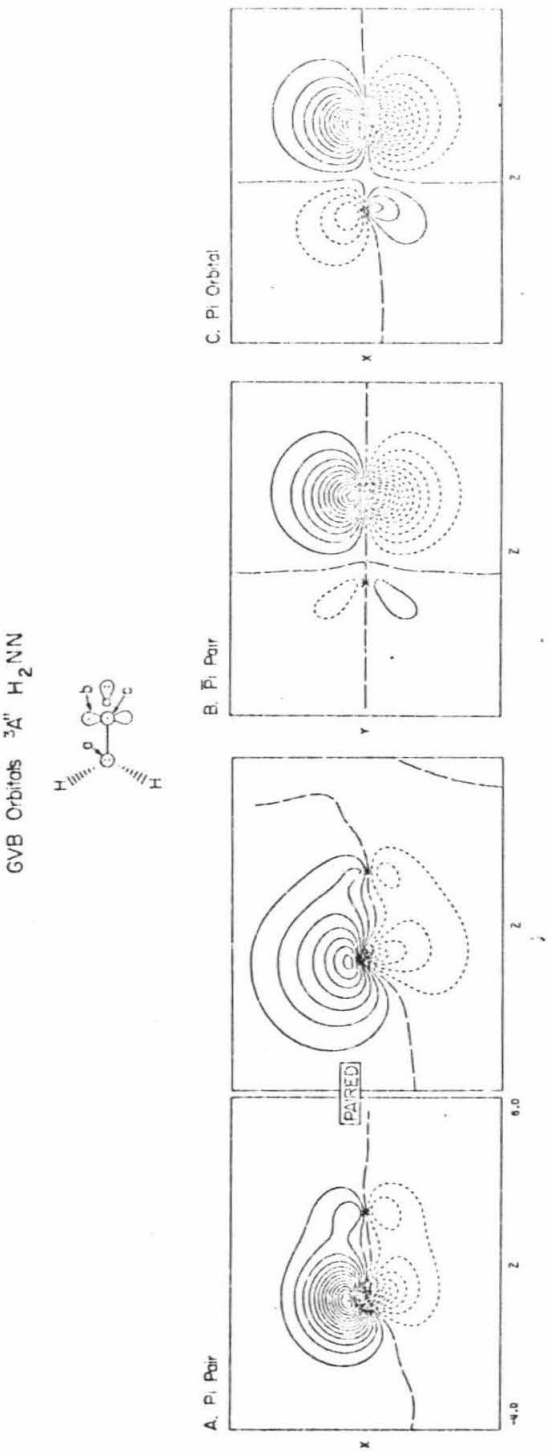
GVB Orbitals $^3A''$ H_2NN
A. Pi Pair
PAIRED
B. Pi Pair
C. Pi Orbital
6.0
-4.0
x
z
y

Because of the strong π bonding of $^1A_1$ ($\bar{\pi}^2$) we assumed that the geometry is planar and did not carry out calculations of the inversion barrier.

B. Ionization Potentials. The first ionization from $^1A_1$ ($\bar{\pi}^2$) is out of the doubly occupied $\bar{\pi}$ orbital, leading to a $^2B_2$ ion at 9.4 eV (see Table III). This same ion state is also obtained from $^3A_2$ ($\pi\bar{\pi}$) by ionization of the unpaired π-electron (8.8 eV indicating the effect on the amino lone pair in this orbital). Ionization of the $\bar{\pi}$-electron of the $^3A_2$ state costs 11.4 eV resulting in a $^2B_1$ ion at 12.1 eV above $^1A_1$. Ionization of an electron from the doubly occupied π lone pair of the $^3A_2$ results in three ions all having the same spatial configuration:

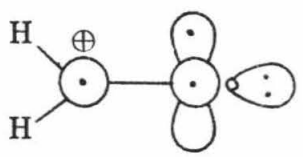

leading to a quartet state and two doublets. Singlet-coupling of the two π-electrons to yield a π-bond results in a $^2B_2$ state at 13.8 eV (13.1 eV above $^3A_2$). The resulting two states have triplet pairing of the $\pi,\bar{\pi}$ orbitals leading to $^4B_2$ of 12.3 eV and $^2B_2$ at 18.7 eV.

C. Excitation Energies. The first excited $^3A_2$ state corresponds not to a $\pi \rightarrow \pi^*$ transition as might have been expected but instead to an excitation of the doubly occupied π lone pair to the singly occupied π orbital. The singlet $\pi \rightarrow \pi^*$ transition is seen at 13.3 eV; since we neither included diffuse functions nor solved self-consistently for this state, this energy is expected to be far too high.

Table IV. Ionization Potentials and Dominant Configurations for Antisymmetrized [GVB(6/15)-CI]

State	Ionization Potential[a] (eV)	Configuration: NH Bonds				NN-sigma bond				pi lone pair				lone pair		2s lone pair		Energy Lowering (hartrees)
		a_1	a_1^*	b_2	b_2^*	σ	σ^*	σ'	$\bar{\sigma}$	π	π'	π^*		π	$\bar{\pi}$	σ	σ^*	
$^3B_2$	9.40	2	0	2	0	2	0	0	0	2	0	0		0	1	2	0	--
		2	0	2	0	2	0	0	0	1	0	0		1	1	2	0	0.0154
		2	0	2	0	1	1	0	0	1	0	0		1	1	2	0	0.0019
		2	0	2	0	2	0	0	0	0	0	0		2	1	2	0	0.0011
$^2B_2$	12.05	2	0	2	0	2	0	0	0	2	0	0		1	0	2	0	--
		2	0	2	0	2	0	0	0	1	0	0		2	0	2	0	0.0359
		2	0	1	0	2	0	0	0	2	0	0		1	1	2	0	0.0139
		2	0	2	0	2	0	0	0	2	0	0		1	0	1	1	0.0121
$^4B_2$	12.27	2	0	2	0	2	0	0	0	1	0	0		1	1	2	0	--
		2	0	2	0	0	2	0	0	1	0	0		1	1	2	0	0.0179
		2	0	1	1	2	0	0	0	1	0	0		1	1	2	0	0.0169
		2	0	2	0	2	0	0	0	0	1	0		1	1	2	0	0.0140
$^2B_2$	13.76	2	0	2	0	2	0	0	0	1	0	0		1	1	2	0	--
		2	0	2	0	0	2	0	0	1	0	0		1	1	2	0	0.0173
		2	0	1	1	2	0	0	0	1	0	0		1	1	2	0	0.0162
		2	0	2	0	2	0	0	0	0	1	0		1	1	2	0	0.0132
$^2B_2$	13.86[b]	2	0	2	0	2	0	0	0	1	0	0		0	2	2	0	--
		2	0	1	1	2	0	0	0	1	0	0		0	2	2	0	0.0138
		2	0	2	0	2	0	0	0	0	1	0		0	2	2	0	0.0120
		2	0	2	0	0	2	0	0	1	0	0		0	2	2	0	0.0111

[a] Planar triplet geometry unless specified.

[b] Planar singlet geometry.

Figure 5. Electronic states of aminonitrene and aminonitrene cation. Energies in electron volts. (1 hartree = 27.2116 eV = 627.5096 kcal $mole^{-1}$)

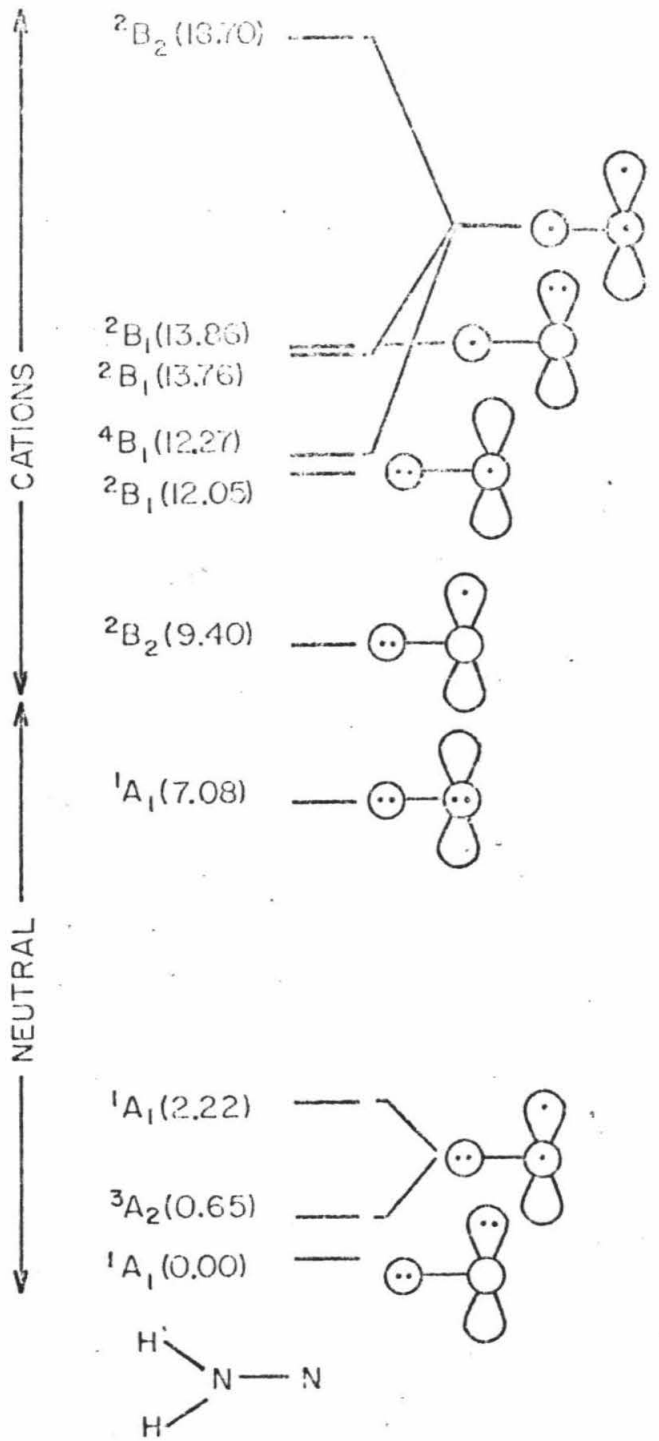
CATIONS
NEUTRAL
$^2B_2$ (13.70)
$^2B_1$ (13.86)
$^2B_1$ (13.76)
$^4B_1$ (12.27)
$^2B_1$ (12.05)
$^2B_2$ (9.40)
$^1A_1$ (7.08)
$^1A_1$ (2.22)
$^3A_2$ (0.65)
$^1A_1$ (0.00)
H
N — N
H

D. Dipole Moments. In GVB wavefunctions the orbitals are unique and localized with chemically identifiable characteristics making it useful to analyze properties such as dipole moments in terms of orbital contributions. In order for the dipole moment to be independent of origin we associate with the electron of each orbital a unit nuclear charge centered at the nucleus on which the orbital is centered (in the VB model). This leads to the results shown in Table IV.

The dipole moment of the $^3A_2$ ($\pi\bar{\pi}$) state is dominated by the nitrene nitrogen 2s pair which hybridizes away from the molecule due to formation of the NN σ bond. This orbital leads to a dipole moment of 2.684 D, while the other orbitals lead to 0.333 D in the opposite direction resulting in a total dipole moment of 2.351 D.

For the $^1A_1$ ($\bar{\pi}^2$) state the major change from $^3A_2$ is the extensive delocalization of the amino π pair due to the lack of a nitrene π electron. Thus the π system of $^1A_1$ has an increased dipole moment of 3.30 D. In response to this shift of π charge to the right, the sigma orbitals all shift charge back to the left. The net increase in dipole moment for $^1A_1$ is 1.69 D leading to a total μ of 4.036 D.

It would be hoped that such analyses will eventually lead to constructing transferable bond dipoles useful in predicting dipole moments of molecules. One of the limits on such procedures can be seen in Table IV where the NH dipole is 0.358 D at an angle of 73.6° with the NN axis in $^3A_2$ and 0.486 D at an angle of 54.0° in $^1A_1$ (the NH angle is is 57.7°). It is not immediately obvious how one could predict the dipoles for the $^3A_2$ case knowing the values for the $^1A_1$ state.

Table IV. Contributions to the Dipole Moment of Aminonitrene (here a positive moment implies movement of electrons toward the nitrene end of the molecule); Based on the GVB(6/15) Wavefunction. [All quantities in atomic units unless indicated otherwise; 1 a.u. = 2.541765 Debye.]

Orbitals	$^3A_2$		$^1A_1$	
	Y	Z	Y	Z
Non GVB (1s)	0.0	0.0	0.0	-0.001
NH Bonds				
Left	-0.360	-0.106	-0.354	-0.257
Right	0.360	-0.106	0.354	-0.257
2s Pair	0.0	1.056	-1.429	0.454
$\bar{\pi}$	0.0	-0.126	1.432	0.442
NN σ Bond	0.0	-0.029	-0.003	-0.091
π Pair	0.0	0.548	0.0	1.297
π	0.0	-0.312	-	-
Total σ	0.0	0.689	0.0	0.291
Total π	0.0	0.238	0.0	1.297
Total				
a.u.	0.0	0.925	0.0	1.588
Debye	0.0	2.351	0.0	4.036

E. Heat of Formation. Since our GVB(6/15)-CI wavefunction for aminonitrene is sufficiently correlated to describe accurately the breaking of the nitrogen-nitrogen bond, we can expect accurate values for the bond dissociation energy for aminonitrene.

From the GVB diagram the dissociated $^1A_1$ state is

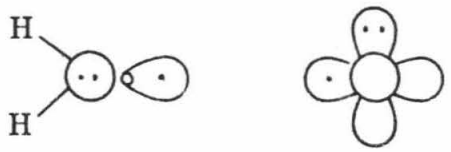

(20)

while the dissociated $^3A_2$ state is

(21)

Here we have retained the planar geometry, forming the NH_2 group to go to the $^2A_2$ excited state rather than the $^2B_1$ ground state. As discussed

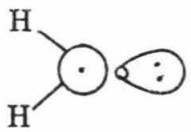

(22)

in section II, the configuration (3) for N in (19) describes neither ^2D nor ^2P (a correct adiabatic description would lead to ^2D here).

In order to obtain bond energies we must carry out consistent calculations of both the molecule and the separate fragments. We elected to do this for the $^3A_2$ state and to calculate the bond energy of $^1A_1$ using the calculated excitation energy.

The basic principles in the CI calculations for bond energies are: (i) Fully correlate (several natural orbitals) the bond pairs that are

broken; (ii) Correlate the orbitals for the other bond pairs and lone pairs associated with the atoms of the broken bond and allow single excitations in these pairs simultaneous with singles in the bond pairs (this allows the important interpair correlations that affect bond energies); (iii) In the case that either the molecule or separated fragment has empty valence orbitals or an open shell configuration include the appropriate strong mixing configurations. In some cases these principles will lead to a HF wavefunction of the dissociated fragment and in others to a correlated wavefunction.[16]

The relevant energies are given in Table V leading to a bond energy of

$$D'_e[H_2N\text{–}N(^3A_2)] = 89.2 \text{ Kcal mole}^{-1}.$$

In Table V we see that the HF wavefunction leads to an error of 43 Kcal in the bond energy and that various levels of GVB (without the additional interpair terms) lead to errors of 25-30 Kcal. Thus these interpair correlation effects are quite important and must be included for results of chemical usefulness.

Since an experimental determination of this bond energy would include the difference in zero-point energies of the molecule and fragments, it is necessary to apply a zero-point vibrational energy correction to D'_e. Estimating the vibrational frequencies for $^3A_2$ aminonitrene based on the average frequencies of hydrazine (as shown in Table VI) and using the experimental values of NH_2, we calculate a zero-point correction 4.0 Kcal mole^{-1}. Thus we predict the dissociation energy for $^3A_2$ aminonitrene to $^2A_1$ NH_2 and ^4S N is $D'_0(H_2NN)$ = 85.2 Kcal mole^{-1}.

Table V. Comparison of Calculated N-N Bond Energies, $D_e(H_2N-N)$, from Various Wavefunctions. Total energies in hartrees, D_e in Kcal mole^{-1}. 1 h = 627.5096 Kcal mole^{-1}.

	HF	GVB(2/5)	GVB(6/15)	GVB(6/15)-CI
$H_2NN(^3A_2)$	-109.98680	-110.014071	-110.05526	-110.08525
$H_2H(^2A_1)$	-55.51338[a]	-55.52523[b]	-55.55379[c]	-55.54874[d]
$N(^4S)$	-54.39441[a]	-54.39441[a]	-54.3992[b]	-54.39441[a]
$D_e(H_2N-N)$ Kcal mole^{-1}	46.6	59.2	6 .2	89.2

[a] HF

[b] GVB(1)

[c] GVB(2)

[d] GVB(2)-CI

Table VI. Vibrational Frequencies Used in Zero-Point Energy Calculation

Vibration		$H_2NN(^3A_2)$	$H_2NN(^1A_1)$ (estimated)[a]	$H_2N(^2A_1)$ (experimental)[b]
NH	a_1	3270	3270	3173
	b_2	3340	3360	3226
NH_2	a_1	1294	1294	1449
	b_2	1016	1016	--
	b_1	873	873	--
NN	a_1	875	1224[c]	--
Total zero-point energy (Kcal $mole^{-1}$)		30.50	31.50	22.56

[a]Based on experimental results in hydrazine; ref. 12.

[b]Ref. 12.

[c]Estimated from $^3A_2$ using ratio of force constants obtained in parabolic fit of bond legnths.

This D_0' applies to dissociation to the $^2A_1$ excited state of NH_2, but we want to obtain the dissociation energy with respect to ground state products $[N(^4S) + NH_2(^2B_1)]$. Using the experimental[17] $^2A_1$–$^2B_1$ splitting for NH_2, 29.3 Kcal mole^{-1}, we calculate

$$D_0[H_2NN(^3A_2)] = 55.9 \text{ Kcal mole}^{-1}.$$

Using the calculated $^3A_2$-$^1A_1$ splitting for H_2NN and correcting for differential zero-point energies, we calculate

$$D_0[H_2NN(^1A_1)] = 70.4 \text{ Kcal mole}^{-1}.$$

This $D_0(^1A_1)$ can now be used to predict the heat for formation of aminonitrene. Using the experimental values[12] for the heat of formation of $NH_2(^2A_1)$ and nitrogen atom (^4S) and the theoretical D_0, we calculate the heat of formation of $^1A_1$ aminonitrene as

$$\Delta H_{f_{0°K}}[H_2NN(^1A_1)] = 70.1 + 112.5 - 70.4 = 112.6 \text{ Kcal mole}^{-1}$$

Using our geometry and predicted vibrational frequencies we find that

$$\Delta H_{f_{298°K}}[H_2NN(^1A_1)] = 114.3 \text{ Kcal mole}^{-1}.$$

Thus we find that aminonitrene is 60 Kcal mole^{-1} higher in energy than the isomeric diimide.[12] Indeed this means that the ground state of aminonitrene is 9.2 Kcal <u>above</u> the energy of

$$N_2 + 2H$$

indicating a rather unstable molecule. Thus if N_2H is stable with $N_2 + H$

then the process of $H_2NN(^1A_1) \rightarrow HNN + H$ is exothermic by more than 9 Kcal (there could still be an energy barrier to this dissociation).

We can now use this D_0 to predict heats of formation for a variety of substituted aminonitrenes. For example, the heat of formation[18] of piperidine is 0.90 Kcal mole^{-1}; combining this with our $D_0(^1A_1)$ and a N–H bond energy of 102 Kcal mole^{-1}, we calculate that piperidine nitrene $\underset{\sim}{2}$, has a heat of formation of

$$\Delta H_{f_{0°K}}(\underset{\sim}{2}) = 30.7 \text{ Kcal mole}^{-1} \qquad (23)$$

Comparing this number to the heat of formation of the cyclic azo compound $\underset{\sim}{1}$ ($\Delta H_f = 26.3$) we conclude that the rearrangement of $\underset{\sim}{2} \rightarrow \underset{\sim}{1}$ should be only 4 Kcal mole^{-1} exothermic. Comparing ($\underset{\sim}{2}$) with the ΔH_f of the tetramethylene biradical the activation energy for blowing the N_2 out of piperidine nitrene, $\underset{\sim}{2}$, is estimated as 31 Kcal mole^{-1}. Such types of estimates should be quite useful in understanding the thermal rearrangements and reactions of nitrenes.

VI. Summary

We find the ground state of aminonitrene is the singlet state ($^1A_1$) with a triplet state ($^3A_2$) at 15.0 Kcal mole^{-1}. This stabilization of the singlet state is due to a large amount of double bond character in the NN bond.

We find the nitrogen-nitrogen bond dissociation energy for aminonitrene to be 70.4 Kcal mole^{-1} for the $^1A_1$ ground state of aminonitrene leading to $\Delta H_{f_{0°K}}$ of 112.6 kcal mole^{-1}.

The dipole moment is found to be 4.036 D for the $^1A_1$ and 2.351 D for the $^3A_2$ state of aminonitrene. The ionization potential in $H_2NN(^1A_1)$ is calculated to be 9.4 eV.

The various properties of the states of aminonitrene are quite consistent with the GVB model for this molecule.

References

(1) This work was supported by a John and Beverly Stauffer Foundation Fellowship, 1975-1976.

(2) J. Chatt, J. Organometallic Chem., 100, 17 (1975).

(3) J. M. Martiques and J. E. Bercaw, J. Am. Chem. Soc., 96, 6229 (1974); J. E. Bercaw, J. Am. Chem. Soc., 96, 5087 (1974).

(4) For example, see P. B. Dervan and T. Uyehara, J. Am. Chem. Soc., 95, 2003 (1976).

(5) P. B. Dervan, private communication.

(6) D. M. Lemal in "Nitrenes", W. Lwowski, Ed., Interscience Publishers, New York (1970).

(7) N. C. Baird and R. F. Barr, Can. J. Chem., 51, 3303 (1973).

(8) W. A. Goddard III, T. H. Dunning, Jr., W. J. Hunt and P. J. Hay, Accts. Chem. Res., 6, 368 (1973).

(9) G. Herzberg, "Molecular Spectra and Molecular Structure," Vol. I, D. Van Nostrand Company, Inc., Princeton (1950).

(10) S. N. Suchard, Spectroscopic Constants for Selected Heteronuclear Diatomic Molecules, Air Force Report No. SAMSO-TR-74-82, U. S. Government Printing Office, Washington, D. C., 1974.

(11) An orbital which is symmetric with respect to the molecular plane but antisymmetric with respect to the perpendicular plane passing through the CC axis is denoted by $\bar{\pi}$.

(12) JANAF Thermochemical Tables, NSRDS-NBS 37, U.S. Government Printing Office, 1970.

(13) Hybridization was determined by Mullikan population analysis of the GVB orbitals. We did not include the contribution of d-functions to the hybridization, since in all cases the contribution was small. E.g., in N-N sigma bond, orbitals are actually $sp^{3.3}\ d^{0.1}$ and $sp^{2.1}\ d^{0.0}$

(14) J. D. Swalen and J. A. Ibers, J. Chem. Phys., 36, 1914 (1962).

(15) W. A. Lathan, L. A. Curtiss, W. J. Hehre, J. B. Lisle, and J. A. Pople, Progress in Physical Organic Chemistry, 11, 175 (1974).

(16) One approach[19] has been to build in only those correlations that do not disappear at $R = \infty$ (leading to HF wavefunctions for the separated fragments). Such an approach can lead to inconsistent levels of correlation and tends to provide too large a bond energy.

(17) G. Herzberg, "Molecular Spectra and Molecular Structure," Vol. III, D. Van Nostrand, Inc., Princeton (1966).

(18) S. W. Benson, "Thermochemical Kinetics," John Wiley and Sons, Inc., New York (1968).

(19) W. J. Stevens, G. Das, A. C. Wahl, M. Krauss, P. Newmann, J. Chem. Phys., 61, 3686 (1974) and references quoted therein.

PART E: MECHANISM OF THE THERMAL AROMATIZATION OF 3,3'-BICYCLOPROPENYLS

The rearrangement of 3,3'-bicyclopropenyls (1) to benzene derivatives (2) is one of the most exothermic unimolecular isomerizations known (ΔH°_{rxn} = 120 kcal/mole[2]). Its mechanism, however, is not well

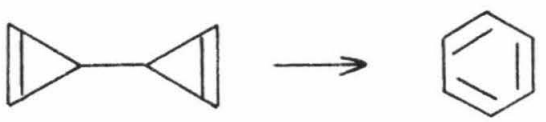

1 2

understood. This rearrangement has been postulated to proceed through Dewar benzene,[3] benzvalene,[4] prismane,[5] diradical,[6] and ionic[3] intermediates, although to date no definitive evidence has been available for distinguishing between these mechanisms.

In 1959, Breslow and Gal[7] first prepared hexaphenylbicyclopropenyl (4) by dimerization of triphenylcyclopropenyl radical (3) and observed its thermal isomerization to hexaphenylbenzene (5). They proposed that the reaction proceeded by initial 2+2 cyclization to hexaphenylprismane (6) followed by rearrangement to hexaphenyl Dewar benzene (7). Subsequent isomerization of 7 would then yield 5. A subsequent study[5] of the isomerization of tetraphenylbicyclopropenyl (8) supported this mechanism, although it did not rule out other possibilities. Pyrolysis of 8 was found to give 1,2,4,5-tetraphenylbenzene (9) and 1,2,3,4-tetraphenylbenzene (10) in a ratio of 10:1 at 135°. The product ratio, as well as the absence of 1,2,3,5-tetraphenylbenzene among the products, was consistent with the prismane mechanism. Isomerization of the proposed tetraphenylprismane by cleavage of the more-substituted

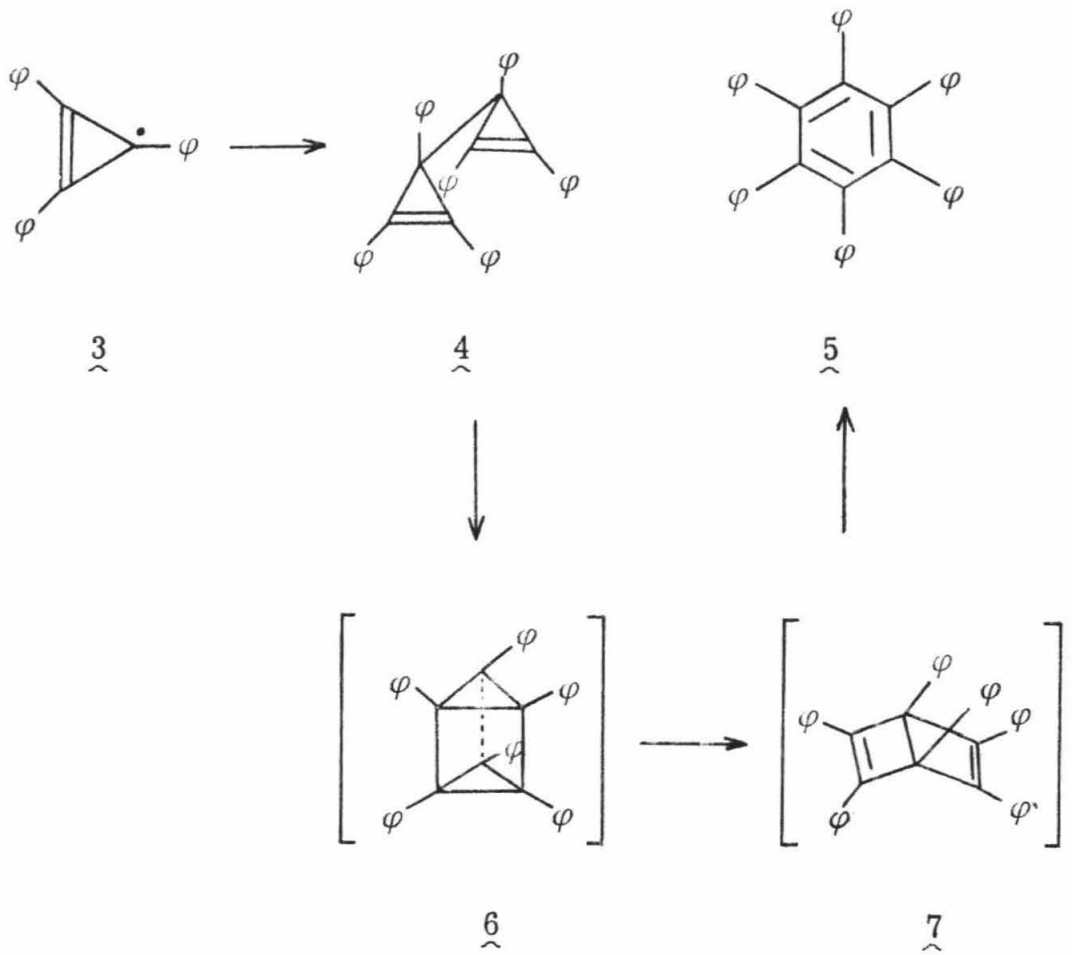

3 4 5

6 7

cyclopropane bonds (path a) would lead to the less sterically hindered Dewar benzene; thus path a would predominate over path b.

In 1973, Weiss and Andrae[3] observed the formation of a Dewar benzene in the thermal rearrangement of 11. Pyrolysis of 11 in refluxing dichloromethane for four weeks led to benzene derivatives 13 and 14 as the sole products; however, after two weeks of pyrolysis, 9% of the Dewar benzene 12 was observed by NMR.[8] In analogy with

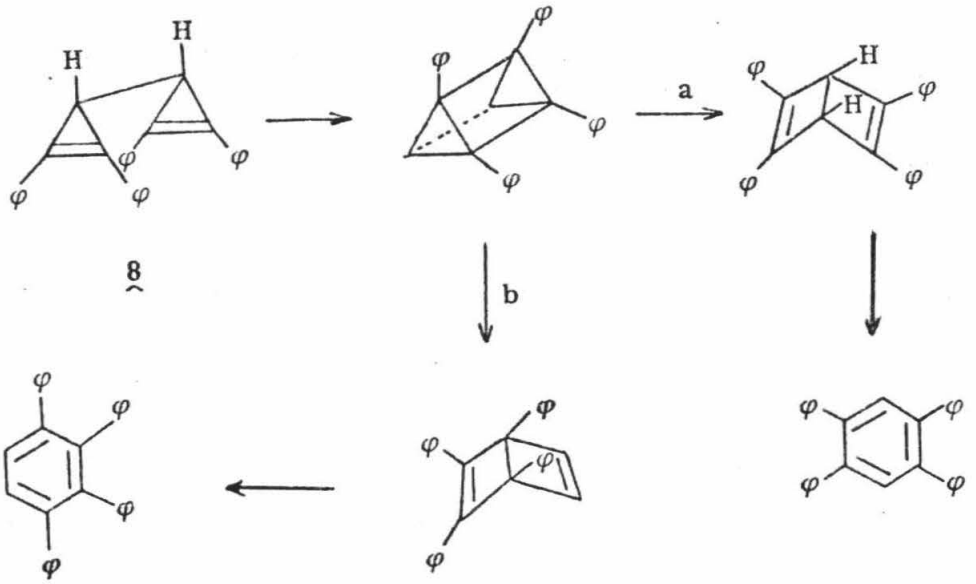

8 9 10

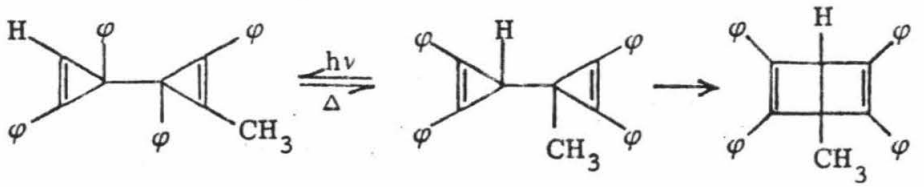

15 11 12

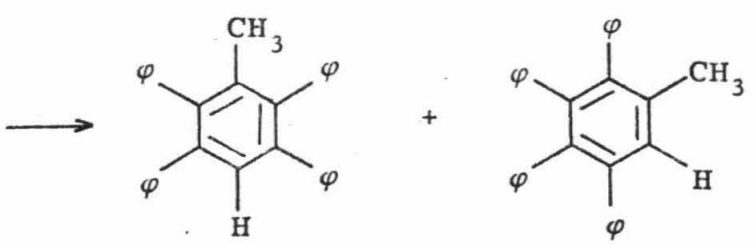

13 14

experiments on the Ag^{I} catalyzed rearrangements of bicyclopropenyls, Weiss and Andrae suggested that the thermal rearrangement involved initial retro-

Scheme I

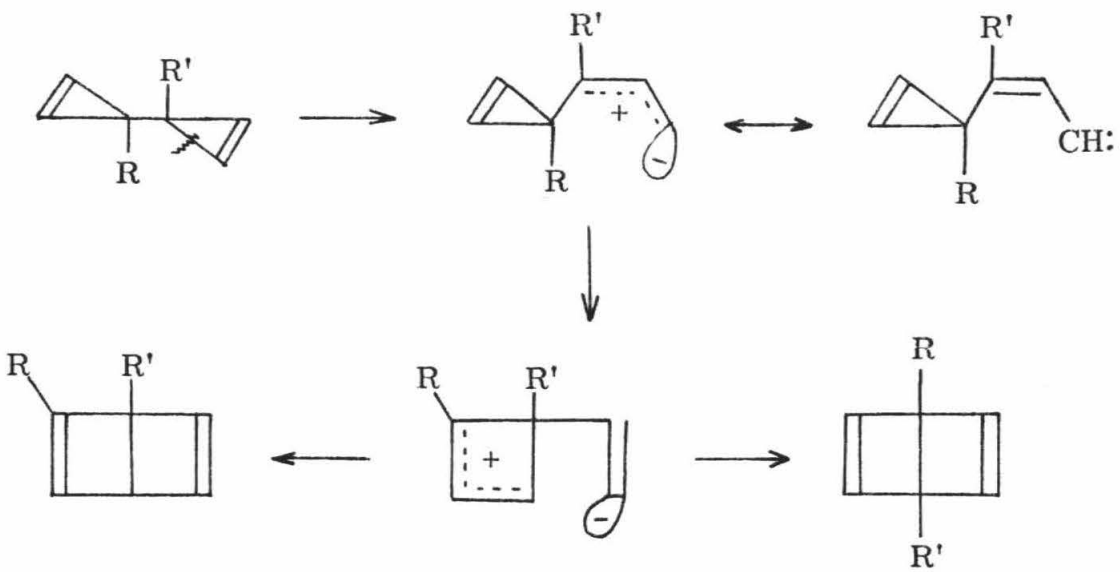

carbene fission of the cyclopropene ring, followed by ring expansion and closure to give the Dewar benzene, as shown in Scheme I. In 1975 Weiss and Kölbl[6] observed the photochemical Cope rearrangement of 11 to an isomeric bicyclopropenyl 15, as well as the thermal Cope rearrangement of 15 to 11. They postulated that the Cope reaction was a two-step process proceeding through an anit-1,4-tricyclohexylene diradical (16). This pathway was claimed to be favorable on the basis of an estimate by the author that 16 has 25 Kcal $mole^{-1}$ less strain energy than the pericyclic transition state (17). In addition to postulating 16 to be an intermediate in the

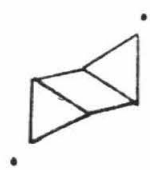

16

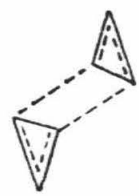

17

Cope rearrangement, Weiss and Kölbl also argued that 16 could be an intermediate in the aromatization process.[9]

Simultaneously with Weiss and Kölbl's observation of a bicyclopropenyl Cope rearrangement, the Cope rearrangement of 3,3'-dimethyl-3,3'-bicyclopropenyl (18) was independently observed by two other research groups. DeWolf, Landheer, and Bickelhaupt[10] observed the rearrangement of 18 to 1,1'-dimethyl-3,3'-bicyclopropenyl (19).

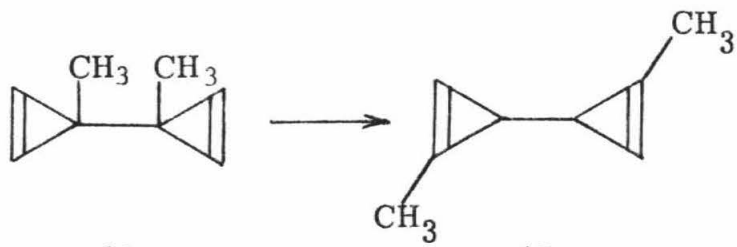

18 19

Two isomers of 19 were found; these were presumed to be diastereomers, although no attempt was made to determine which was d,l and which meso. The ratio of the isomeric products was found to vary from 10:1 at 256° to 1:1 at 320°. In addition further pyrolysis of the mixture of isomers of 19 was found to give a 2:1 ratio of m- and p-xylene (10% yield). No mechanism for the aromatization was suggested, but in previous studies[4] of the pyrolysis of 3,3'-tetramethylenebicyclopropenyl (20) by these authors a benzvalene intermediate had been proposed. This mechanism involved initial retrocarbene fission leading to a vinyl carbene (21), which then could add across the double bond of the other ring to yield the benzvalene (22). Aromatization of 22 was then assumed to lead to the observed tetralin product (23).

20 21

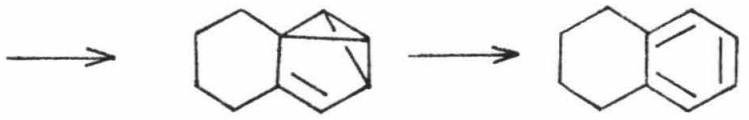

22 23

Bergman and Shea[11] have also observed the Cope rearrangement of 18 to the two diastereomers of 19 and have assigned the stereochemistry of each diastereomer. The method of assignment is discussed in the next section.

The present work is concerned with the kinetics of the Cope rearrangement and the aromatization process. During this study it occurred to us that determination of the ratios of isomeric xylene products formed on thermal aromatization of the two diastereomers of 19 might provide a definitive solution to the aromatization mechanism problem. We therefore set out to preparatively separate the two diastereomers and to carry out the pyrolysis of the pure isomers.

II. Assignment of Stereochemistry to meso and dl-19

The stereochemistries of meso- and dl-19 were determined by chemical correlation with compounds whose configuration could be determined directly (Scheme II). Because our supply of 19 from the pyrolysis of 18 was very limited, the following method, involving methylenecyclopropanes 24 as relay compounds, was chosen.

First, usable quantities of 24 were prepared independently by addition of CBr_2 to 2,5-hexadiene, followed by reduction with zinc in acetic acid and elimination/isomerization using KOtBu/DMSO. This sequence gave the two diastereomers of 24 in a 1:2 ratio, the minor isomer (which proved to be the meso; vide infra) eluting first from a Carbowax vpc column. A 2:1 mixture of diastereomers 19 was then purified by vpc and converted to the diastereomers 24 by base-catalyzed isomerization, again using KOtBu/DMSO. Analytical vpc showed that this reaction gave a 2:1 mixture of diastereomers 24. In this case, however, the early-eluting diastereomer of 24 was formed in major amount. The fact that different bismethylenecyclopropane (24) diastereomer ratios were obtained from 2,5-hexadiene and 19 shows that equilibration of the diastereomers does not occur in KOtBu/DMSO. We therefore conclude that in the 19 → 24 reaction, the major (early-eluting) diastereomer in the 19 mixture corresponds stereochemically to the major diastereomer in the 24 mixture.

After attempts at kinetic resolution of the diastereomers of 24 (using both asymmetric hydroboration[12a] and epoxidation with a

Scheme II

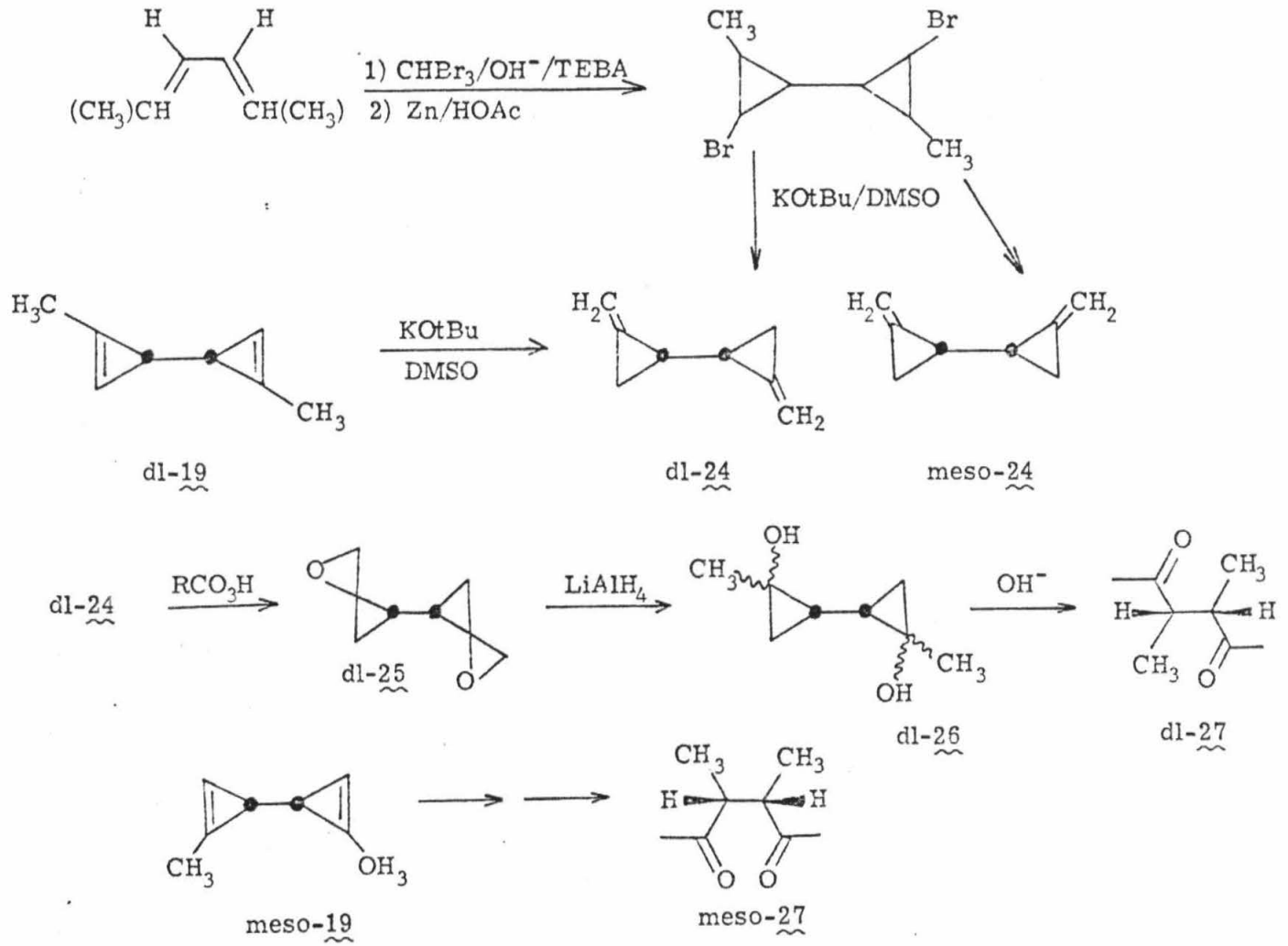
1) $CHBr_3/OH^-$/TEBA
2) Zn/HOAc
KOtBu/DMSO
KOtBu
DMSO
RCO_3H
$LiAlH_4$
OH^-
dl-19
dl-24
meso-24
dl-25
dl-26
dl-27
meso-19
meso-27

deficiency of (+)-monoperchamphoric acid[12b] failed to produce optical activity in either isomer, we decided to correlate the diastereomers of 19 by chemical conversion to meso- and dl-2,4-hexanediones 27 using the route outlined in Scheme II (for brevity, only the correlation of dl-19 is shown in detail). Epoxidation of 24 with m-chloroperbenzoic acid gave the mixture of epoxides 25. These were subjected to ring-opening reduction with $LiAlH_4$, and the cyclopropanols 26 treated with dilute base. Predominant ring cleavage at the less-substituted carbon, according to precedent[13a], gave diketone 27. Control experiments showed that meso- and dl-27 underwent only slight interconversion by epimerization under the reaction conditions. The stereochemistries of meso- and dl-27 were then assigned through the kinetic resolution[12a] of dl-27 by asymmetric hydroboration (see Experimental).

III. Mechanistic Considerations

Possible mechanisms for the aromatization process fall into two general groups. The first (Group A) postulates some sort of initial bonding interaction between the two cyclopropenyl rings (examples are the concerted double ring expansion and the classical Breslow mechanism), and the other (Group B) involves cyclopropene ring bond cleavage as the initial critical step. Comparison of the xylene ratios from pure meso- and dl-19 allows us to distinguish between these two groups, because (as

outlined in detail below) Group B mechanisms, involving initial ring bond cleavage, destroy the stereochemical distinction between these diastereomers. Thus if one of the Group B mechanisms is operating, we would expect very similar xylene ratios from each. Additionally, as is outlined in detail below, we are able to distinguish among the Group A and Group B mechanisms by considering additionally the xylene ratios formed from 18.

A) Group A Mechanisms

1) Prismane Mechanism

Initial formation of a prismane from 18, d,l-19 and meso 19, followed by isomerization to the corresponding Dewar benzenes and aromatization, would predict formation of xylenes as is shown in Scheme III. Meso- 18 and 19 should form the same prismane intermediate and thus would give an identical mixture of o- and p-xylenes, while d,l-19 would give m- and p-xylenes.

2) The Weiss Biradical Mechanisms

The Weiss mechanism involves formation of a common intermediate for the Cope and aromatization processes. The products expected from an anti-1,4-tricyclohexylene intermediate are shown in Scheme IV. All three isomers are expected to give a different mixture of xylenes. If, as Weiss suggests, there is an additional pathway for aromatization including "prefulvene" intermediates (e.g. benzvalene), we would still predict substantially different product distributions from each of the isomers.

Scheme III

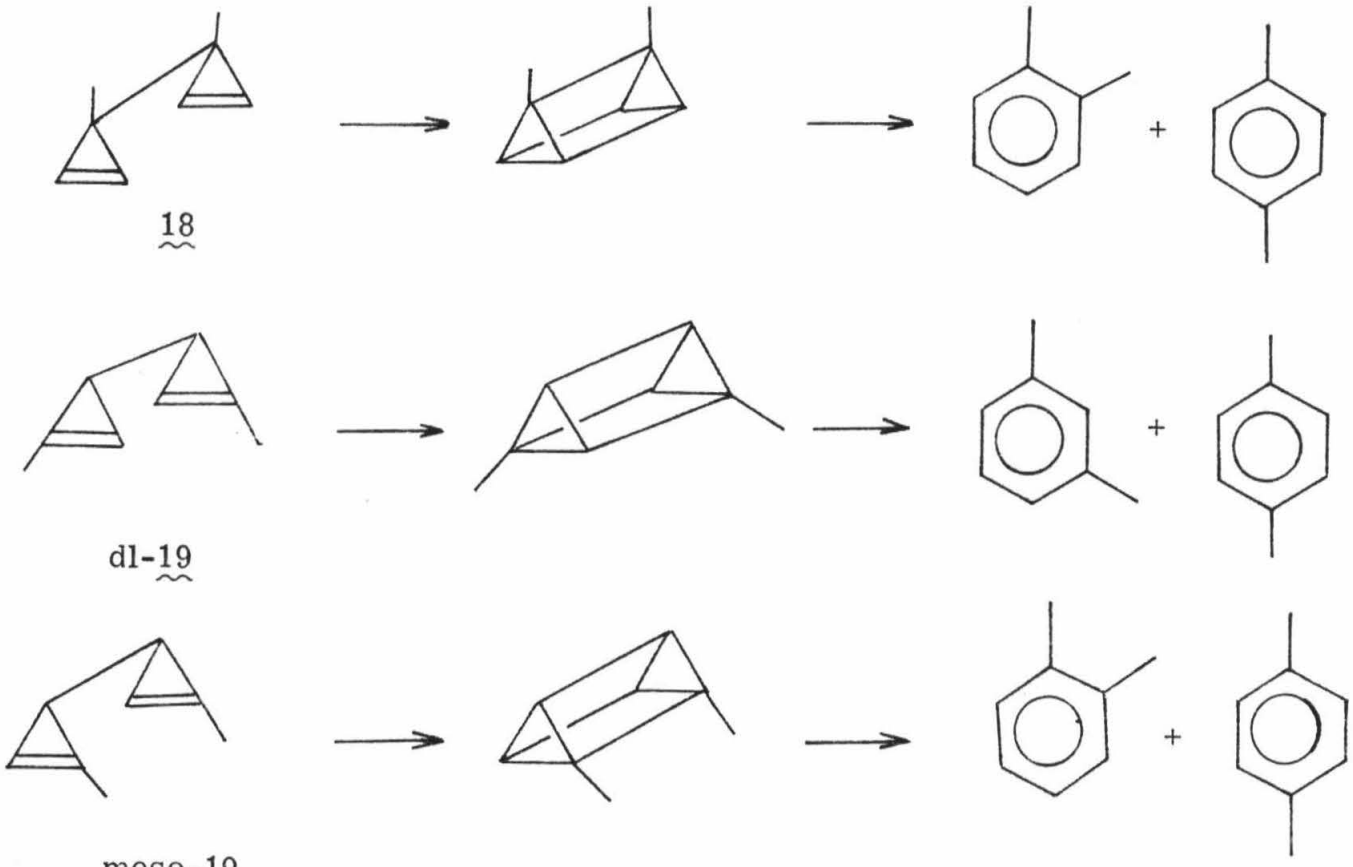

18

dl-19

meso-19

Scheme IV

18

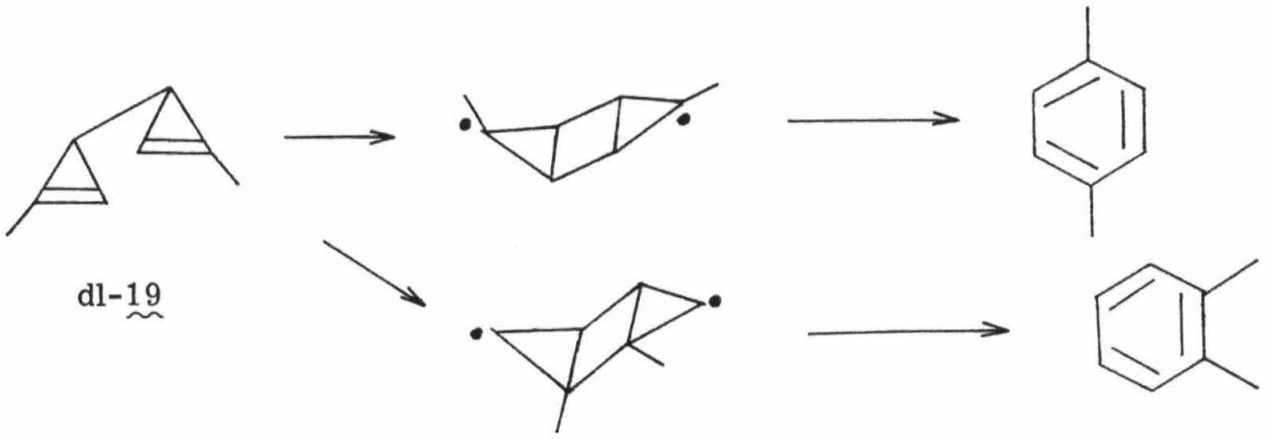

dl-19

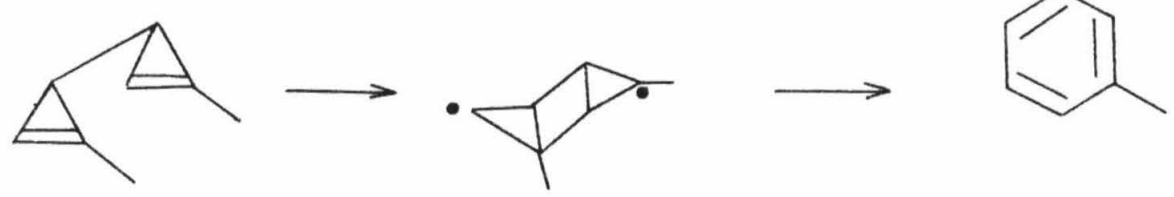

meso-19

3) The Concerted Ring Expansion Mechanism

A fourth mechanism not previously proposed involves concerted ring expansion of both cyclopropenes to give a Dewar benzene directly. As can be seen from Scheme V, in this pathway both 18 and d,l-19 are predicted to give p-xylene exclusively while meso-19 is expected to yield m-xylene. Note that there is no pathway for formation of o-xylene.

B) Group B Mechanisms

1) The Benzvalene Mechanism

The mechanism of deWolf, Landheer, and Bickelhaupt involves retro-carbene fission of one cyclopropene followed by addition of the carbene carbon to the other ring. This benzvalene would then aromatize to give benzene derivatives. The predicted products from our labelled bicyclo-propenyls are shown in Scheme VI. Assuming that vinylcyclopropane rearrangement in the benzvalene is slow relative to aromatization, the two diastereomers of 19 are predicted to give the same product distributions, while 18 is predicted to yield exclusively o-xylene.

2) The "Benzvalene-like" Diradical Mechanism

A slight variation on the benzvalene mechanism involves initial ring bond cleavage to give the 1,3 diradical (28) followed by ring closure to give the bicyclo [3,1,0] hexenediyl (29). Cleavage of the internal cyclopropropyl bond yields xylene. As shown in Scheme VII, 18 would yield exclusively o-xylene while d,l-19 and meso-19 would yield a mixture of all three xylenes.

Scheme V

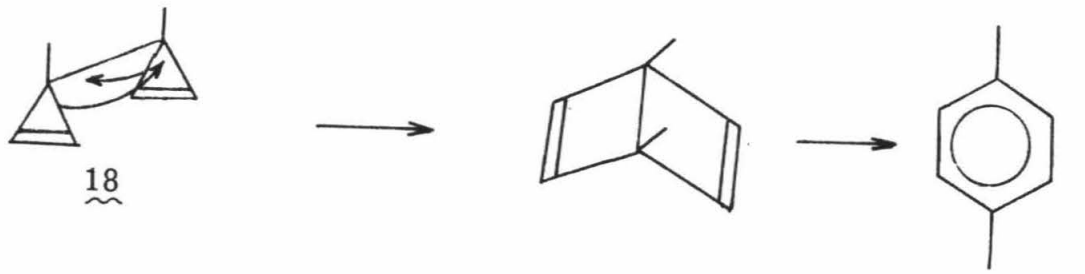

18

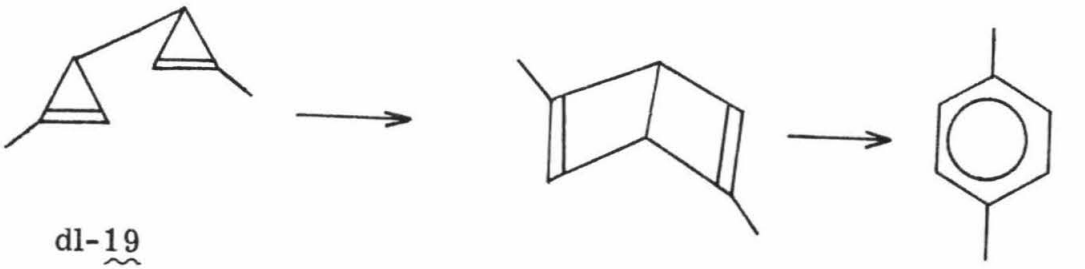

dl-19

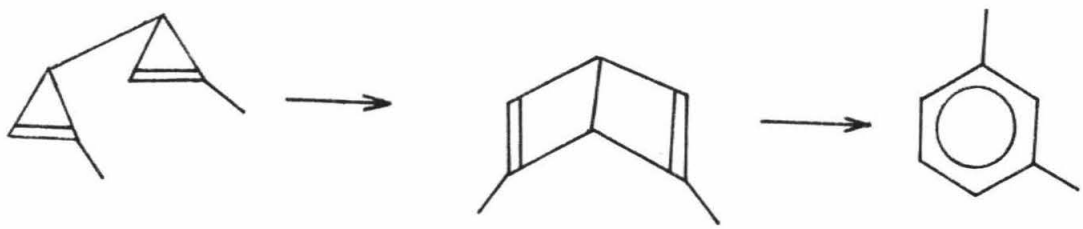

meso-19

Scheme VI

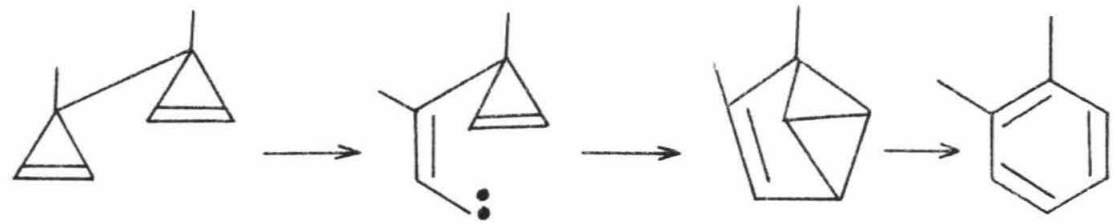

18

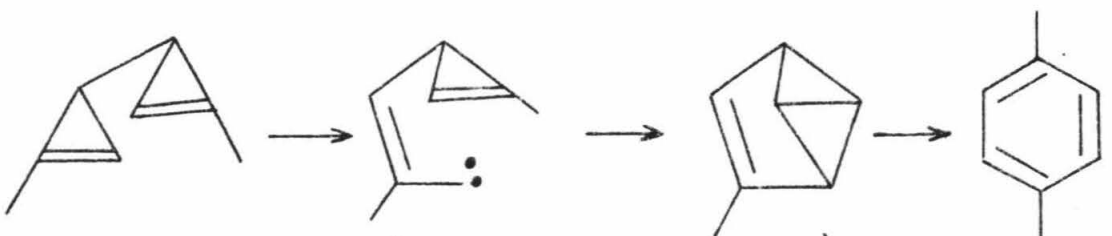

dl-19

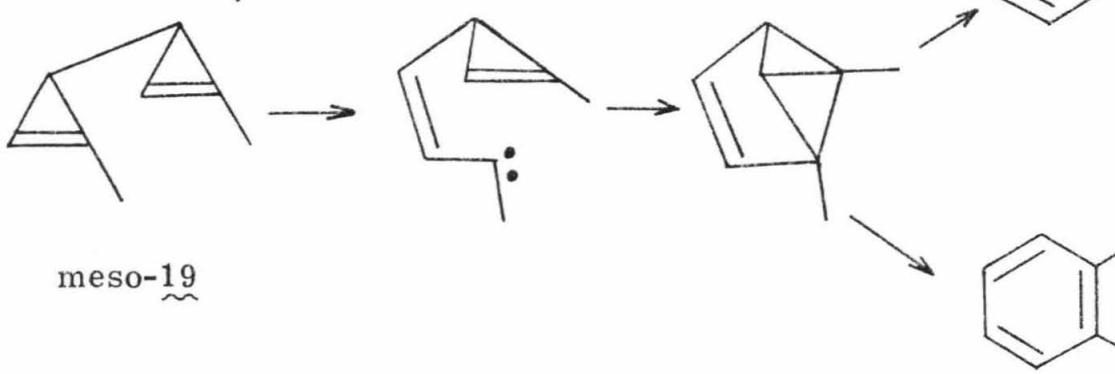

meso-19

Scheme VII

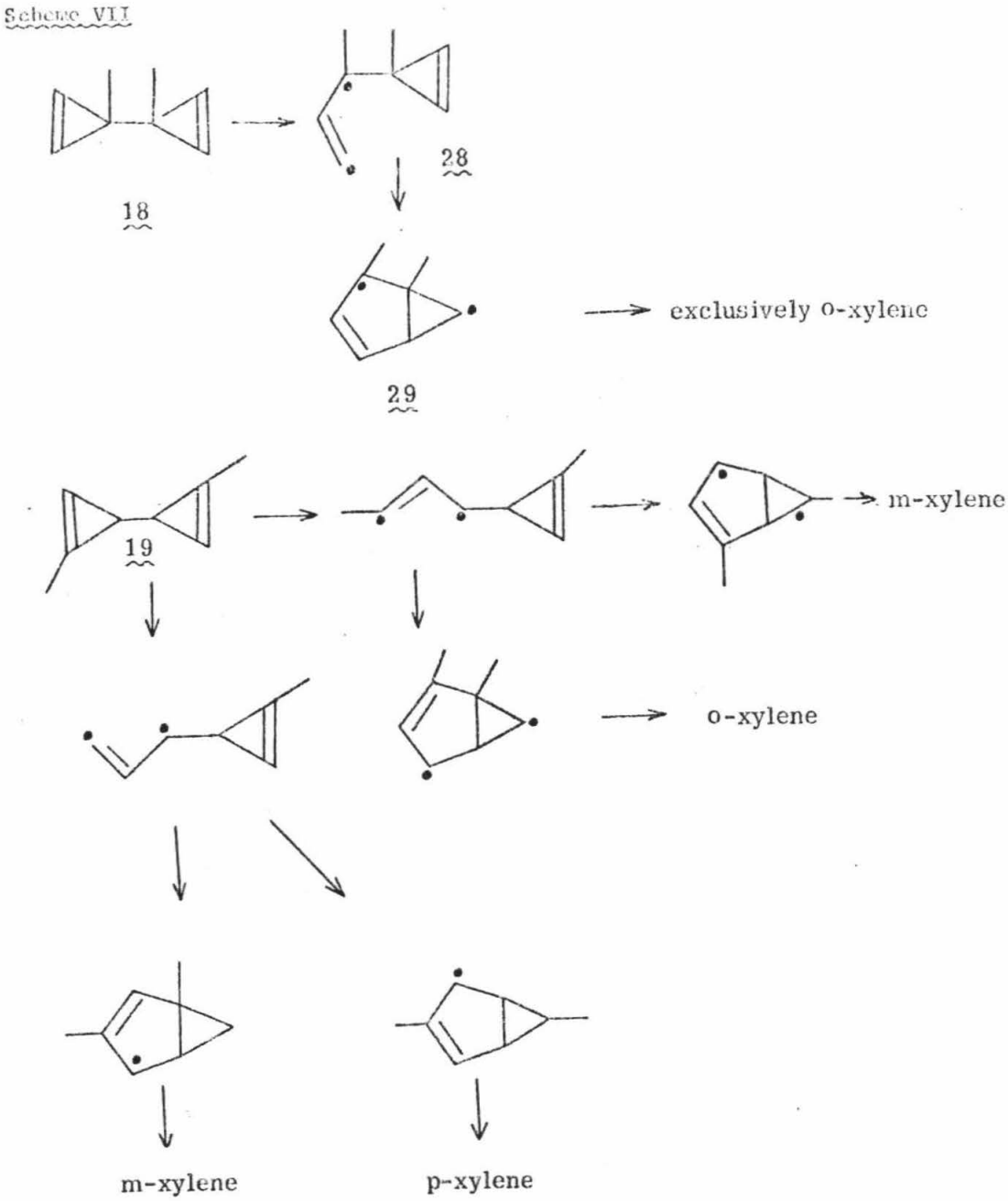
18
28
29
exclusively o-xylene
19
m-xylene
o-xylene
m-xylene
p-xylene

3) The Weiss "Ag^{I}-Type" Mechanism

In their original work Weiss and Andrae had proposed the mechanism shown in Scheme I involving a cyclopropenylcarbinyl cation ring expansion. This mechanism predicts that 18 should give both o- and p-xylenes but no m-xylenes, while d,l-19 and meso-19 would yield a mixture of all three xylenes.

IV. Results

Pyrolyses of 3,3'-dimethyl-3,3'-bicyclopropenyl (18) were carried out in both flow and static systems. Under all conditions used, xylenes were the products observed at complete conversion. At earlier reaction times, however, the buildup and disappearance of two new products were observed. These compounds were obtained in nearly pure form (>95%) by preparative vapor phase chromatography. The liquid phase used for the separation proved to be crucial. The use of standard "olefin-separation" phases[14a] resulted in decomposition of the bicyclopropenyls and, in at least one case[14b], resulted in quantitative isomerization to the Dewar benzenes. Hence, the only acceptable phase for vpc analysis of the bicyclopropenyls was the relatively inert SE-30. The sensitivity of the bicyclopropenyls also necessitated the use of glass columns in all vpc work. The stereochemistry of the pure diastereomers was then determined as outlined in Section II. When 18 was pyrolyzed in a flow system, the d,l/meso ratio of 19 was found to vary from 10:1 to 1:1 over a 40° temperature range. It appeared that this temperature variation might be due to thermal interconversion of the products d,l- and meso-19 under the reaction conditions. The thermal reactions of all three isomers were therefore examined in more detail using a static pyrolysis system.

Pure samples of 18, 19a, and 19b were obtained by preparative vpc and pyrolyzed at 166.5°. Samples were analyzed at various time intervals ranging from 200 sec to 5000 sec; the data are shown in Figures 1,2, and 3. Rate constants were determined by computer simulation of concentration-

Figure 1: Time dependence of products formed on pyrolysis of 3,3'-dimethyle-3,3'-bicyclopropenyl (18) at 165.5°. Solid lines are computer simulated percentages.

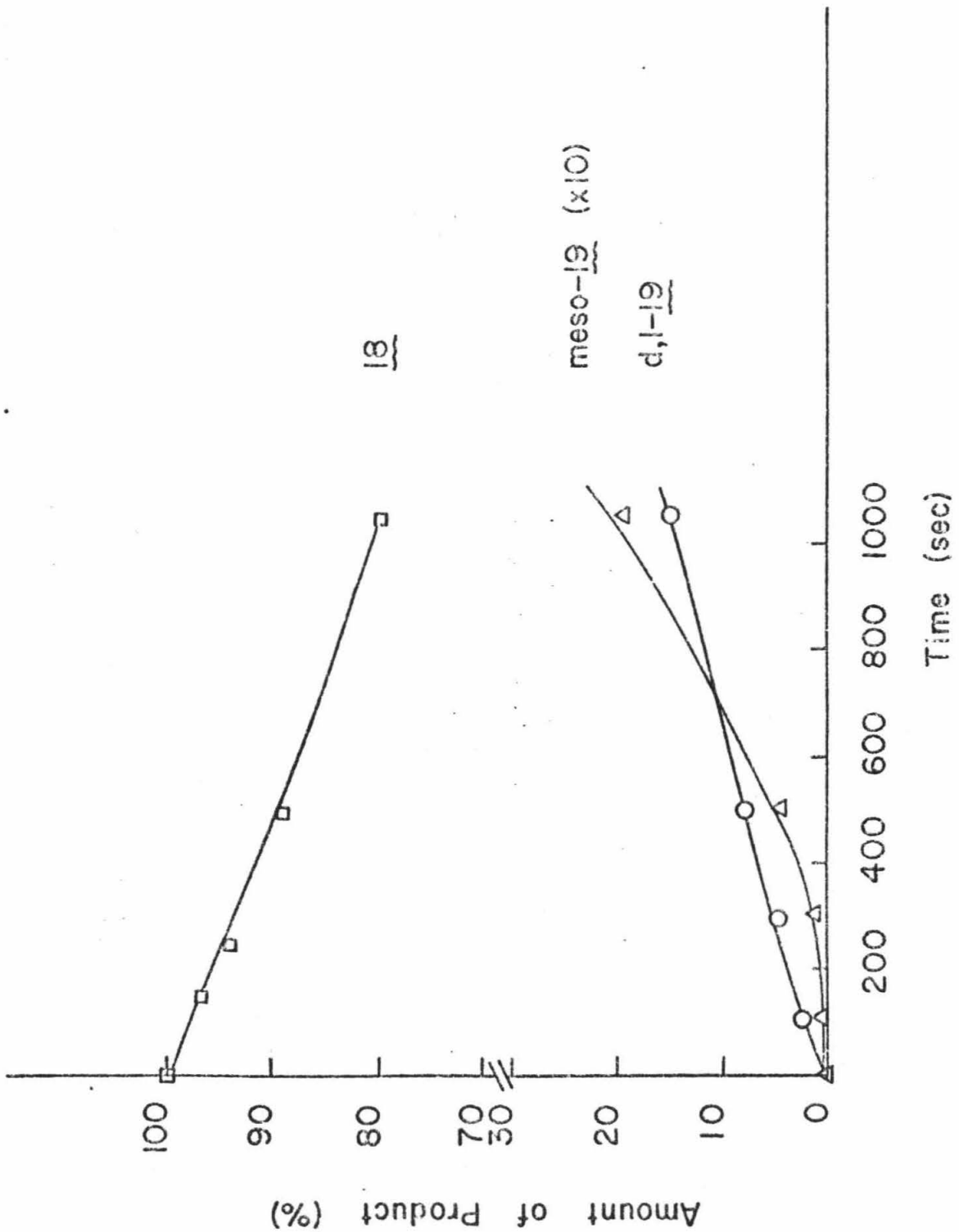
18
meso-19 (x10)
d,l-19
Amount of Product (%)
100
90
80
70
50
20
10
0
200
400
600
800
1000
Time (sec)

Figure 2: Time dependence of products formed on pyrolysis of d,l-1,1'-dimethyl-3,3'-bicyclopropenyl (d,l-19) at 165.5°. Solid lines are computer simulated percentages.

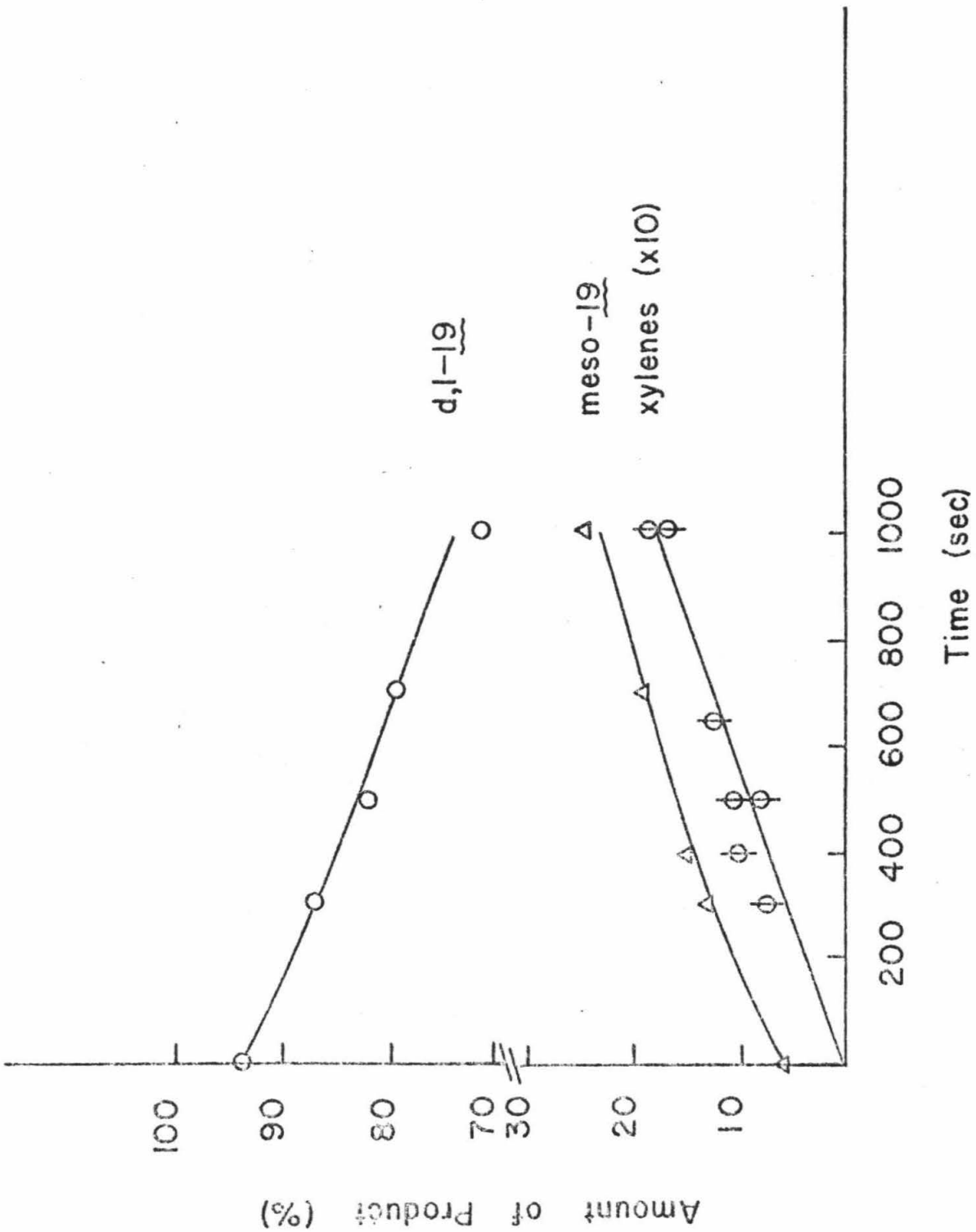
d,l-19
meso-19
xylenes (x10)
Amount of Product (%)
100
90
80
70
30
20
10
200
400
600
800
1000
Time (sec)

Figure 3: Time dependence of products formed on the pyrolysis of meso-1,1'-dimethyl-3,3'-bicyclopropeny (meso-19) at 165.5°. Solid lines are computer simulated percentages.

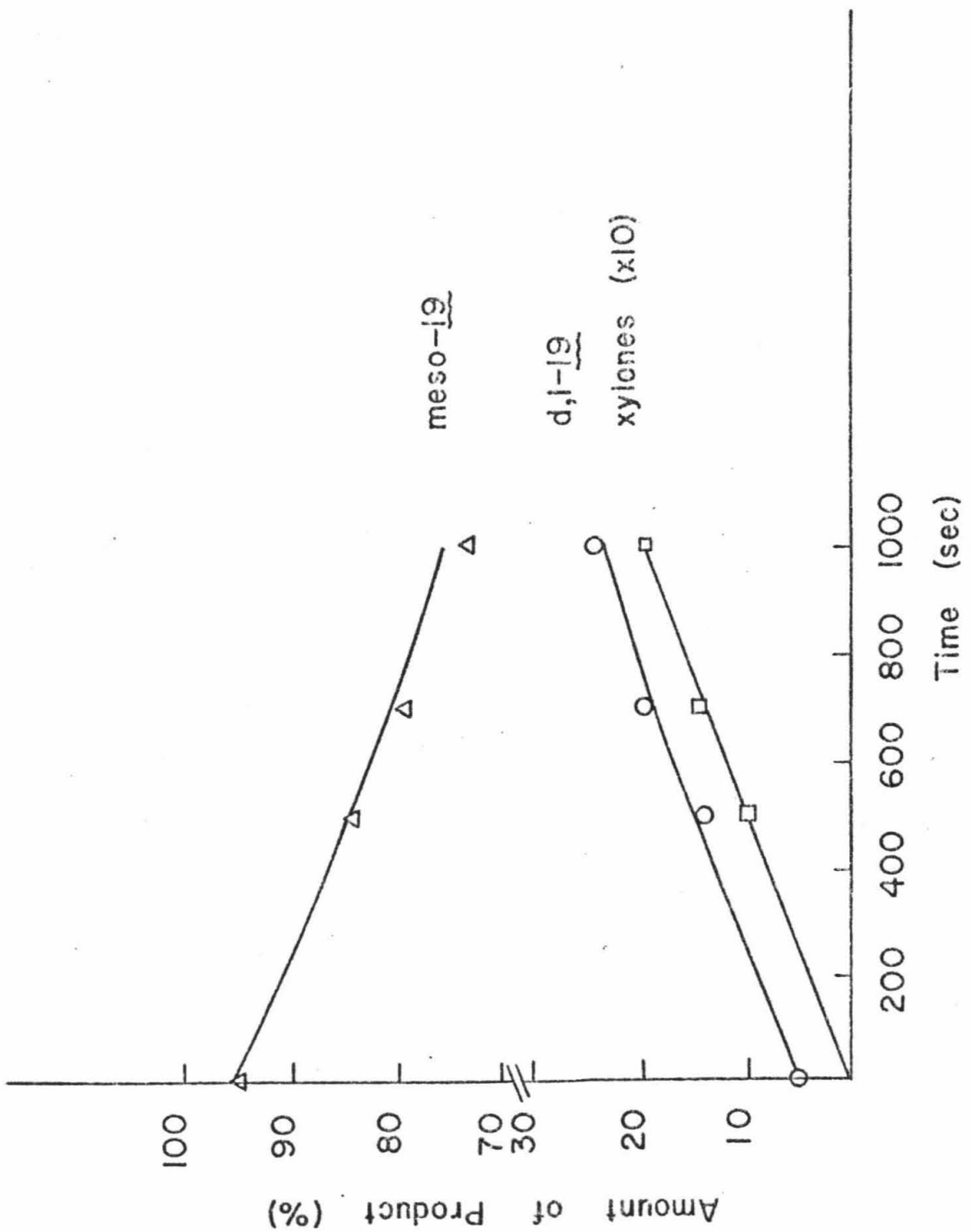
meso-19
d,l-19
xylenes (x10)
Amount of Product (%)
100
90
80
70
30
20
10
200
400
600
800
1000
Time (sec)

vs.-time curves using the MS1M4 program.[15] The calculated rate constants are listed in Table I for the interconversion of the dimethylbicyclopropenyls and for their conversion to xylenes. The zero-time xylene distributions were extrapolated from the data shown in Figure 4-6 and are listed in Table II. It was extremely important that the xylene ratios be taken as close as possible to zero-time due to two complicating factors. First, in the pyrolysis of 18, the formation of any substantial amount of the Cope products (19) resulted in xylenes formed from both 18 and 19. Second, the aromatization of pure dl- and meso-19 occurred at a rate competitive with that of interconversion of the diastereomers. With some effort, we were able to analyze accurately for xylene formation at conversions of starting material as low as 1%.

To determine the temperature dependence of the kinetic (zero-time) dl/meso ratio, the pyrolysis of 18 was also carried out at 196.5°. At both temperatures the dl/meso ratio extrapolates to 130 ± 10 at zero time (e.g. Figure 7) and shows no measurable variation with temperature.

Figure 4: Time dependence of the percentage of each xylene produced on pyrolysis of dl-19 at low percent conversion.

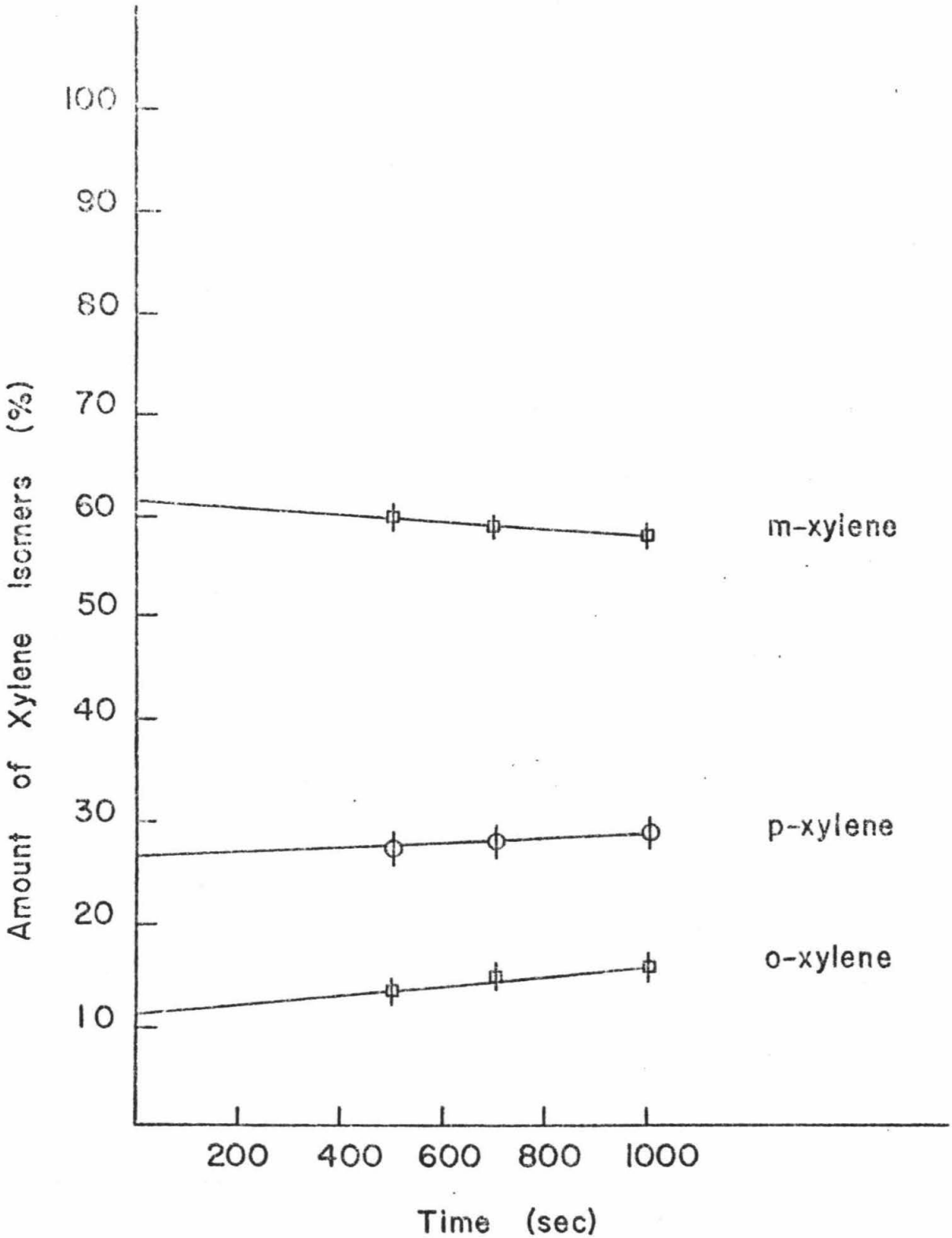
100
90
80
70
60
50
40
30
20
10
Amount of Xylene Isomers (%)
m-xylene
p-xylene
o-xylene
200
400
600
800
1000
Time (sec)

Figure 5: Time dependence of the percentage of each xylene produced on pyrolysis of meso-19 at low percent conversion.

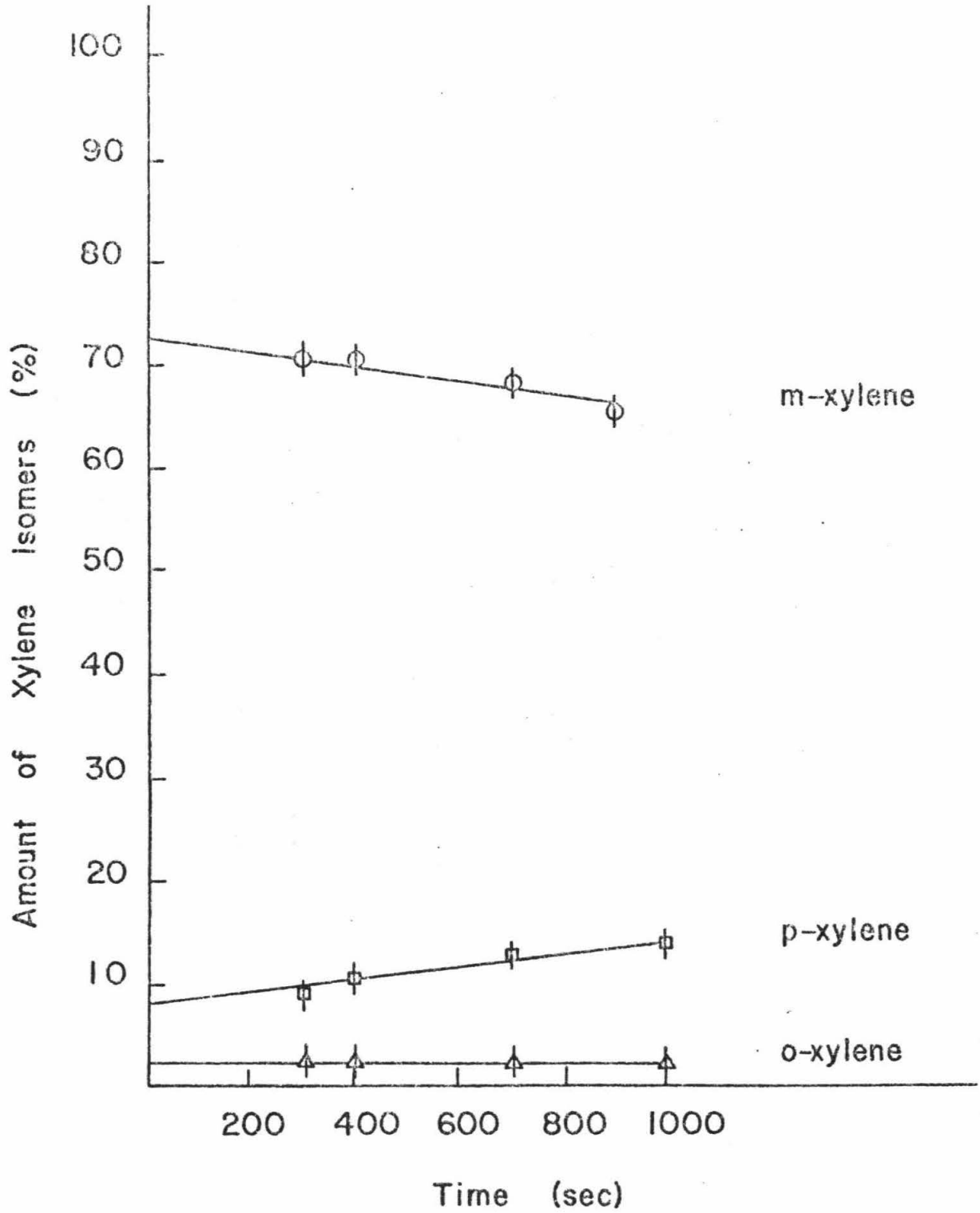
100
90
80
70
60
50
40
30
20
10
Amount of Xylene Isomers (%)
m-xylene
p-xylene
o-xylene
200
400
600
800
1000
Time (sec)

Figure 6: Time dependence of the percentage of each xylene produced on pyrolysis of 18 at low percent conversion.

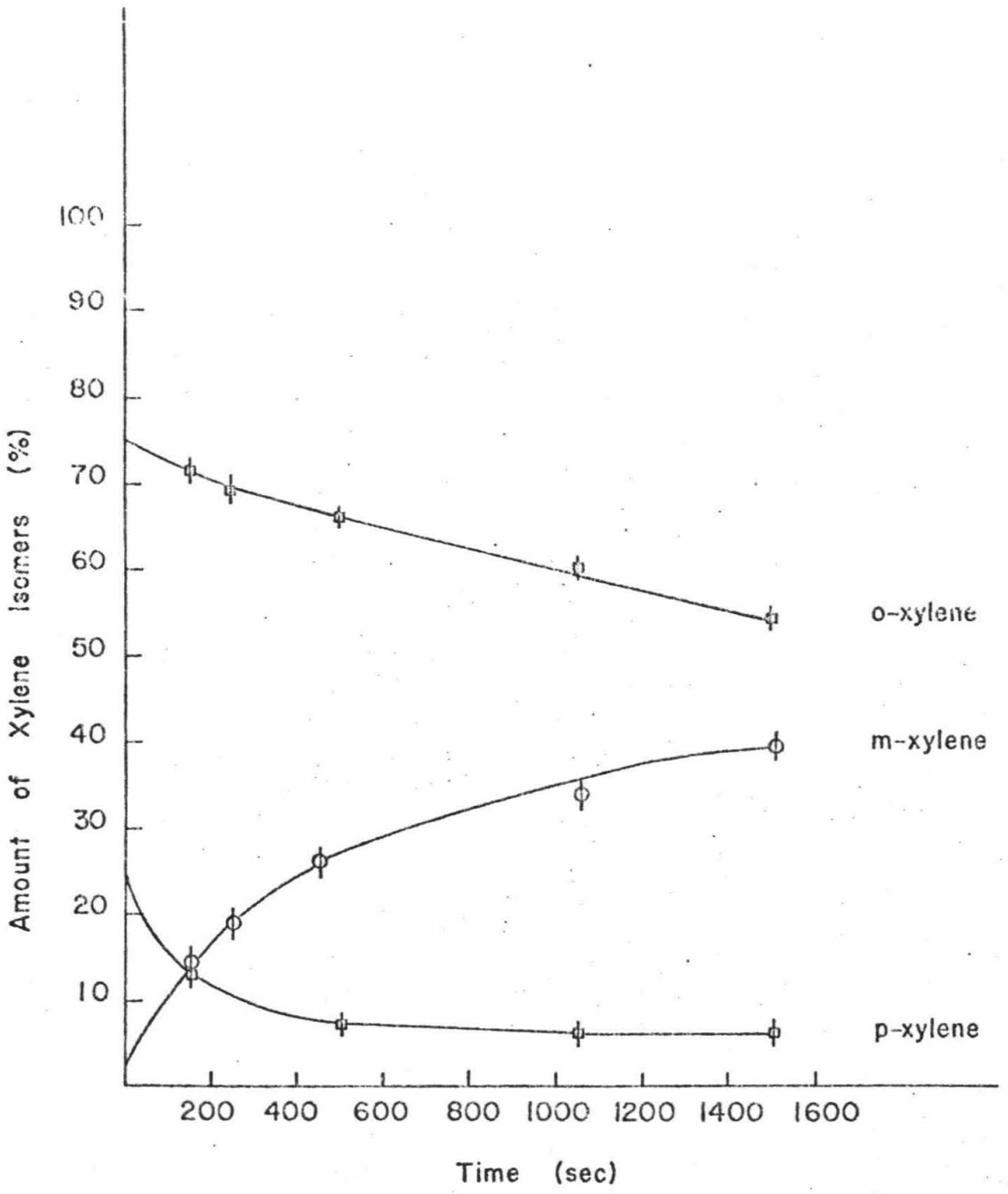
Amount of Xylene Isomers (%)
100
90
80
70
60
50
40
30
20
10
200
400
600
800
1000
1200
1400
1600
Time (sec)
o-xylene
m-xylene
p-xylene

Figure 7: Extrapolation to zero time of dl-19/meso-19 ratio from pyrolyses of 18 at 165.5°.

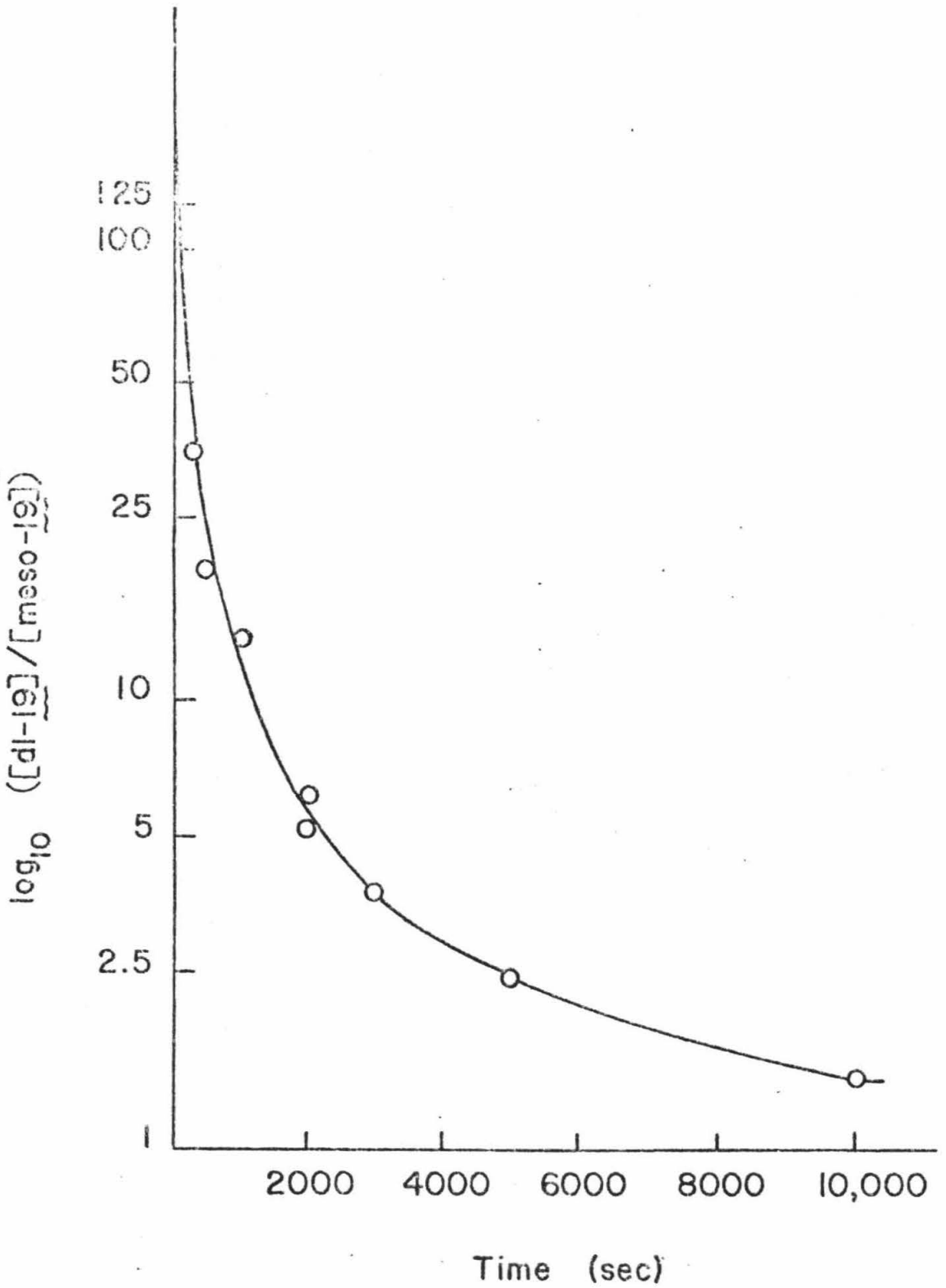
125
100
50
25
10
5
2.5
1
2000
4000
6000
8000
10,000
Time (sec)
log10 ([dl-19]/[meso-19])

V. Discussion

a) Cope Rearrangement and Bicyclopropenyl Interconversion

The pyrolysis of 3,3'-dimethyl-3,3'-bicyclopropenyl (18) yields both d,l- and meso-1,1'-dimethyl-3,3'-bicyclopropenyl (19) in a ratio of 130 ± 10 at zero time. As shown in Scheme VIII two different transition states are available for the Cope rearrangement with the chair conformer yielding d,l and the boat giving meso. Goldstein[15] has suggested that the Cope rearrangement in acyclic systems might be proceeding through other transition states (e.g. twist, plane, and anchor conformers). In the bicyclopropenyl case, however, the rigidity of the system prevents rearrangement through many of the conformations which might be available in more flexible acyclic systems. Additionally the unusual symmetry of the bicyclopropenyl molecule allows the chair and boat conformers to interconvert by a simple rotation rather than a ring flip. Thus it seems likely that the difference in free energy of activation ($\Delta\Delta G^{\ddagger}$) for the formation of d,l and meso-19 accurately reflects the free energy difference between the chair and boat transition states. The experimental $\Delta\Delta G^{\ddagger}$ of 4.3 kcal/mole (166°) is in good agreement with the $\Delta\Delta G^{\ddagger}$ for the acyclic system (~ 6 kcal/mole at 498°).[17] Our results confirm that the variable dl/meso ratios observed by deWolf, Landheer, and Bickelhaupt were the result of thermal interconversion of dl and meso-19 at the temperatures required for reaction. In view of this, one might ask whether this interconversion occurs via retro-Cope rearrangement to 18 (Scheme IX). The following reasoning

Scheme VIII

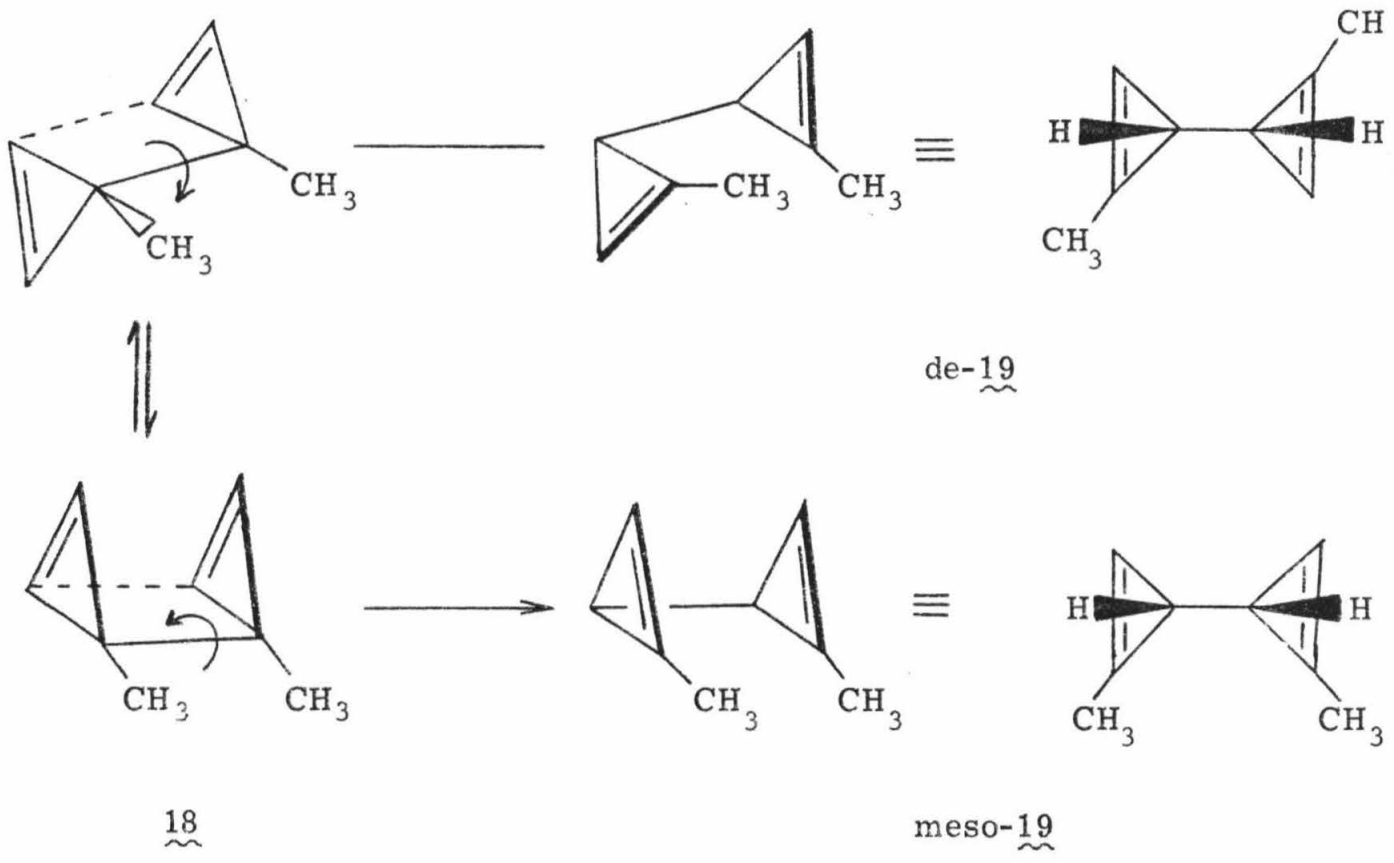
CH3
CH3
CH3
CH3
≡
CH
H
H
CH3
de-19
CH3
CH3
CH3
CH3
≡
H
H
CH3
CH3
18
meso-19

Scheme IX

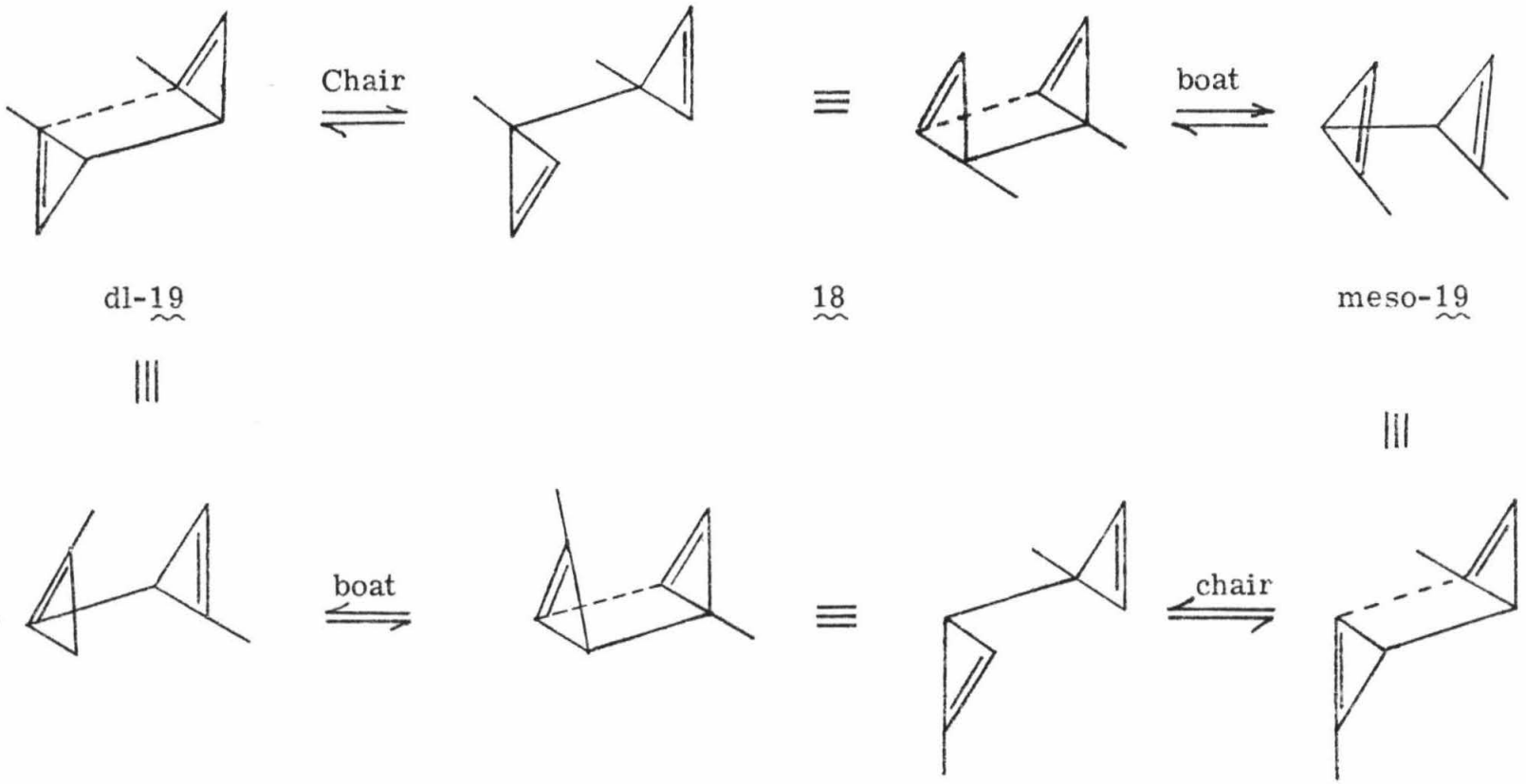

rules out this possibility. The rate of rearrangement for dl-19 to meso-

$$\text{dl-19} \underset{k_1}{\overset{k_2}{\rightleftharpoons}} 18 \underset{k_4}{\overset{k_3}{\rightleftharpoons}} \text{meso-19}$$

19 is limited by the rates of dl-19 → 18 and 18 → meso-19. However, the observed rate for the interconversion of dl-19 → meso-19 is two orders of magnitude faster than the rate for 18 → meso-19. Therefore the reverse Cope rearrangement cannot be operating at a significant rate under our pyrolysis conditions. An additional piece of evidence against interconversion by the reverse Cope rearrangement is our failure to detect any 3,3'-dimethyl-3,3'-bicyclopropenyl or any 1,3'-dimethyl-3,3'-bicyclopropenyl in the pyrolyses of pure dl-19 and meso-19.

A reasonable mechanism for the interconversion of dl- and meso-19 involves initial ring opening of one cyclopropene followed by bond rotation and ring closure as shown in Scheme IX. This mechanism would predict that the rate of interconversion should be approximately the same whether one starts with dl or meso-19. These ratios are found to be identical within experimental error (Table I).

b) Aromatization

The relative rates of formation of each of the xylene isomers from each of the three bicyclopropenyls allows us to distinguish clearly between the various mechanisms proposed in part III. Our data show that d,l and meso-19 yield very similar percentages of xylenes (mostly para- and meta-), while 18 gives a quite different ratio (mostly ortho). We can therefore rule out all Group A pathways--i.e., the prismane mechanism,

Weiss's biradical mechanism, and any other pathways which would retain the stereochemical distinctions between d,l- and meso-19. In addition the benzvalene or "benzvalene-like" diradical mechanism fails to predict accurately the xylene distributions for the three isomers.

The only reasonable mechanism consistent with our observations is the Weiss "Ag^{I}-Type" mechanism. This involves the zwitterionic form (32) of the ring-opened bicyclopropenyl. While this species might

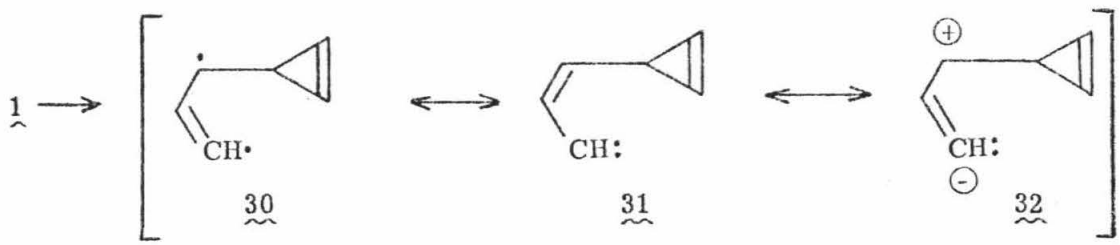

be important in solution, it is unlikely to play any role in the gas-phase due to the greatly unfavorable energy required by charge separation. Recent theoretical calculations [17] indicate that ring-opening of a cyclopropene (33) most likely leads to a 1,3-diradical-type state (34) which then converts to the slightly lower energy "carbene" state (35). When the symmetry of the system is perturbed (for example by the extra cyclopropene ring in 18) configurations 34 and 35 can mix. Thus it seems likely that the initial ring-opened intermediate formed by ring cleavage in a substituted cyclopropene should have large contributions from configurations resembling 34 and 35, and thus the intermediate should possess significant radical character at carbon 3.

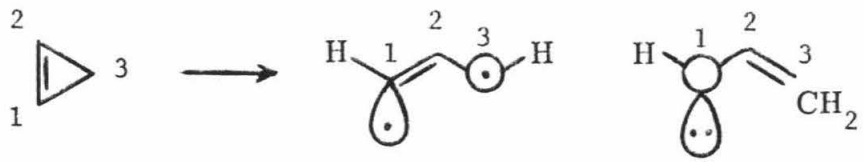

33 34 35

We now propose that 1,2-vinyl migration occurs in 30 to yield a cyclobutenyl radical (36). 1,2-vinyl shifts of this nature are well-

30 36

precedented; e.g., the Δ^2-cyclopentenyl methyl radical (37) rearranges rapidly[19] to 4-cyclohexenyl radical (38). Ring expansion in 30

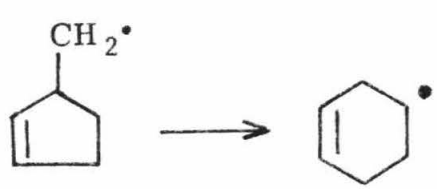

37 38

should be even more facile than in 37, since we are not only relieving greater strain in the cyclopropene but also forming an allylic radical.

This "modified Weiss mechanism" is outlined in detail in Schemes X and XI. This hypothesis accounts for the observation that, in the case of the pyrolysis of 18, rearrangement gives both o- and p-xylene but not m-xylene. In addition, since ring closure by path b (Scheme X) involves greater steric hindrance and yields the least substituted double bond, we would expect path a to predominate. Thus, we expect 18 to yield only two xylenes with the major isomer being o-xylene, as is found experimentally. Scheme XI allows us to predict which xylenes should predominate in pyrolysis of dl-19 and meso-19. On a purely statistical basis, we would predict the ratio of o-/m-/p-xyxlens to be 1:4:3. Since pathway a involves cleavage of the more substituted cyclopropene bond and thus might be preferred over pathway b, we expect a greater predominance of m-xylene. Experimentally we find a o:m:p ratio of 1:9:2.5 for dl-19 and 1:6:2.5 for meso-19. Thus the xylene ratios from pyrolysis of all three isomers strongly support the mechanism outlined in Schemes X and XI.

The best evidence for this mechanism would, of course, be the direct observation of a Dewar benzene intermediate. Although this has not been possible in the gas phase reactions due to the low-steady concentration of Dewar benzenes (estimated to be $<<10^{-6}$), it has been possible to detect spectroscopically the presence of a Dewar benzene in the thermal rearrangement of 18 in solution. In conjunction with Turro and Schuster,[20] we have observed chemiluminescent rearrangement of 18 to xylenes. Furthermore we have shown that the chemiluminescent species is a ground

Scheme X

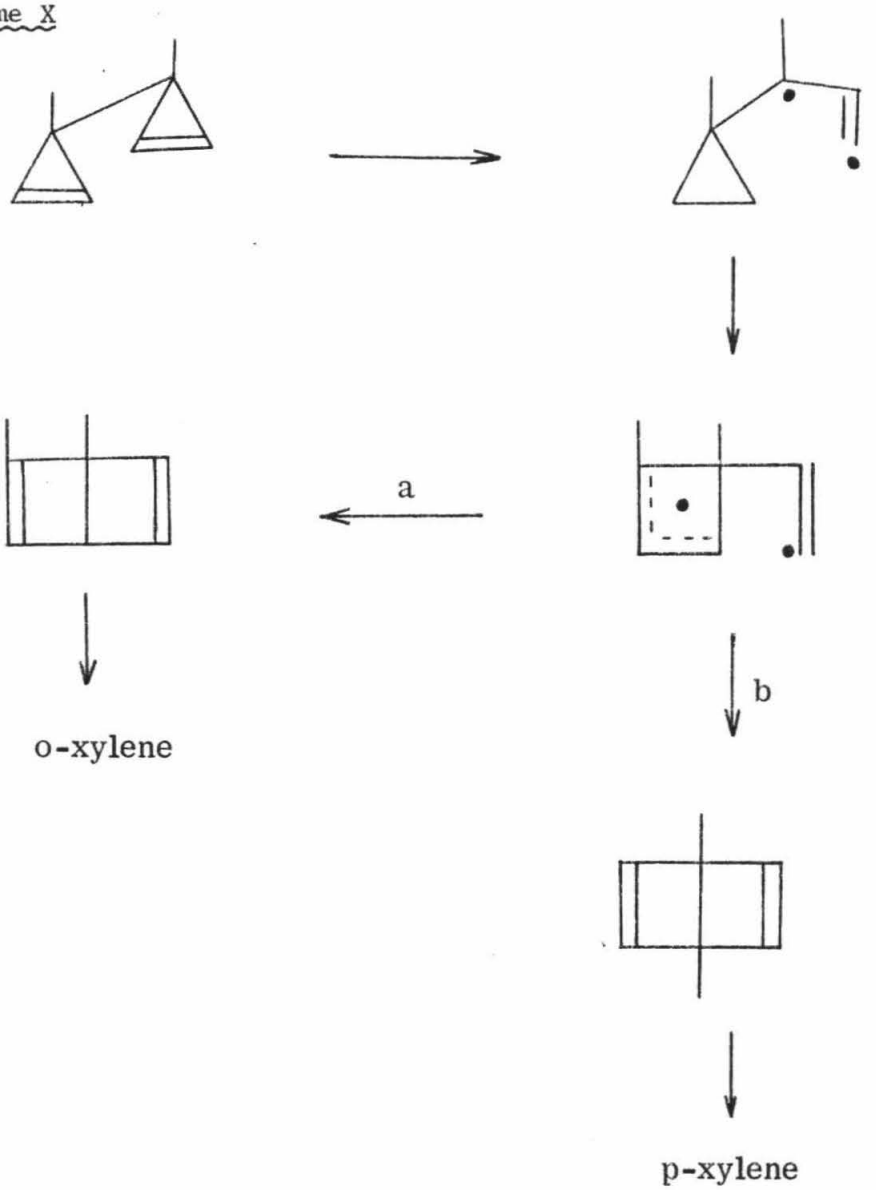

Scheme XI

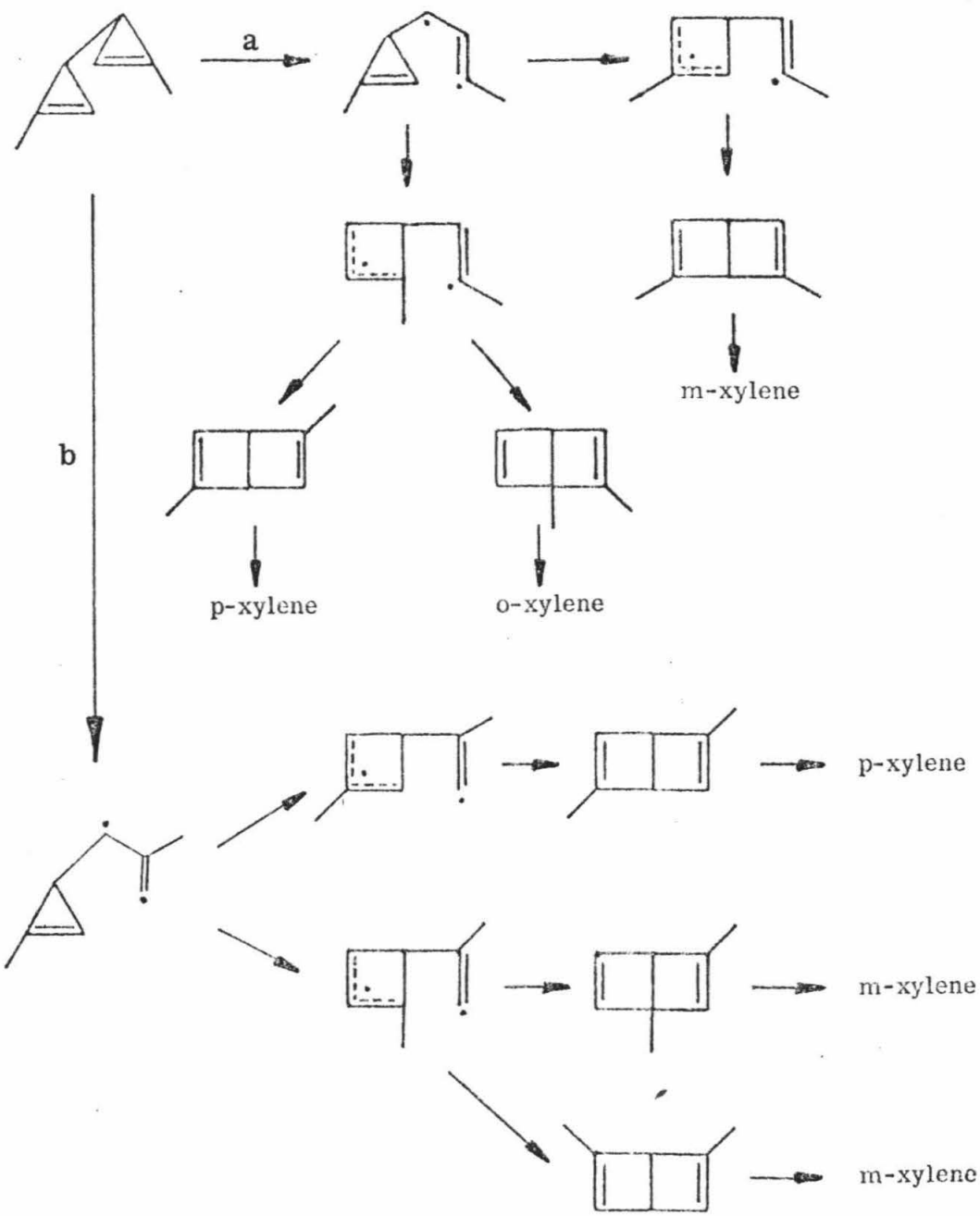

state intermediate in the rearrangement of 18. Of the three plausible ground state intermediates (prismanes, benzvalenes, Dewar benzenes), only Dewar benzenes have been found to chemiluminesce with sufficient intensity to account for the bicyclopropenyl pyrolysis results.

Measurements of the chemiluminescence yields suggest that at least 50% of the reaction must be proceeding by way of the Dewar benzene intermediate. Thus this solution data clearly fit the postulated gas-phase mechanisms. While it is always possible for a different mechanism to be operating in the solution chemistry, we feel that the mechanism outlined in Scheme X and XI present by far the most coherent and economical picture of the aromatization of bicyclopropenyls.

VI. Experimental

Materials. N-pentane (reagent grade) was stirred with concentrated sulfuric acid until no further coloration resulted. The pentane was then stirred overnight with 0.5 N $KMnO_4$ in 3M H_2SO_4, washed with water and aqueous $NaHCO_3$, and dried over M_5SO_4. The pentane was distilled from P_2O_5 through a one-meter distillation column packed with glass helices.[21]

3,3'-Dimethyl-3,3'-bicyclopropenyl was prepared by the method of de Wolf, et al.[22]

Trans-1,2-dimethylcyclohexane was purified by preparative vpc. All bicyclopropenyls were purified just prior to use by preparative vpc on a Varian Aerograph 90-P gas chromatograph using a 20' x 1/4" glass column packed with 30% SE-30 on 60/80 Chromosorb WAW-DMCS. The column temperature was 60-70°C, the injector temperature 60°C, and the detector temperature was 80°C. Other preparative vpc columns used: Column A: 10' x 1/4" glass 15% carbowax 1500 on 60/80 Chromosorb WAW-DMCS; Column B: 10' x 1/4" glass 5% Diethylene Glycol Succinate (DEGS) on 60/80 Chromosorb WAW-DMCS.

Apparatus. Static Pyrolysis of the bicyclopropenyls was carried out in a reactor of 200 ml volume (Figure 8). The reactor was constructed of lead-alkaline glass (Corning 0120) and was joined to a Teflon stopcock A by a length of capillary tubing to minimize dead space. Fused to the capillary tubing and extending into the center of the flask was a thermocouple well. Stopcock A was connected to a vacuum manifold which included

a small coil trap, 14/20 joint B, vacuum stopcock and 14/20 joint C, vacuum stopcock D, vacuum stopcock and 14/20 joint E, and large trap F. System pressure was monitored by a mercury manometer at G.

The reaction flask was immersed in a 6-l copper beaker containing a high temperature silicon oil (Lauda Ultra-Therm 330-SCB). Also immersed in the bath was a high-speed Sargent stirrer. Heat was supplied by two 500-W base heaters, one of which was connected to a thermoregulator. The temperature was measured by inserting an iron-constanan thermocouple into the reacter thermacouple well; voltage was read on a Leeds and Northup millivolt potentiometer (Model 8686). Temperature could be routinely kept constant during a run to better than ± 0.2°.

The reaction vessel was conditioned by heating bicyclopropenyl 18 in it at 195° for 24 hr. Rate constants were determined using the following procedure. The entire system was evacuated to less than 0.05 torr by a Welch Pump. An appropriate mixture of bicyclopropenyls and internal standard (trans-1,2-dimethylcyclohexane) was degassed at joint C (stopcock A closed). The stopcock to the pump was closed and the mixture allowed to vaporize into the manifold (15-20 torr). Stopcock C was closed and then degassed pentane was vaporized into the manifold from point E to give a total pressure of ~150 torr. The Teflon stopcock A was opened and the manifold mixture expanded into the reaction vessel to give a total pressure of 100 torr. The remaining manifold mixture was condensed, and the system was re-evacuated. After the mixture had been pyrolyzed, stopcocks C and D were closed, and the Teflon stopcock opened momentarily. The material which expanded into the manifold was condensed with liquid nitrogen

at point B. The aliquot was removed from the line and stored at -50°C until analysis.

All analytical vpc was done on either a Hewlett-Packard 5751 gas chromatograph with flame ionization detector or a Perkin Elmer 3920 gas chromatograph. Peak areas were integrated using a Spectro-Physics Autolab System I computing integrator. Two different analytical columns were necessary to determine the dl/meso ratio and to determine the o:m:p-xylene ratios. To measure the relative amounts of 18, dl-19, meso-19, and xylenes, a 20' x ¼" glass column packed with 30% SE-30 on 60-80 Chromosorb WAW-DMCS was used. This column was temperatured-programmed with a rise in temperature of 1° C/minute after an initial period of 60 minutes at 60° C. VPC analysis of the xylenes required the use of an "internal tandem" 20' x ¼" glass column packed with 15' of 30% SE-30 on chromosorb WAW (60/80) followed by 5' of 5% DC-SSS and 5% Bentone-34 on chromosorb WAW (60/80). This column was usable for separation of xylenes if temperature-programmed at 50° for 64 min (to elute the bicyclopropenyls) and then at 1°/min to 85°. Under these conditions the retention times were: p-xylene, 94.4 min; m-xylene, 96.9 min; o-xylene, 101.0 min.

Figure 8. Apparatus for Gas Phase Kinetics

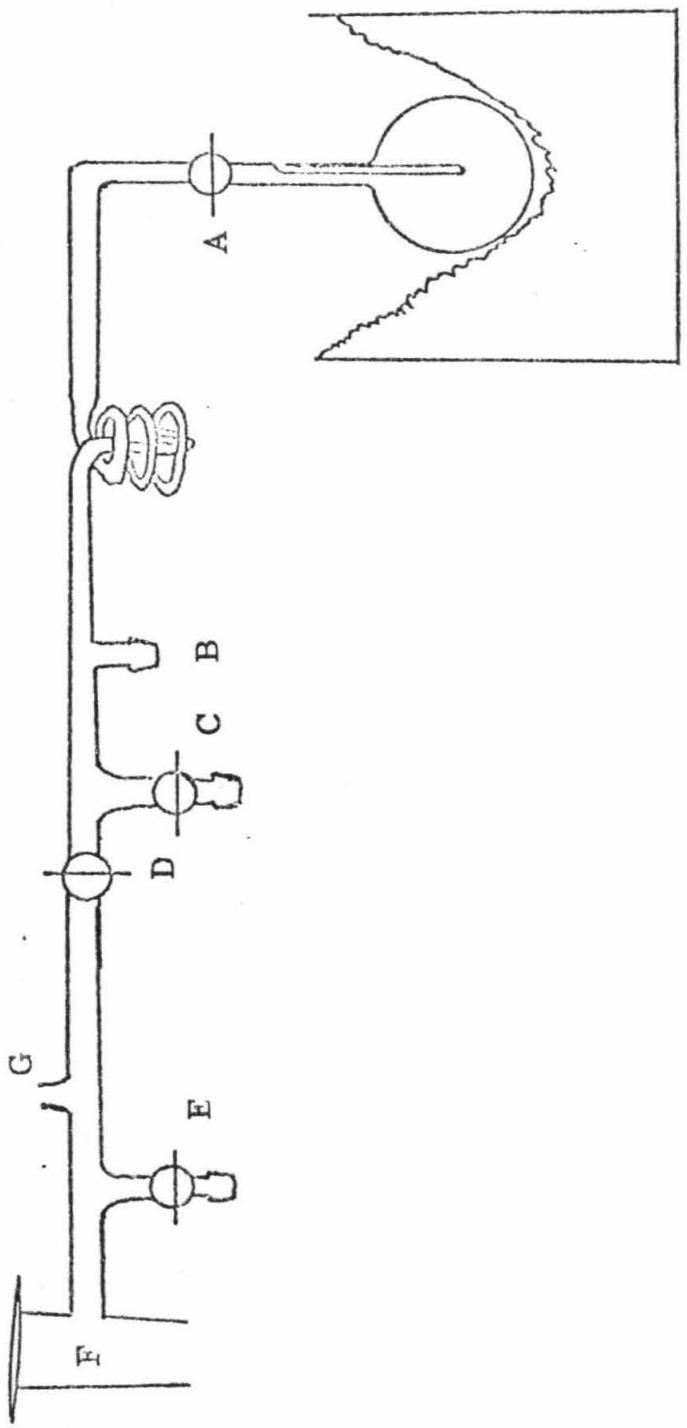
A
B
C
D
E
F
G

References and Notes

1. John and Beverly Stauffer Foundation Fellow, 1975-76.

2. Estimated using standard group equivalent values and a cyclopropene strain energy of 54 Kcal/mole; c.f. S. W. Benson, "Thermochemical Kinetics", John Wiley & Sons, N.Y., 1968.

3. R. Weiss and S. Andrae, Angew. Chem. Int. Ed. (Engl.), 12, 150, 152 (1973).

4. a) I. J. Landheer, W. H. de Wolf, and F. Bickelhaupt, Tet. Letters, 349 (1975).

   b) ibid., 2813 (1974).

5. R. Breslow, P. Gal, H. W. Chang and L. J. Altman, J.Amer.Chem.Soc., 87, 5139 (1965).

6. a) R. Weiss and H. Kölbl, J.Amer.Chem.Soc., 97, 3222 (1975);

   b) ibid., 97, 3224 (1975).

7. R. Breslow and P. Gal, J. Amer. Chem. Soc., 81, 4747 (1959).

8. From the experimental data given, it is not clear whether 12 is in fact an intermediate of the major pathway or merely a side reaction product.

9. The authors did not correlate this proposed diracidal intermediate with their previous observations of dewar-benzene formation.[3]

10. W. H. de Wolf, I. J. Landheer and F. Bickelhaupt, Tet. Letters, 179 (1975).

11. J.H. Davis, K.J. Shea and R.G. Bergman, Angew. Chem., 88, 254

(1976).

12. (a) H. C. Brown and G. Zwiefel, J. Amer. Chem. Soc., 83, 486 (1961); (b) J. F. Collins and M. A. McKervey, J. Org. Chem., 34, 4172 (1969).

13. (a) C. H. DePuy and F.W. Breitbeil, J. Amer. Chem. Soc., 85, 2176 (1963).

14. (a) The following phases were tried: 1,2,3-tris(2-cyanoethozy)propane (TCEP); β,β-oxydipropionitrilephenyl acetonitrile, carbo 20M, Diethylene glycol succinate; (b) TCEP

15. M. J. Goldstein and M. S. Benzon, J. Amer. Chem. Soc., 94, 7149 (1972).

16. Available from the Quantum Chemistry Program Exchange.

17. W. Von E. Doering and W. R. Roth, Tetrahedron, 18, 67 (1962).

18. J. H. Davis, R. G. Bergman and W. A. Goddard, J. Amer. Chem. Soc., 98, 4015 (1976).

19. L. H. Slaugh, J. Amer. Chem. Soc., 87, 1522 (1965).

20. N. J. Turro, G. B. Schuster, R. G. Bergman, K. J. Shea, and J. H. Davis, J. Amer. Chem. Soc., 97, 4758 (1975).

21. D. D. Perrin, W. L. F. Armarego, and D. R. Perrin, "Purification of Laboratory Chemicals", Pergamon Press, Oxford, 1966.

22. W.H. de Wolf, W. Stohl, I.J. Landheer and F. Bickelhaupt, Rec. Trav. Chim. Pays-Bas, 96, 405 (1971).